McLure, Lindsey Elizabeth Robertson (2015) The role of cardiac magnetic resonance imaging in the assessment of right ventricular function in pulmonary hypertension. MD thesis.

http://theses.gla.ac.uk/6884/

Copyright and moral rights for this thesis are retained by the author

A copy can be downloaded for personal non-commercial research or study, without prior permission or charge

This thesis cannot be reproduced or quoted extensively from without first obtaining permission in writing from the Author

The content must not be changed in any way or sold commercially in any format or medium without the formal permission of the Author

When referring to this work, full bibliographic details including the author, title, awarding institution and date of the thesis must be given.

Glasgow Theses Service
http://theses.gla.ac.uk/
theses@gla.ac.uk

THE ROLE OF CARDIAC MAGNETIC RESONANCE IMAGING IN THE ASSESSMENT OF RIGHT VENTRICULAR FUNCTION IN PULMONARY HYPERTENSION

Lindsey Elizabeth Robertson McLure

MBChB, BSc (Hons), MRCP

Submitted in fulfilment of the requirements for the Degree of Doctor of Medicine.

The University of Glasgow

June 2015

Table of Contents

List of Tables 6
List of Figures 8
List of Abbreviations 10
Acknowledgements 16
Author's Declaration 17
Summary 18
Publications relating to this thesis 20
Presentations to Learned Societies 21
1 Introduction 24
1.1 Overview of pulmonary hypertension 24
1.1.1 Pulmonary arterial hypertension (Group 1) 25
1.1.2 PH due to lung disease and/or hypoxia (Group 3) 27
1.1.3 CTEPH (Group 4) 27
1.1.4 Treatment of PH 28
1.1.5 Specific drug therapy for PH 30
1.1.6 Natural history of pulmonary hypertension 31
1.2 The Right Ventricle 33
1.2.1 Assessment of the RV 35
1.2.2 RV in pulmonary hypertension 35
1.3 Cardiac Magnetic Resonance (CMR) Imaging 37
1.3.1 Introduction 37
1.3.2 Basic Physics of CMR 37
1.3.3 Main sequences in CMR 39
1.3.4 Components of a modern CMR scanner 40
1.3.5 Limitations of CMR 41
1.3.6 Ventricular Morphology and Function by CMR 41
1.3.7 Flow Analysis 43
1.3.8 Contrast Enhanced CMR imaging 44
1.3.9 MR Pulmonary Circulation 44
1.4 CMR Assessment of Pulmonary Hypertension 45
1.4.1 Ventricular Volumes 45
1.4.2 Ventricular Mass 46
1.4.3 Interventricular Septal Configuration 47

1.4.4 RV Diastolic Function 48
1.4.5 Right Ventricular Contractility 48
1.4.6 Contrast Enhanced Perfusion CMR 49
1.4.7 Stress CMR 50
1.4.8 CMR flow measurements 51
1.4.9 Distensibility of Pulmonary Artery 52
1.4.10 CMR Pulmonary Angiography 53
1.4.11 CMR Pulmonary Perfusion Imaging 53
1.4.12 Pulmonary Artery Pressure Estimation by CMR 53
1.4.13 NMR Spectroscopy 54
1.4.14 Summary of CMR 54
1.5 Inert gas rebreathing 55
1.6 Evaluation of Pulmonary Hypertension 56
1.7 Follow up assessment of PH patients 63
1.7.1 WHO Functional Class 66
1.7.2 Quality of life (QoL) 66
1.7.3 Exercise Testing 66
1.7.4 Echocardiography 67
1.7.5 Biomarkers 68
1.7.6 Haemodynamics 69
1.7.7 Cardiac Magnetic Resonance Imaging 70
1.8 Hypotheses and Aims 75
2 Materials and Methods 78
2.1 Introduction 78
2.2 Cardiac Magnetic Resonance Imaging 85
2.2.1 CMR protocol 85
2.2.2 Preparation of patient for CMR scan 85
2.2.3 Cardiovascular Magnetic Resonance Imaging 86
2.2.4 CMR image acquisition and analysis 87
2.2.5 Analysis of CMR images 92
2.2.6 Intra-observer variability of CMR analysis in this thesis 97
2.3 WHO Functional Class (WHO FC) 99
2.4 Six-minute walk test 99
2.4.1 Test protocol 99
2.5 Right heart catheterisation 100

2.6 Inert gas rebreathing 104
2.6.1 Principles and operational detail..... 104
2.7 Statistical methods. 108
3 Non-invasive stroke volume measurement by cardiac magnetic resonance imaging and inert gas rebreathing in pulmonary hypertension. 110
3.1 Introduction..... 110
3.2 Methods and Materials 111
3.2.1 Patients and Protocol 111
3.2.2 Right heart catheterisation and thermodilution measurements ... 112
3.2.3 CMR image acquisition and analysis 112
3.2.4 Inert Gas Rebreathing..... 113
3.2.5 Statistical Analysis..... 113
3.3 Results..... 113
3.4 Discussion 120
4 Comparison of right ventricular function, assessed by cardiac magnetic resonance imaging, in patients with idiopathic pulmonary arterial hypertension versus connective tissue disease associated pulmonary arterial hypertension: A cross-sectional study. 125
4.1 Introduction..... 125
4.2 Methods 127
4.2.1 Study population..... 127
4.2.2 Study design 127
4.2.3 Cardiac magnetic resonance (CMR) image acquisition and analysis 127
4.2.4 Right heart catheterisation 128
4.2.5 Six-minute walk test 128
4.2.6 Statistical analysis..... 128
4.3 Results..... 129
4.3.1 Patient characteristics..... 129
4.3.2 CMR measurements..... 130
4.3.3 Correlation between mPAP and CMR measurements..... 135
4.3.4 Survival analysis..... 140
4.4 Discussion 140
5 Changes in right ventricular function measured by CMR imaging in pulmonary hypertension patients receiving disease-targeted therapy: A longitudinal study. 146

5.1 Introduction 146
5.2 Materials and Methods 148
5.2.1 Study design 149
5.2.2 Cardiac magnetic resonance (CMR) image acquisition and analysis 150
5.2.3 Right heart catheterisation 151
5.2.4 6-minute walk test 151
5.2.5 WHO functional class 152
5.2.6 Statistical analysis 152
5.3 Results 153
5.3.1 Participants 153
5.3.2 Response to disease-targeted therapy 155
5.3.3 CMR assessments 155
5.4 Discussion 162
6 General discussion and summary 169
7 Appendices 173
7.1 Appendix 1: Euro-MR introductory letter 173
7.2 Appendix 2: Euro-MR Newsletter 174
List of References 176

List of Tables

Table 1-1: Clinical classification of pulmonary hypertension (Nice, 2013) 25
Table 1-2: Definition of patient status as guided by the European Society of Cardiology / European Respiratory Society guidelines..... 64
Table 1-3: Current measurements with established importance for assessing disease severity, stability and prognosis in pulmonary arterial hypertension. 65
Table 2-1: Baseline diagnostic investigations at the Scottish Pulmonary Vascular Unit. 79
Table 2-2: Inclusion and exclusion criteria for entry into cardiac magnetic resonance studies at Scottish Pulmonary Vascular Unit. 81
Table 2-3: Measurements obtained from cardiac magnetic resonance imaging for this thesis. 94
Table 2-4: Intra-observer variability data of CMR analysis. 97
Table 2-5: Summary of Bland-Altman analyses performed. 98
Table 2-6: World Health Organisation functional classification in pulmonary hypertension..... 99
Table 2-7: Haemodynamic measurements performed during right heart catheterisation. 103
Table 3-1: Baseline characteristics of the subjects in the study. 114
Table 3-2: Results of diagnostic evaluation. 115
Table 3-3: Summary of Bland-Altman analyses performed. 119
Table 3-4: Results of Bland-Altman analyses performed in the presence and absence of lung disease..... 120
Table 4-1: Measurements obtained in this study from cardiac magnetic resonance imaging. 128
Table 4-2: Baseline characteristics for patients enrolled in this study. 130
Table 4-3: Baseline cardiac magnetic resonance measurements for enrolled patients. 131
Table 4-4: Correlations between mean pulmonary artery pressure measurements and cardiac magnetic resonance measurements. 136
Table 5-1: EURO-MR: Outline and study timetable. 148
Table 5-2: Measurements made from cardiac magnetic resonance imaging in this study. 151

Table 5-3: World Health Organisation functional classification of pulmonary hypertension..... 152
Table 5-4: Baseline characteristics for patients enrolled in this study. 154
Table 5-5: Baseline and four month cardiac magnetic resonance variables in the cohort group..... 156

List of Figures

Figure 1-1: Signalling pathways involved in the pathogenesis of pulmonary hypertension. 29
Figure 1-2: Natural history of pulmonary hypertension. 32
Figure 1-3: Anatomy of the heart. 33
Figure 1-4: Planimetry of the right ventricle. 43
Figure 1-5: Cardiac magnetic resonance short axis image from a patient with pulmonary hypertension. 47
Figure 1-6: Delayed contrast enhanced cardiac magnetic resonance images of a patient with pulmonary hypertension. 50
Figure 1-7: Pre (A) and post (B) treatment cardiac magnetic resonance images. 71
Figure 2-1: Flow chart of patient journey at the Scottish Pulmonary Vascular Unit. 80
Figure 2-2: Consent form for CMR clinical research project. 82
Figure 2-3: Patient information sheet. 83
Figure 2-4: Cardiac magnetic resonance imaging at the Scottish Pulmonary Vascular Unit. 87
Figure 2-5: Typical orthogonal scout images used to localise the heart within the thoracic cavity. 88
Figure 2-6: Planning of cine cardiac magnetic resonance image acquisition. 90
Figure 2-7: Planimetry analysis of the right ventricle. 95
Figure 2-8: Velocity encoded flow maps of the pulmonary artery to determine stroke volume. 96
Figure 2-9: Right heart catheterisation at the Scottish Pulmonary Vascular Unit. 101
Figure 2-10: Swan-Ganz Pulmonary Artery Catheter. 102
Figure 2-11: Sulphur hexafluoride concentration during rebreathing. 106
Figure 2-12: A semi-logarithmic plot of normalised nitrous oxide against time. 107
Figure 3-1: Correlation plot and Bland-Altman analysis comparing stroke volume measured by thermodilution and CMR (aortic flow). 116
Figure 3-2: Correlation plot and Bland-Altman analysis comparing stroke volume measured by thermodilution and CMR (pulmonary artery flow). 117
Figure 3-3: Correlation plot and Bland-Altman analysis comparing stroke volume measured by thermodilution and inert gas rebreathing. 118

Figure 4-1: Bar graphs depicting ventricular dimensions and function measured by CMR in IPAH and CTDPAH patient groups..... 132
Figure 4-2: Correlation plots between mean pulmonary artery pressure measurements and cardiac magnetic resonance measurements in IPAH and CTDPAH patients..... 137
Figure 4-3: Kaplain-Meier survival curves for IPAH and CTDPAH patient groups. 140
Figure 5-1: Study protocol. 149
Figure 5-2: Change in 6 minute walk distance from baseline (0 months) to 4 months. 155
Figure 5-3: Changes in cardiac magnetic resonance measurements from the left heart: Between baseline and 4 months of disease targeted therapy..... 157
Figure 5-4: Changes in cardiac magnetic resonance measurements from the right heart: Between baseline and 4 months of disease targeted therapy..... 158
Figure 5-5: Pearson correlations between change in right ventricular function and change in six minute walk distance. 160
Figure 5-6: Pearson correlations between change in left ventricular function and change in six minute walk distance..... 161

List of Abbreviations

ABGs	arterial blood gases
ATS	American Thoracic Society
BSA	body surface area
BNP	brain natriuretic peptide
CAMPHOR	Cambridge pulmonary hypertension outcome review
CCB	calcium channel blocker
ceCMR	contrast enhanced - cardiac magnetic resonance
CHD	congenital heart disease
CHF	chronic heart failure
CI	cardiac index
CMR	cardiac magnetic resonance
CMRI	cardiac magnetic resonance imaging
CO	cardiac output
COPD	chronic obstructive pulmonary disease
CoV	coefficient of variation
CPET	cardiopulmonary exercise testing
CT	computed tomography
CTD	connective tissue disease
CTPA	computed tomography pulmonary angiogram
CTDPAH	connective tissue disease associated pulmonary arterial hypertension
CTEPH	chronic thromboembolic pulmonary hypertension
CXR	chest X-ray
DLCO	diffusing capacity for carbon monoxide
DCE	delayed contrast enhancement
Ds-CMR	dobutamine stress-cardiac magnetic resonance
ECG	electrocardiogram

ED	end diastole
EDV	end diastolic volume
EDVI	end diastolic volume index
EF	ejection fraction
ES	end systole
ESV	end systolic volume
ESVI	end systolic volume index
ET	endothelin
EURO-MR	European magnetic resonance study
FEV_1	forced expiratory volume in 1 second
FISP	fast imaging with steady state precession
FoV	field of view
FLASH	fast low angle shot
FVC	forced vital capacity
Gd-DTPA	gadolinium-diethylene triaminepentaacetic acid
GE	gradient echo
H^+	hydrogen atom
HLA	horizontal long axis
HR	heart rate
HRCT	high resolution computed tomography
IGR	inert gas rebreathing
ILD	interstitial lung disease
IPAH	idiopathic pulmonary arterial hypertension
IVS	interventricular septum
L.M.	Lindsey McLure
LV	left ventricle/ventricular
LVCI	left ventricular cardiac index
LVEDV	left ventricular end diastolic volume

LVEDVI	left ventricular end diastolic volume index
LVEF	left ventricular ejection fraction
LVESV	left ventricular end systolic volume
LVESVI	left ventricular end systolic volume index
LVH	left ventricular hypertrophy
LVM	left ventricular mass
mPA	main pulmonary artery
mPAP	mean pulmonary artery pressure
MR	magnetic resonance
MRA	magnetic resonance angiography
MRI	magnetic resonance imaging
MVO_2	mixed venous oxygen saturation
n	number
N_2O	nitrous oxide
NIH	National Institutes of Health
NMR	nuclear magnetic resonance
NO	nitric oxide
NSF	nephrogenic systemic fibrosis
NTproBNP	N-terminal pro-brain natriuretic peptide
NYHA	New York Heart Association
O_2	oxygen
PA	pulmonary artery
$P_{A\text{-}a}O_2$	alveolar-arterial oxygen partial pressure gradient
PAH	pulmonary arterial hypertension
PAH-QuERI	PAH Quality Enhancement Research Initiative
PAOP	pulmonary artery occlusion pressure
PAP	pulmonary artery pressure
PBF	pulmonary blood flow

PDE type-5	phosphodiesterase type-5
PEA	pulmonary endarterctomy
PFO	patent foramen ovale
PFTs	pulmonary function tests
PH	pulmonary hypertension
PoPH	portopulmonary hypertension
PVOD	pulmonary veno-occlusive disease
PVR	pulmonary vascular resistance
PVRI	pulmonary vascular resistance index
PWP	pulmonary wedge pressure
PWV	pulse wave velocity
QOL	quality of life
r	correlation coefficient
RAC	relative area change
RAP	right atrial pressure
RCT	randomised controlled trial
REPAIR	Right vEntricular remodelling in Pulmonary ArterIal hypeRtension
RF	radiofrequency
RHC	right heart catheterisation
ROI	region of interest
RR	respiratory rate
RV	right ventricle/ventricular
RVCI	right ventricular cardiac index
RVEDV	right ventricular end-diastolic volume
RVEDVI	right ventricular end-diastolic volume index
RVEF	right ventricular ejection fraction
RVESV	right ventricular end-systolic volume
RVESVI	right ventricular end-systolic volume index

RVF	right ventricular failure
RVH	right ventricular hypertrophy
RVIP	right ventricular insertion point
RVM	right ventricular mass
RVMI	right ventricular mass index
RVSD	right ventricular systolic dysfunction
RVSV	right ventricular stroke volume
RVSVI	right ventricular stroke volume index
SA	short axis
SD	standard deviation
SE	spin echo
SEM	standard error of the mean
SF_6	sulphur hexafluoride
SPVU	Scottish Pulmonary Vascular Unit
SSc	systemic sclerosis
SSc-PAH	pulmonary arterial hypertension associated with systemic sclerosis
SSFP	steady state free precession
SV	stroke volume
SVI	stroke volume index
T	Tesla
TAPSE	tricuspid annular plane systolic excursion
TD	thermodilution
TE	echo time (during CMR image acquisition)
TI	inversion time (during CMR image acquisition)
TLC	total lung capacity
TR	repetition time (during CMR image acquisition)
TR	tricuspid regurgitation
TTCW	time to clinical worsening

TTE	trans-thoracic echocardiography
VLA	vertical long axis
VMI	ventricular mass index
V/Q	ventilation to perfusion ratio
VO_2	oxygen uptake
WHO	World Health Organisation
WHO FC	World Health Organisation functional class
6MWD	six-minute walk distance
6MWT	six minute walk test
Δ	change
% predicted	percent predicted

Acknowledgements

I would like to thank my supervisor, Professor Andrew Peacock, for his valuable advice, encouragement, patience and assistance throughout this project. I would also like to thank Dr Martin Johnson and Dr David Welsh for their support and guidance.

I am extremely grateful to Ms Tracey Steedman for her assistance in teaching me the techniques of cardiac magnetic resonance imaging.

I would like to thank my colleagues in the Scottish Pulmonary Vascular Unit, Colin Church, Waiting Lee, Agnes Crozier, Jim Mearns and Val Pollock, for their assistance in both clinical and research matters.

I would like to extend a great deal of gratitude to the patients studied in this thesis.

Finally, I would like to thank my family for their support and patience during this project.

Author's Declaration

The experimental design of the work presented in this thesis was that of the author and her supervisor, Professor Andrew Peacock. All experimental work was carried out by the author with the exception of the acquisition of a proportion of the cardiac magnetic resonance scans (performed by Tracy Steedman, Glasgow Cardiac magnetic Resonance Unit, Western Infirmary, Glasgow).

I declare that this thesis has been composed by myself and is a record of work performed by myself. It has not previously been submitted for a higher degree.

Lindsey E R McLure
June 2015

Summary

Pulmonary hypertension (PH) is a rare disease of the pulmonary arteries. It is characterised by vascular proliferation and remodelling resulting in a progressive increase in pulmonary vascular resistance and right ventricular failure. The functional capacity of the right ventricle is the major prognostic determinant in PH, and death usually results from right ventricular failure. Although recent therapeutic advances have improved the short-to-medium term outlook of PH patients, early death due to right ventricular failure remains inevitable in many patients. The imperative role of RV performance in the clinical status and long-term outcome in PH patients is evident. Evaluation of right ventricular function is essential in the management of patients with pulmonary hypertension. Current methods of assessment of PH patients are suboptimal.

The right ventricle is difficult to assess due to its position and geometry. Recent developments in imaging techniques, such as cardiac magnetic resonance (CMR) imaging and echocardiography, have improved our understanding of the structure and function of the right ventricle. Assessment of RV function is complex and no single measurement is generally accepted in clinical practice. The experimental work performed in this thesis aimed to improve our understanding of RV function in PH patients and to provide clarity in the role of CMR in the non-invasive assessment and monitoring of pulmonary hypertension patients.

A non-invasive measurement of stroke volume would be beneficial to monitor disease progression in pulmonary hypertension patients. Chapter 3 demonstrated that cardiac magnetic resonance imaging provided non-invasive measurements of stroke volume that were as accurate as those obtained by thermodilution measured during right heart catheterisation. Inert gas rebreathing using photoacoustic analysis also provided accurate non-invasive measurements of stroke volume. Chapter 4 compared two patient groups: idiopathic pulmonary arterial hypertension (IPAH) and pulmonary hypertension associated with connective tissue disease (CTDPAH). We clarified that there was no significant differences in RV structure and performance between these two distinct patient groups to account for the poorer prognosis in the CTDPAH group.

Treatments for PH are always expensive, sometimes invasive and carry significant side effects. It is imperative that we are able to assess the patient's response to therapy in a clinically meaningful, accurate and non-invasive manner. The importance of escalating therapy if a patient does not respond to initial treatment has been emphasised in recently published guidelines. Current monitoring techniques have acknowledged limitations and are suboptimal. Chapter 5 presents the results obtained from my contribution to the prospective, longitudinal multinational EURO-MR study. Longitudinal CMR examination identified significant improvements in cardiac function with the introduction of disease-targeted therapy. Baseline and 4 months post therapy CMR scans were compared. It is anticipated that CMR could be a useful monitoring technique for patients with pulmonary hypertension.

Publications relating to this thesis

Changes in right ventricular function measured by cardiac magnetic resonance imaging in patients receiving pulmonary arterial hypertension-targeted therapy: The EURO-MR study.
Peacock AJ, Crawley S, **McLure L**, Blyth K, *et al*
Circ Cardiovasc Imaging. 2014 Jan;7(1):107-14.

Non-invasive stroke volume measurement by cardiac magnetic resonance imaging and inert gas rebreathing in pulmonary hypertension.
McLure LE, Brown A, Lee WN, Church AC, Peacock AJ, Johnson MK.
Clin Physiol Funct Imaging 2011 May;31(3):221-6

Cardiac magnetic resonance imaging for the assessment of the heart and pulmonary circulation in pulmonary hypertension.
McLure LE, Peacock AJ.
Eur Respir J. 2009 Jun;33(6):1454-66. Review.

Imaging of the heart in pulmonary hypertension.
McLure LE, Peacock AJ.
Int J Clin Pract Suppl. 2007 Sep;(156):15-26. Review.

Presentations to Learned Societies

Non-invasive measurement of stroke volume using an inert gas rebreathing device in patients with pulmonary hypertension.
Lindsey ER McLure
Oral presentation
The Royal Medico-Chirurgical Society of Glasgow
Research Prize Night - Winner
6th March 2008
Royal College of Physician and Surgeons of Glasgow

Cardiac Function determined by MR correlates with Pulmonary Artery Pressure in Pulmonary Arterial Hypertension (PAH) but there was no difference between Idiopathic PAH and Connective Tissue Disease PAH.
L.E.R. McLure, A.C. Church, K.G. Blyth, M.K. Johnson, A.J. Peacock
Poster presented at American Thoracic Society 2008

Non-invasive measurement of stroke volume using an inert gas rebreathing device in patients with pulmonary hypertension.
L.E.R. McLure, A. Brown, W.N. Lee, A.C. Church, A.J. Peacock, M.K. Johnson,
Poster presented at European Respiratory Society 2008

Non-Invasive Assessment of Pulmonary Blood Flow using an Inert Gas Rebreathing Device in Patients with Pulmonary Hypertension.
Lindsey ER McLure
Oral Presentation
British Thoracic Society Winter Meeting
5th December 2007

Effects of treatment for pulmonary hypertension on pulmonary artery distensibility determined by cardiac magnetic resonance imaging.

LER McLure, AJ Peacock

Poster presented at European Respiratory Society 2007

Chapter 1

Introduction

1 Introduction

This chapter aims to discuss the background and rationale of the work performed for this thesis. An overview of pulmonary hypertension (PH) is undertaken, focussing on clinical classification, pathobiology and management. The natural history of PH and the pivotal role of the right ventricle are described. The principal technique used in this thesis is cardiac magnetic resonance (CMR) imaging. This technique is described in detail and a comprehensive review of its use in PH is undertaken. Inert gas rebreathing (IGR) is a further technique employed in this thesis. The history of IGR is described and its role in the clinical setting is discussed. The initial evaluation of a patient with PH is described, including the importance of diagnostic investigations in terms of prognosis. This is followed by a comprehensive discussion of current methods used in the longitudinal assessment of PH and their limitations. Finally, the hypotheses and aims of this thesis are outlined.

1.1 Overview of pulmonary hypertension

Pulmonary hypertension (PH) is a disease of the pulmonary arteries that is characterised by vascular proliferation and remodelling (1, 2) resulting in a progressive increase in pulmonary vascular resistance (PVR) and right ventricular failure. The functional capacity of the right ventricle is the major prognostic determinant in PH, and death usually results from RV failure (3-6). PH is a haemodynamic and pathophysiological condition defined as an increase in mean pulmonary arterial pressure (mPAP) ≥ 25mmHg at rest as assessed by right heart catheterisation. A resting mPAP between 8 and 20mmHg should be considered normal. Further studies are required to determine the natural history of individuals with a resting mPAP between 21 and 24mmHg.

The most recent clinical classification of PH was proposed, by worldwide experts, at the fifth World Symposium on PH held in 2013 in Nice, France (7). PH is classified into five diagnostic groups with specific histological, clinical, and therapeutic features. Despite possible comparable elevations of pulmonary pressure in the different clinical groups, the underlying mechanisms, the

diagnostic approaches, and the prognostic and therapeutic implications are completely different. Please see table 1.1.

Table 1-1: Clinical classification of pulmonary hypertension (Nice, 2013)

1. Pulmonary arterial hypertension (PAH)

- 1.1 Idiopathic
- 1.2 Heritable
- 1.3 Drugs and toxins induced
- 1.4 Associated with (APAH)
  - 1.4.1 Connective tissue diseases
  - 1.4.2 HIV infection
  - 1.4.3 Portal hypertension
  - 1.4.4 Congenital heart diseases
  - 1.4.5 Schistosomiasis

1'. Pulmonary veno-occlusive disease/pulmonary capillary haemangiomatosis

1''. Persistent pulmonary hypertension of the newborn

2. Pulmonary hypertension due to left heart disease

3. Pulmonary hypertension due to lung diseases and/or hypoxia

4. Chronic thromboembolic pulmonary hypertension

5. PH with unclear and/or multifactorial mechanisms

In this thesis, the patients enrolled were diagnosed with either PAH, PH due to lung disease and/or hypoxia or CTEPH. I will, therefore, elaborate further on each of these conditions.

1.1.1 Pulmonary arterial hypertension (Group 1)

PAH comprises the idiopathic (IPAH) and familial forms and the forms associated with connective tissue diseases, congenital heart defects with systemic-to-pulmonary shunts, portal hypertension, and human immunodeficiency virus (HIV)

infection. They share comparable clinical and haemodynamic pictures and virtually identical pathological changes of the lung microcirculation.

Pathological lesions affect the distal pulmonary arteries (< 500µm of diameter) in particular and are characterised by medial hypertrophy, intimal proliferative and fibrotic changes, adventitial thickening with moderate perivascular inflammatory infiltrates, complex lesions (plexiform, dilated lesions), and thrombotic lesions. Pulmonary veins are classically unaffected. The exact processes that initiate the pathological changes seen in PAH are still unknown although it is recognised that PAH has a multifactorial pathobiology that involves various biochemical pathways and cell types.

Recent registries have described the epidemiology of PAH (8, 9). The lowest estimates of the prevalence of PAH and IPAH are 15 cases and 5.9 cases/million adult population, respectively. The lowest estimate of PAH incidence is 2.4 cases/million adult population/year. Recent data from Scotland and other countries have confirmed that PAH prevalence is in the range 15–50 subjects per million population in Europe (8, 9). In the subgroup of APAH, 15.3% had connective tissue diseases (CTDs; mainly systemic sclerosis), 11.3% had CHD, 10.4% had portal hypertension, 9.5% had anorexigen-associated PAH and 6.2% had HIV infection (8, 9).

IPAH

IPAH is the most prevalent type of PAH. IPAH corresponds to sporadic disease, without any family history of PAH or known triggering factor. Mutations in the bone morphogenetic protein receptor 2 gene can be detected in 11-40% of apparently sporadic cases, thus representing a major genetic predisposing factor to PAH (10).

PAH associated with CTD (CTDPAH)

Connective tissue disease (CTD) is the second most prevalent type of PAH after IPAH in registries. The prevalence has been estimated to be 2.3-10 cases per million in the general population (8, 9, 11). Compared with IPAH, patients with CTDPAH are mainly women (women/men ratio 4:1), are older (mean age at diagnosis, 66 years), may present with concomitant disorders (pulmonary

fibrosis, left heart disease), and have shorter survival (12). The unadjusted risk of death for systemic sclerosis-associated PAH compared with IPAH is 2.9200 and the predictors of outcome are the same as for IPAH (right atrial pressure [RAP], pulmonary artery pressure [PAP], and cardiac index [CI]). Between 7% and 12% of patients with systemic sclerosis (SSc) and around 0.5-14% of patients with systemic lupus erythematosus are reported to have PAH, making these the two most frequent causes of PAH-CTD (12-14). In these patients, PAH may occur in association with interstitial fibrosis or as a result of an isolated pulmonary arteriopathy. Pulmonary venous hypertension from left heart disease may also be present. Histopathological changes in PAH associated with CTD are generally indistinguishable from those of classical IPAH, although there is more frequent involvement of the pulmonary veins (15).

1.1.2 PH due to lung disease and/or hypoxia (Group 3)

Based on published series, the incidence of significant PH in COPD patients with at least one previous hospitalization for exacerbation of respiratory failure is 20%. In advanced COPD, PH is highly prevalent (> 50%) (16, 17), although in general it is of only mild severity. In interstitial lung disease, the prevalence of PH is between 32 and 39% (18). The combination of lung fibrosis with emphysema is associated with a higher prevalence of PH (19).

The pathophysiological mechanisms involved in this setting are multiple and include hypoxic vasoconstriction, mechanical stress of hyperinflated lungs, loss of capillaries, inflammation, and toxic effects of cigarette smoke. Pathological changes include medial hypertrophy and intimal obstructive proliferation of the distal pulmonary arteries. A variable degree of destruction of the whole vascular bed in emphysematous or fibrotic areas may also be present.

1.1.3 CTEPH (Group 4)

No specific genetic mutations have been linked to the development of CTEPH. It is suggested that the prevalence of CTEPH is up to 3.8% in survivors of acute pulmonary embolism (20). CTEPH can be found in patients without any previous clinical episode of acute pulmonary embolism or deep venous thrombosis (up to 50% in different series) (21).

Pathological lesions are characterised by organised thrombi tightly attached to the pulmonary arterial medial layer in the elastic pulmonary arteries, replacing the normal intima. These may completely occlude the lumen or form different grades of stenosis, webs and bands (22). In the non-occluded areas, a pulmonary arteriopathy indistinguishable from that of PAH (including plexiform lesions) can develop (23). The obstructive lesions observed in the distal pulmonary arteries of non-obstructed areas (virtually identical to those observed in PAH) may be related to a variety of factors, such as shear stress, pressure, inflammation, and the release of cytokines and vasculotrophic mediators. Collateral vessels from the systemic circulation (from bronchial, costal, diaphragmatic and coronary arteries) can grow to reperfuse at least partially the areas distal to complete obstructions. Pulmonary thromboembolism or *in situ* thrombosis may be initiated or aggravated by abnormalities in either the clotting cascade, endothelial cells, or platelets, all of which interact in the coagulation process (24). In most cases, it remains unclear whether thrombosis and platelet dysfunction are a cause or consequence of the disease. Inflammatory infiltrates are commonly detected in the pulmonary endarterectomy (PEA) specimens. Thrombophilia studies have shown that lupus anticoagulant may be found in approximately 10% of such patients, and 20% carry antiphospholipid antibodies, lupus anticoagulant, or both. A recent study has demonstrated that the plasma level of factor VIII, a protein associated with both primary and recurrent venous thromboembolism, is elevated in 39% of patients with CTEPH. No abnormalities of fibrinolysis have been identified.

1.1.4 Treatment of PH

Prior to the availability of treatment, PAH patients had a life expectancy of less than 3 years (4, 25). Modern drug therapy leads to a significant improvement in patients' symptomatic status and a slower rate of clinical deterioration. A meta-analysis performed on 23 RCTs in PAH patients (published prior to October 2008) reports a 43% decrease in mortality and a 61% reduction in hospitalisations in patients treated with specific drug therapies vs. patients randomised to placebo (26). These results, achieved after an average treatment period of 14.3 weeks, support the efficacy of the currently approved PAH treatments. Despite this finding, PAH remains a chronic disease without a cure. The medical and

interventional treatments for more advanced cases are still invasive and prone to significant side effects.

The guidelines state that the use of one of the three major classes of PH-specific therapies, the prostanoids, endothelin antagonists, or PDE-5 inhibitors, is up to the discretion of the treating physician. Combination therapy, using two or more classes of drugs simultaneously, is one way of escalating treatment, and has been used successfully in the treatment of systemic hypertension and heart failure (27, 28). It is also an attractive option for the management of PAH because three separate signalling pathways known to be involved in the disease are targeted by present therapies:

1) Prostacyclin pathway;
2) Endothelin pathway;
3) Nitric oxide (NO) pathway.

Figure 1-1: Signalling pathways involved in the pathogenesis of pulmonary hypertension.

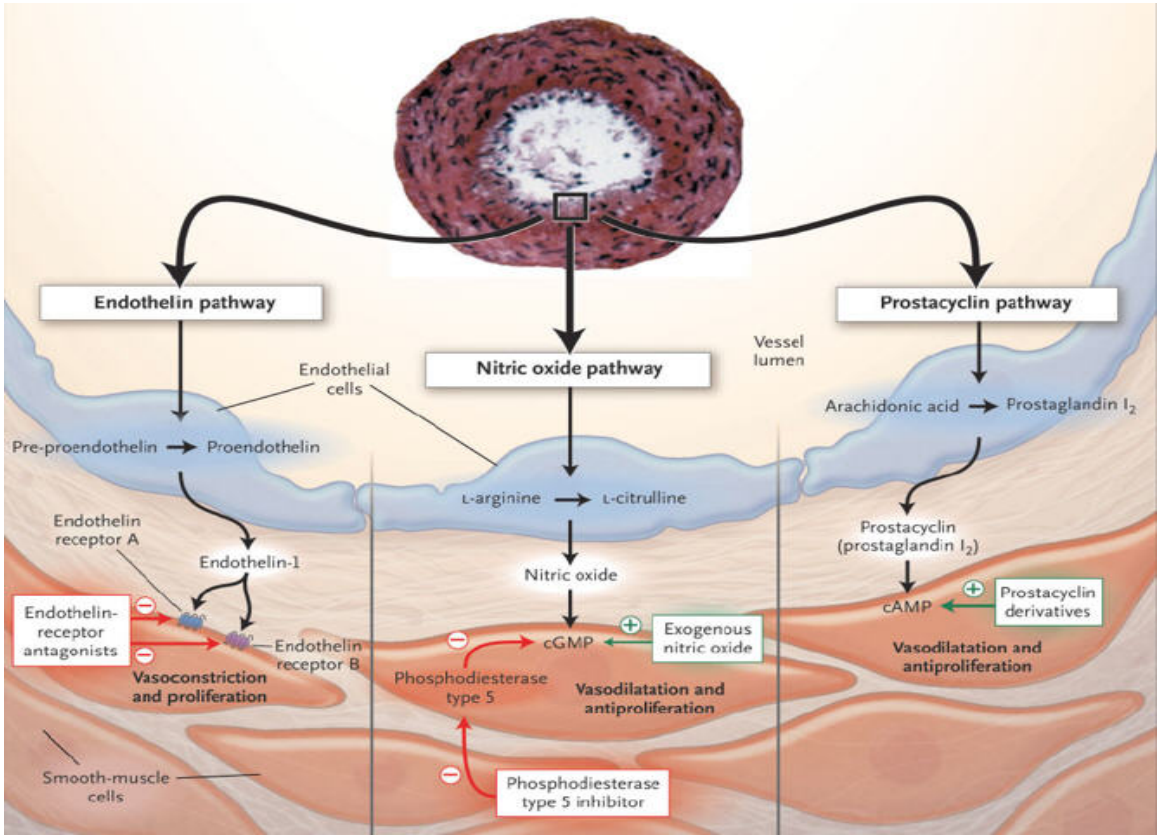

Figure adapted from the New England Journal of Medicine.

1.1.5 Specific drug therapy for PH

Calcium channel blockers

Smooth muscle cell hypertrophy, hyperplasia, and vasoconstriction are known to contribute to the pathogenesis of IPAH and this has led to the use of traditional vasodilators since the mid 1980s, principally involving the use of calcium channel blockers (CCBs). It has been increasingly recognised that only a small number of patients with IPAH who demonstrate a favourable response to acute vasodilator testing at the time of RHC benefit from CCBs (29, 30).

Prostanoids

Prostacyclin is produced predominantly by endothelial cells and induces potent vasodilatation of all vascular beds. This compound is the most potent endogenous inhibitor of platelet aggregation and it also appears to have both cytoprotective and antiproliferative activities (31). Dysregulation of the prostacyclin metabolic pathways has been shown in patients with PAH as assessed by reduction of prostacyclin synthase expression in the pulmonary arteries and of prostacyclin urinary metabolites (32). The clinical use of prostacyclin in patients with PAH has been extended by the synthesis of stable analogues that possess different pharmacokinetic properties but share qualitatively similar pharmacodynamic effects.

Endothelin receptor antagonists

Activation of the endothelin system has been demonstrated in both plasma and lung tissue of PAH patients (33). Although it is not clear if the increases in endothelin-1 plasma levels are a cause or a consequence of PH (34), these data support a prominent role for the endothelin system in the pathogenesis of PAH (35). Endothelin-1 exerts vasoconstrictor and mitogenic effects by binding to two distinct receptor isoforms in the pulmonary vascular smooth muscle cells, endothelin-A and endothelin-B receptors. Endothelin-B receptors are also present in endothelial cells, and their activation leads to release of vasodilators and antiproliferative substances such as NO and prostacyclin that may counterbalance the deleterious effects of endothelin-1. Despite potential differences in receptor isoform activity, the efficacy in PAH of the dual

endothelin-A and endothelin-B receptor antagonist drugs and of the selective ERA compounds appears to be comparable.

Phosphodiesterase type-5 inhibitors

Inhibition of the cGMP-degrading enzyme PDE type-5 results in vasodilatation through the NO/cGMP pathway at sites expressing this enzyme. Since the pulmonary vasculature contains substantial amounts of PDE type-5 the potential clinical benefit of PDE type-5 inhibitors has been investigated in PAH. In addition, PDE type-5 inhibitors exert antiproliferative effects (36, 37).

Emerging treatments such as tyrosine kinase inhibitors, soluble guanylate cyclase activators (riociguat) and prostacyclin receptor agonists (selexipeg) are currently being evaluated in PAH.

1.1.6 Natural history of pulmonary hypertension

Obliteration of pulmonary capillary beds and vasoconstriction lead to elevated pulmonary vascular resistance (PVR) and increased RV afterload. Right ventricular adaptation is the main determinant of clinical outcome and survival. In early disease, vasodilatation of non-diseased pulmonary capillary beds compensates for the loss of functional beds elsewhere, thereby maintaining PVR and pulmonary artery pressures. Patients often have few symptoms as stroke volume (SV) and cardiac output (CO) at rest and during exercise are preserved. The negative impact on cardiopulmonary function becomes clinically apparent when around 70% of the pulmonary capillary beds are occluded. Patients experience increasing exertional limitation as SV and CO response to exercise become progressively restricted. In advanced disease, CO eventually becomes compromised at rest resulting in overt RHF, cardiovascular collapse and death (Figure 1.2).

Figure 1-2: Natural history of pulmonary hypertension.

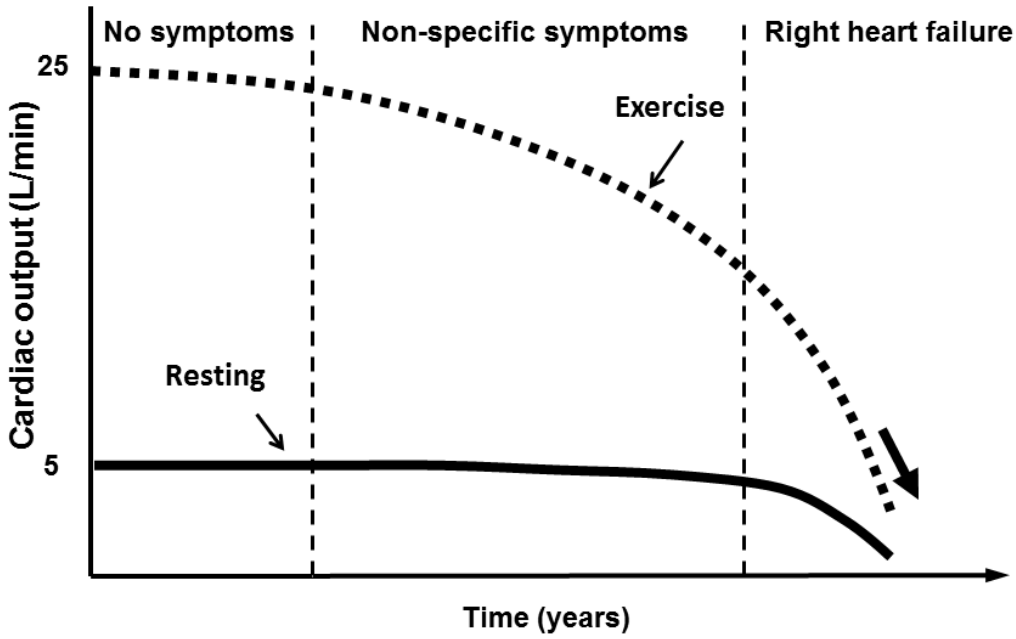

Patients are asymptomatic when both resting and exercise CO are preserved. Non-specific symptoms develop on exertion when exercise CO becomes restricted without affecting resting CO. Right heart failure ensues when resting CO is also compromised.

1.2 The Right Ventricle

Figure 1-3: Anatomy of the heart.

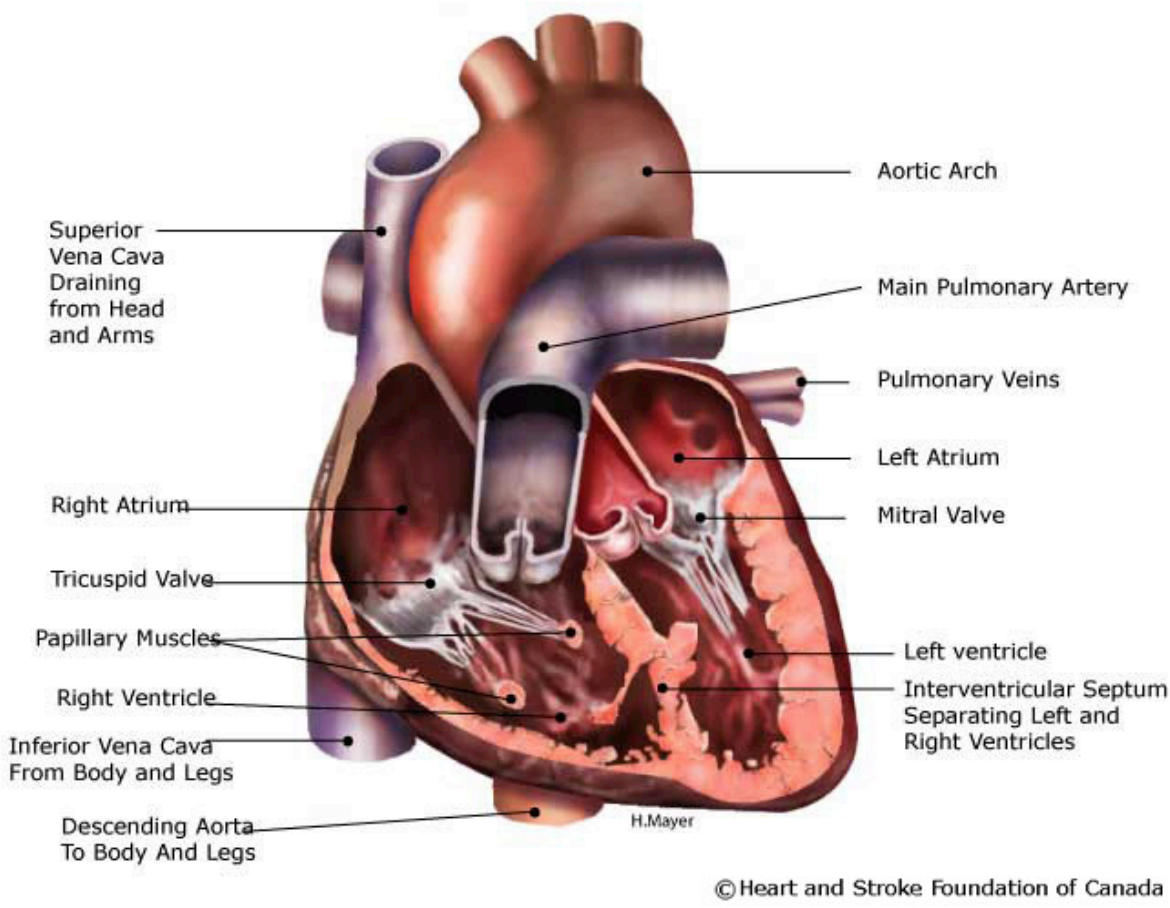

Figure adapted from Heart and Stroke Foundation of Canada.

The functional capacity of the right ventricle (RV) is the major prognostic determinant in PH, and death usually results from RV failure (3-6). Developments in CMR and echocardiography within the past 2 decades have led to new insights into the structure and function of the RV. The important role of RV performance in the clinical status and long term outcome of patients with PH, congenital heart disease, and LV dysfunction has become increasingly evident (38, 39).

The RV differs substantially from the LV in its morphology, structure, and function. These differences are present from the very early embryological origin of both ventricles (40, 41). LV myocardial precursor cells originate from the primary heart field in the anterior plate mesoderm, whereas RV precursor cells originate from the secondary heart field. Their different embryological origins probably explain why RV myocytes respond differently from LV myocytes to

abnormal haemodynamic loading conditions (42, 43). During fetal life, the RV pumps blood to the systemic circulation and placenta and contributes more than the LV (~65%) to total cardiac output (CO) (44). After birth, the LV becomes the systemic ventricle, whereas the RV remodels to become the subpulmonary ventricle, which supports the low-resistance pulmonary circulation. Once this adaptation has occurred, the RV loses its capacity to revert to its fetal phenotype and is limited in its ability to respond to abnormal haemodynamic loading, especially to increased pressure loading (42).

The RV has complex 3D geometry, with a triangular appearance in the sagittal plane and a crescent shape in the coronal plane. The normal RV has an inflow component formed by the atrioventricular septum, tricuspid valve and subvalvular apparatus, an apical trabecular component and an outflow tract which continues into the pulmonary trunk. The RV inflow and outflow regions are separated by the crista ventricularis and the RV is “wrapped around” the LV. The RV is closely connected to the LV: they share a wall (interventricular septum); the RV free wall is attached to the anterior and posterior interventricular septum; and they have mutually encircling epicardial fibres and share the same intrapericardial space. The RV is characterised by a thin wall (3-5mm in adults) and normally has one sixth of the muscle mass of the LV. It pumps the same stroke volume (SV) as the LV but with approximately 25% of the stroke work because of the low resistance of the pulmonary vasculature. In health, the pulmonary circulation is a compliant, high flow, low resistance system and is nearly maximally vasodilated at rest. Healthy pulmonary arteries exhibit very low basal smooth muscle tone and normal PVR is approximately one-fifteenth of normal systemic vascular resistance. This allows the pulmonary circulation to accommodate the entire cardiac output, which flows through the lungs at pressures far lower than those seen in the systemic circulation. These low pressures prevent fluid from migrating into the interstitial space, optimising the conditions for gas exchange and allowing the RV to operate at minimum energy cost.

Nearly all studies of ventricular fibre structure have been performed on the LV. Dissection studies have shown that its fibres course in a helical continuum between the subendocardium and subepicardium. The LV has a middle layer

containing circumferential constrictor fibres that provide the main driving force of the LV by reducing ventricular diameter. Since myocardial fibres only shorten by 15%, however, an essential contribution to LV ejection is shortening of the ventricle through contraction of its oblique fibres. A third component of ejection is torsion i.e. rotation of the LV apex relative to the base. The RV also has helical fibres and undergoes torsion. However, the RV lacks a middle layer and must rely more heavily on longitudinal shortening than does the LV (45) for generation of SV. The interventricular septum is generally considered part of the LV although the septum contains longitudinal fibres belonging to the RV. There are fibres that course between them at both the superficial and deeper layers, and the two ventricles interact functionally.

The RV also differs from the LV in its physiology. RV pressure-volume loops have a trapezoidal shape with a less well-defined isovolumic periods compared with the typical rectangular LV pressure-volume loops (46-48). RV output is highly sensitive to afterload and fairly mild increases in afterload lead to reduced RV CO. This sensitivity could explain why systemic arterial hypertension is better tolerated than PH.

1.2.1 Assessment of the RV

The RV is difficult to assess. The RV inflow and outflow tracts are positioned in different planes and are difficult to image simultaneously with 2D techniques. The normal RV has a thin wall and is, therefore, difficult to visualise and differentiate from the surrounding structures. Prominent RV trabeculations further complicate border detection, which is required for calculation of RV volumes and mass, irrespective of the imaging technique employed. Assessment of RV function is complex and no single functional parameter is generally accepted in clinical practice. This situation contrasts with assessment of LV performance, in which LV ejection fraction (LVEF) is a generally accepted parameter to assess systolic function.

1.2.2 RV in pulmonary hypertension

The functional capacity of the right ventricle (RV) is the major prognostic determinant in PH, and death usually results from RV failure (3-6). It is unknown

why some patients with markedly elevated pulmonary artery pressures maintain well-preserved cardiac function for several years, while others with equal or less severe PH suffer rapidly progressive right heart failure. Although pulmonary pressure rise is the distinctive characteristic of this disease, the level of pulmonary artery pressure itself has only modest prognostic significance in patients with PAH. One factor that has hindered the understanding of RV performance in patients with PH has been the lack of techniques that give a reliable picture of right ventricular morphological and functional change in the face of increasing outflow obstruction. However, in patients with PAH, RV dysfunction has not received the same scientific interest as the mechanisms of PAH.

Significant morphological and functional adaptive changes of the RV develop in patients affected by PH. The first adaptation that occurs is myocardial hypertrophy, followed by progressive contractile impairment. Possible mechanisms involved in the progression of RV myocardial contractile dysfunction include:

i) ischaemia,
ii) changes in gene expression of the sarcomere proteins,
iii) activation of myocardial renin–angiotensin system.

However, afterload mismatch remains the main determinant of RV dysfunction in patients with PH. RV dilatation occurs in order to compensate a reduced fractional shortening by an increase in preload, so that stroke volume is maintained. As contractile dysfunction progresses, RV failure occurs and it is characterized by high RV filling pressures, diastolic dysfunction, and reduced cardiac output (CO). The decrease in CO is also due to the functional tricuspid regurgitation caused by tricuspid annular dilatation and impaired leaflet coaptation. Augmented RV volume is the result of chamber remodelling, owing to the increase in cardiac myocyte length as a consequence of newly synthesized sarcomeres assembled in series. With hypertrophy and dilatation, the RV progressively becomes more spherical, its cross-sectional area enlarges, and the interventricular septum flattens, causing also LV diastolic dysfunction. Diastolic dysfunction is the most frequent type of LV impairment in patients with PAH. Usually, patients with PAH show a delayed relaxation pattern of LV filling and a small end-diastolic LV volume. The reduced LV end-diastolic volume contributes

to the decrease in stroke volume. Reduction of LV ejection fraction may occur in patients with PAH but this is a rather uncommon finding.

1.3 Cardiac Magnetic Resonance (CMR) Imaging

1.3.1 Introduction

CMR imaging is well established in clinical practice for the diagnosis and management of a wide spectrum of cardiovascular disease. Its advancing role is related to technical improvements, which allow increasingly rapid and robust data acquisition. Use of CMR represents the specialised application of magnetic resonance (MR) to the cardiovascular system, employing specialised receiver coils, pulse sequences, and gating methods. Images may be performed with ECG gating/triggering and with respiratory suppression (breath holding or navigator gating), thereby reducing image artefacts.

CMR is fundamentally safe. No short or long-term ill effects have been reported at current field strengths (less than 3 Tesla). MR does not interfere with the electron shells involved in chemical binding (e.g. DNA) that can be altered by ionizing radiation. The phenomenon of MR is restricted to atomic nuclei with unpaired spin e.g. hydrogen, carbon, oxygen, sodium, potassium, and fluorine. The majority of clinical CMR imaging involves the hydrogen nucleus, which is abundant in water, fat, and muscle.

1.3.2 Basic Physics of CMR

MRI is based on *nuclear magnetic resonance*, the phenomenon of the resonance of atomic nuclei in response to radiofrequency (RF) waves. The hydrogen (H^+) atom is the simplest and most abundant element in the body and consists of one proton nucleus orbited by one electron. The H^+ nucleus can therefore also be termed a proton, and current clinical MRI techniques are based on receiving and processing RF signals from protons. Protons have a magnetic axis which is normally randomly orientated. When a magnetic field is applied, the protons align in synchrony and spin around an axis in line with the main magnetic field. This spinning is termed precession. The rate at which protons precess is measured by the precession frequency, which changes linearly with increasing

magnetic field strengths. When protons precess in synchrony they are said to be in-phase. There is loss of synchrony with time, and this is also termed out-of-phase. At equilibrium within a magnetic field, overall proton alignment is in the direction of the main magnetic field and they have net longitudinal magnetisation. This equilibrium can be disturbed by transmission of RF energy at the precession frequency of the proton which is 63 megaHertz (MHz) for water protons at 1.5 Tesla (T) which is the strength of most commercially used magnets.

The degree of proton excitation is proportional to the amplitude and duration of the RF pulse. After excitation, proton relaxation occurs as the energy is dissipated and this process is defined by two parameters known as T1 and T2. T1 relaxation times measure the time after excitation to recover the longitudinal magnetisation found in the equilibrium state. Transverse magnetisation decays at a rate measured by T2, which is faster than the rate of T1 recovery. T1 and T2 relaxation vary according to the environment of the H^+ atom within tissues and imaging sequences can be designed with different preference (or weighting) to one of these relaxation parameters for tissue characterisation, known as T1-weighted (T1W) and T2-weighted (T2W) acquisitions. The values for T2 are always below that of T1, and T1 represents the upper limit of T2. T1 and T2 values tend to parallel each other when proton motion is relatively random, e.g. in adipose tissue (which has a short T1 and T2) and in free water (which has a long T1 and T2). Tissues with a more organised structure contain abundant bound water. In this case proton motion is not random, there is increased transverse decay from the exchange of energy between protons, and T2 values become shorter than those of T1.

Localisation of anatomical position within a selected imaging slice or volume is done with the application of frequency- and phase-encoding gradients. The corresponding direction of application of these gradients is known as the frequency encode or phase encode direction. With modifications of the phase encoding gradients flowing blood can be differentiated from stationary anatomy via alterations in the phase of the MR signal. The velocity of material is proportional to the phase change or phase shift caused by its movement during gradient application.

Transmission and reception of RF energy is via special aerials known as coils with subsequent conversion of these raw data into images using ultrafast computers and a process known as Fourier transformation.

1.3.3 Main sequences in CMR

There are two fundamental types of sequence commonly used in CMR: *gradient echo* (GE) and *spin echo* (SE). As a general rule, with GE sequences both blood and fat appear white and so this technique is also known as white blood imaging. By contrast, in SE sequences blood is usually black but fat is white, giving rise to the term black-blood imaging. SE sequences are more useful for anatomical imaging as opposed to the functional imaging performed with GE sequences. Variations in GE sequences are fast low-angle shot (FLASH), fast imaging with steady-state free precession (SSFP), and velocity mapping. GE imaging also forms the basis of the inversion recovery technique.

Cine imaging using SSFP (or cines) are obtained by rapid repetition of a variant of the basic GE sequence to obtain a series of cardiac images at progressively advancing points of the cardiac cycle which when put together form a cine loop. The weighting of SSFP sequences depends on the ratio of T2/T1, therefore most fluids and fat have a high signal and appear white. However, muscle and many other solid tissues have along value for T1 and a short value for T2. This means that their signal intensity is reduced to shades of grey.

Velocity mapping (or flow velocity mapping) techniques can determine the average velocity within a single imaging voxel, typically 1 x 1 x 10mm^3. The operator selects the required plane and sets a maximal encoding velocity (Venc). The Venc represents the practical upper limit of velocities that can be depicted unambiguously and should ideally be set to a numerical value just greater than the true velocity. Problems occur if it is set much higher or lower than this value – with the former leading to less sensitivity and the latter causing misrepresentation via the phenomenon of aliasing. Velocity mapping sequences are also used to calculate overall flow in a major vessel throughout the cardiac cycle.

1.3.4 Components of a modern CMR scanner

The scanner itself is comprised of a superconducting magnet (made of Niobium, low resistance wire) bathed within supercooled liquid Helium (circulating at around -250ºC). The smaller gradient magnet coils are housed on the inner circumference of the main magnet and the whole apparatus is enclosed within a copper lined room designed to deflect commercial radio waves that might interfere with its operation. Copper lined channels in one wall of this box allow transmission of tubing from infusion pumps in the control room and the delivery of drugs or oxygen to the patient during scanning. The floor beneath the MR scanner must be reinforced to accommodate the weight of the main electromagnet.

The MR signal is received by a phased array chest coil. This is a dedicated receiver coil that lies on top of the chest. It contains several component coils, the arrangement of which is designed to maximise MR signal strength but minimise interference from tissue movement and system noise (i.e. optimise the signal to noise ratio). ECG-gating is used to synchronise imaging cycles with the motion of the heart. The R wave of a 3-lead ECG, recorded continuously, is used to trigger the excitatory RF pulse. Gradient echo sequences, which have a short TR, can be used to generate video-quality cine loops. This capability has revolutionised cardiac imaging as end-diastolic and end-systolic phases can be defined on the resulting cine images and end-diastolic and end-systolic volumes can be accurately measured. Individual lines of K-space (representing individual phase encoding steps) are filled during consecutive heart beats; therefore each cine loop takes at least 5 cardiac cycles to complete, depending on the sequence being used. To minimise motion artefact on the resulting images, patients are asked to hold their breath in expiration during most gradient echo sequences. In longer pulse sequences this is not possible and the patient must be allowed to breath freely, but they are asked to do so as smoothly as possible.

Once the predetermined K-space volume has been filled, the digital data is fed into a ‘Reconstructor’ computer which performs Fourier Transform Image Reconstruction and generates pixelated grey-scale data that is presented to the user on a flat screen monitor as a completed MR image. During any MR examination the user can alter the operation of the gradient coils and select a

variety of pulse sequences using a modified keyboard and mouse. Individual parameters within these sequences e.g. TR, TE, flip angle, can be modified as the operator desires. Images can be saved to an internal database and to external compact disc drives. The same PC workstation can be used for image analysis using the necessary software.

1.3.5 Limitations of CMR

CMR is expensive, not widely available and requires significant operator expertise. It can be a difficult examination for PH patients to complete due to time duration and breath holding requirements. Claustrophobia is a significant problem. This can be overcome in the majority of patients by using mild sedation, although this is often inappropriate in PH patients. Ferromagnetic objects must not enter the MR scanner area because they will become projectiles. This is an extremely important safety issue. Common practice is to specifically check and verify that each medical device present in patients is MR compatible. The radiofrequency field, which is used for excitation, can induce heating of tissue and implanted devices. It is possible to stimulate sensitive tissues such as peripheral nerves owing to the rapidly changing gradient magnetic fields used to generate images. Myocardial stimulation has not been described with current hardware.

1.3.6 Ventricular Morphology and Function by CMR

CMRI is regarded as the “gold standard” for quantifying ventricular volume, mass, structure and function. Impressive results for accuracy have been demonstrated by several investigators in various disease states (49-53). The interstudy reproducibility of CMR-derived parameters of ventricular function and mass is good for both the left and right ventricle and is superior to two-dimensional and M mode echocardiography (54-56). The results from a study performed by Grothues *et al* demonstrate that the interstudy reproducibility of the RV is lower than for the LV, although CMR is still a reliable method and can be considered the gold standard for serial assessment of RV volumes, function and mass (57).

MRI produces tomographic still images that can accurately and reproducibly assess left ventricular and right ventricular chamber sizes, wall thickness and mass. The multifaceted nature of MRI enables it to be used not only for morphological assessment, but also for functional assessment. Conventional gradient-recalled echo or steady-state-free-precession pulse (SSFP) sequences can be used to construct a cine image, which is a movie of 15-20 frames in which the full cardiac cycle can be seen; each movie frame represents approximately 30-40ms of the cycle. Recent technological advances enable the implementation of SSFP sequences which provide a substantially higher signal-to-noise ratio than can be obtained by conventional gradient-echo techniques. The contrast between myocardium and cavity blood (58) make planimetry of the interface accurate and easily reproducible for assessment of left and right ventricular function. The SSFP technique is the preferred cardiac CMR pulse sequence for acquisition of volumetric data sets of the left and right ventricle. Cine mode MRI allows regional and global systolic function to be evaluated because wall motion abnormalities can be identified. Ventricular volumes, ejection fraction, and myocardial mass are usually obtained from a stack of contiguous “bright blood” cine CMR 5-10mm slices covering the LV and RV acquired in short axis or transverse orientation. Endocardial and epicardial contours are drawn during post processing on end-diastolic and end-systolic frames, and LV and RV volumes are calculated as the sum of individual slice volumes. Ventricular mass is the product of myocardial volume and muscle specific density (1.05g/cm^3). A previous criticism of this technique has been the time required to analyse the cine data to generate accurate volume and mass data. New PC-based software solutions with intensity based thresholding for semiautomated myocardial-blood border definition has enabled analysis to become less time consuming.

Figure 1-4: Planimetry of the right ventricle.

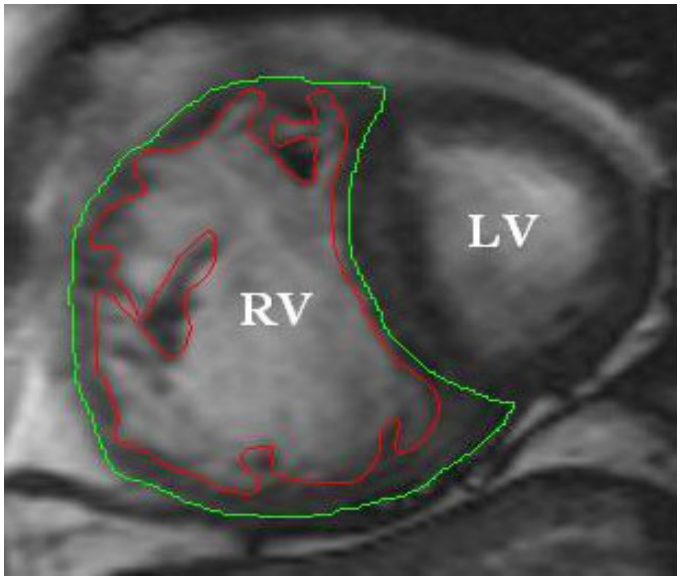

Epicardial and endocardial borders of the right ventricular myocardium are manually traced at end-diastole on this short axis CMR image. This scan is taken from a patient with idiopathic pulmonary hypertension. Right ventricular dilatation, hypertrophy and increased trabeculation are evident. (RV = right ventricle; LV = left ventricle).

1.3.7 Flow Analysis

Phase contrast velocity mapping is an MR sequence used to measure velocity and flow in blood vessels, or within the heart, in which each pixel in the image displays the signal phase, which is encoded. Volumetric flow (ml/sec) is obtained in each time frame by multiplying the spatial mean velocity (cm/sec) of blood flow with the cross sectional area of the vessel (cm^2). Integrating the volumetric flow curve over systole gives the stroke volume (SV). This imaging technique has been available for over 20 years (59). Velocity encoded imaging has been shown to be a reliable method to measure blood flow in different vessels of the body. Analogous to Doppler echocardiography, this technique allows the calculation of stroke volume, cardiac output, ejection fraction, valvular regurgitant fractions, and quantification of cardiac shunts, while mitral and tricuspid transvalvular flow profiles allow the assessment of ventricular diastolic filling patterns (E and A waves). Cardiac output and the pulmonary-to-systemic flow ratio (Qp:Qs) measured with the use of this technique have been shown to be accurate (60, 61). SV calculated from flow measurements in the pulmonary artery corresponds well with volumetric measurements of the RV in healthy subjects. Phase contrast

MR flow is less accurate in patients with either cardiac arrhythmia during acquisition or turbulent blood flow; the presence of these is a general limitation of this technique. Of note, even when appropriate methods of acquisition have been used, there can be inaccuracies of flow measurement on some CMR systems caused by background phase errors due to eddy currents or uncorrected concomitant gradients.

1.3.8 Contrast Enhanced CMR imaging

Gadolinium is a contrast agent utilised in MR scanning. It has seven unpaired electrons in its outer shell, and it hastens T1 relaxation, thereby increasing signal in the area of interest. Gadolinium alone is cytotoxic, but not if chelated with diethylenetriamine pentaacetic acid (DTPA). It has similar pharmacokinetic properties to iodinated X-ray contrast but with minimal nephrotoxicity and anaphylaxis risk. Attention has been drawn, however, to recent reports identifying a possible link between exposure to gadolinium-containing agents used in patients with end-stage renal disease and a rare, potentially life threatening condition referred to as nephrogenic systemic fibrosis (NSF). Regulatory authorities advise caution in the administration of gadolinium-containing agents in renally impaired patients.

In addition to evaluating the first-pass transit of gadolinium contrast, images can be obtained 10-15 minutes later, in a pseudoequilibrium phase. Gadolinium is avidly retained in abnormal myocardial regions resulting in a shortened T1 and increased signal intensity. The bright areas on the resulting images are described as areas of delayed contrast enhancement (DCE). DCE is not biologically specific and has been described in a variety of illnesses. Myocardial infarction, fibrosis and inflammation have all been shown to result in DCE using gadolinium as an intravenous contrast agent (62-66).

1.3.9 MR Pulmonary Circulation

Several methods have been proposed for MRI imaging of the pulmonary vasculature, both with and without the use of gadolinium. 3D gadolinium-enhanced magnetic resonance angiography is now the most commonly applied. Contrast-enhanced MR angiography utilises 3D ultrafast imaging sequences (T1

weighted) after intravenous injection of gadolinium and uses the first pass of this contrast agent (67). Limitations of MR angiography include a lower spatial resolution and longer breath hold when compared to CT.

Preliminary protocols are being developed to image lung perfusion into the diseased lung. These will allow for quantitative analysis of lung perfusion. This technique may allow for perfusion/functional assessment pre and post disease targeted therapy.

1.4 CMR Assessment of Pulmonary Hypertension

It is recognised that the response of the RV in PH is the most important determinant of patient outcome. A range of haemodynamic, structural and functional measures associated with the RV have prognostic importance in PH and, therefore, have potential value as measurements for the evaluation and follow up of patients. If these measures are to be used clinically, we require simple, reproducible, accurate, easy to use, and non-invasive methods to assess them. CMRI is regarded as the “gold standard” method for assessment of the RV. CMR is only reliable when adequately standardised. Measurement accuracy depends on optimisation of image acquisition and consistency in postprocessing. Imaging acquisition can be influenced by inconsistent breath-holding and different scanning parameters. Postprocessing requires extensive manual contouring, which is operator dependent. Measurement variability is related to difficulties in defining the tricuspid and pulmonary valve planes and in identifying the endocardial border owing to the extensive trabeculations that characterise the right ventricle. Manual analysis offers better control over delineation than semi-automated analysis, reflected in improved interobserver reproducibility (68). However it is time consuming and requires end-systole to be predefined. This can be difficult in PH due to abnormal interventricular septal motion.

1.4.1 Ventricular Volumes

Right ventricular end-diastolic (RVEDV) and end-systolic volumes (RVESV) are significantly elevated in PH patients when compared to control subjects (49, 69-71). RV ejection fraction (EF) is impaired in PH compared to healthy subjects

(69, 70, 72). RVEF, calculated by measuring end-diastolic and end-systolic RV volume, is a prognostic indicator in PAH (73). RV stroke volume (SV) (69) and RVCO are significantly reduced in patients with PH compared to healthy control subjects (72). A CMR study of 64 patients with IPAH confirmed that a large RV volume and a low SV measured at baseline were strong independent predictors of mortality and treatment failure (73).

LVEDV, LVSV and LV peak filling rate were significantly smaller in patients with PH compared to healthy controls (69). A reduced LVEDV at baseline predicts a poor outcome (73). A CMR study by Noordegraaf *et al* compared patients with PH secondary to emphysema and healthy controls. A significantly reduced LV ejection fraction was demonstrated in the emphysematous patients although especially in those without RV hypertrophy (72). Decreased LV volumes can be explained by the increased PVR, which limits RV SV and therefore the volume available for LV filling. LV septal bowing further reduces the LV volume in early diastole, thus limiting the LV filling process during the most important phase of rapid filling. Gan and colleagues investigated the contribution of direct right to left ventricular interaction to LV filling and SV in PAH patients and controls using CMR (74). They confirmed a close relationship between LVEDV and SV and concluded that ventricular interaction mediated by the IVS impairs LV filling, contributing to a decreased SV.

1.4.2 Ventricular Mass

CMR has confirmed a significantly higher RV mass in PH patients compared with healthy volunteers. Right ventricular hypertrophy is a consequence of the increased pulmonary afterload (51). The left ventricular mass does not differ significantly from normal values in PH patients (51). A study by Saba *et al* including 26 patients who underwent CMR and echocardiography examination shortly after right heart catheterisation showed that a *ventricular mass index* > 0.6 (obtained by dividing RVM by LVM) had a sensitivity of 84% and specificity of 71% for detecting pulmonary hypertension of various aetiologies (75). The *VMI* was more accurate than echocardiography in diagnosing PH and demonstrated excellent correlation (r=0.81) with the mPAP determined during right heart catheterisation (75). This correlation was superior to that obtained from RVM alone. A recent, larger study by Roeleveld *et al,* however, showed a much

weaker correlation between the *VMI* and mPAP (r=0.56) although the *VMI* was found to be the best among five different CMR-based methods for the estimation of mPAP (76).

1.4.3 Interventricular Septal Configuration

Distortion of the normal shape of the interventricular septum (IVS) has been reported in situations of RV pressure and/or volume overload (77). Patients with PH show characteristic changes in the movement and shape of the IVS as a result of increased RV pressure. Cine CMRI demonstrates how the IVS flattens and bows during diastole and systole. This can be expressed quantitatively as curvature, and the degree of curvature has been shown to be related to systolic PAP (78). Severe left ventricular septal bowing (LVSB) is often considered to be associated with an unfavourable prognosis in PH (4).

Figure 1-5: Cardiac magnetic resonance short axis image from a patient with pulmonary hypertension.

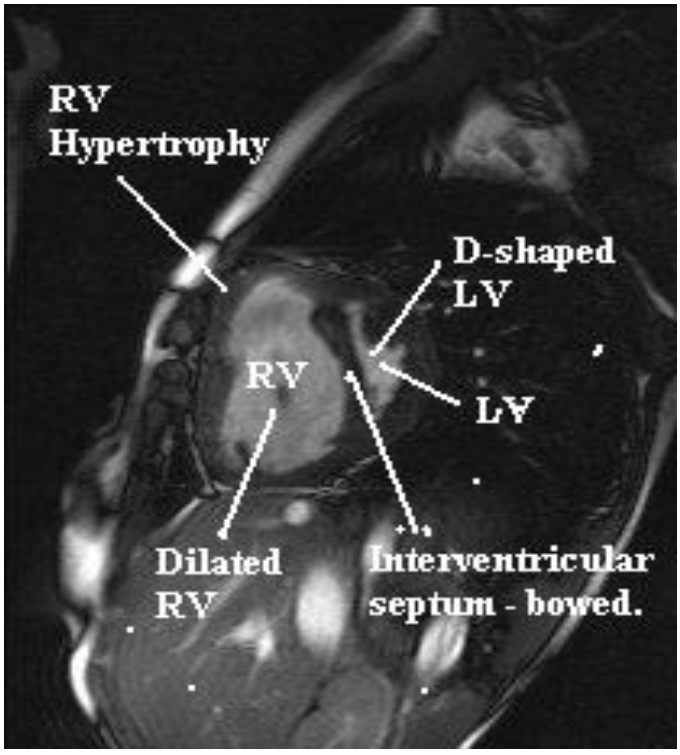

A short axis cine image at mid-ventricular level in early diastole. The CMR image was acquired from a patient with severe IPAH. The RV is grossly dilated and hypertrophied. The distorted IVS is bowed towards the LV (D-shaped) due to RV pressure overload.

1.4.4 RV Diastolic Function

Diastolic function has been shown to be abnormal in diseases affecting the LV and is often an early sign of ventricular dysfunction. It is targeted therapeutically. In PAH, a prolonged post-systolic isovolumetric time interval, between PV closure and TV opening is seen (79-82). Several reports have shown that this post-systolic isovolumetric period is related to disease severity (83) and was previously interpreted as a reflection of RV diastolic dysfunction (81, 84-87). Gan *et al* showed that this, determined by CMRI, can be a marker for RV dysfunction, correlating positively with ventricular mass and PVR (80). More recently the use of MRI-tagging techniques has shown that the underlying mechanism of increased post-systolic time is increased RV contraction rather than impaired relaxation time (88, 89). One consequence of this prolonged RV contraction time is leftward septal bowing impairing early LV diastolic filling (74). This, together with a low SV, might explain why LV end-diastolic volume (LVEDV) is such a good prognostic parameter in PAH; impaired LVEDV is an independent predictor of mortality, while a further decrease in LVEDV is among the strongest predictors of mortality in PAH. Other significant predictors include a decrease in SV and progression of RV dilatation (73, 90).

To simplify RV assessment, surrogate measurements are being developed. Recently, geometric shortening measured in the longitudinal or, more significantly, transversal plane using CMRI has been shown to have a stronger relation to RVEF than tricuspid annular plane systolic excursion (TAPSE) (91). A more recent publication by Mauritz and colleagues showed that geometric changes in the transversal plane are particularly important for monitoring the RV in end-stage disease (92).

1.4.5 Right Ventricular Contractility

Recent advances in MR scanner hardware and software have enabled CMR guidance of endovascular catheters under real time imaging (magnetic resonance fluoroscopy). This CMR approach is a promising tool for assessing RV contractility in the clinical setting (93). Interventional CMR allows RV pressure-volume loops to be created from which 3 key measures are extracted:1) Systolic function (Emax; end-systolic pressure divided by ESV) 2) Afterload (Ea; end-

systolic pressure divided by SV) and 3) Ventricular-arterial coupling (Emax/Ea). In patients with PAH, Kuehne and colleagues (93) found that while systolic function was increased, the increase in arterial elastance was relatively greater leading to ventricular-arterial decoupling. These findings have been echoed more recently in a larger cohort of patients with PH (albeit using different definitions of Emax and Ea) (94). CMR-guided RHC has been successful in assessing the changes in PVR after nitric oxide inhalation in patients with IPAH (95). Reduction or elimination of x-ray radiation, added anatomic and functional information available with MR, and the relative ease and accuracy of phase contrast MR flow quantification may make this technique an attractive method for invasive measurement of PVR. This is a single centre experience and major limitations are cost and availability of MR compatible equipment. This procedure is not suitable for serial follow up due to its invasive nature.

1.4.6 Contrast Enhanced Perfusion CMR

An interesting pattern of hyperenhancement within the RV is described with delayed contrast CMR in patients with PH. This delayed contrast enhancement pattern has a mid-wall distribution involving the RV septal insertion points and the IVS (96). A higher degree of enhancement was correlated with worse RV function and haemodynamics. When contrast enhancement was present in the IVS it was associated with septal bowing on cine-CMR. This data was confirmed by McCann and colleagues (66). This has led to speculation that it may reflect pathological fibrosis (96) and hence a source of ventricular arrhythmias (66). Proving its histological basis is difficult. Its position is inaccessible to in-vivo biopsy. Pathological correlation in a patient who had died 6 weeks after CMR (97) showed myocardial disarray and plexiform fibrosis at the insertion regions where LGE occurred. These histological features are normally found in the insertion regions since they represent crossing points for left and right ventricular fibres with collagen in between (98). Hence LGE may reflect pooling of gadolinium with an area of normal myocardium whose architecture has been accentuated by hypertrophy and mechanical stress.

Figure 1-6: Delayed contrast enhanced cardiac magnetic resonance images of a patient with pulmonary hypertension.

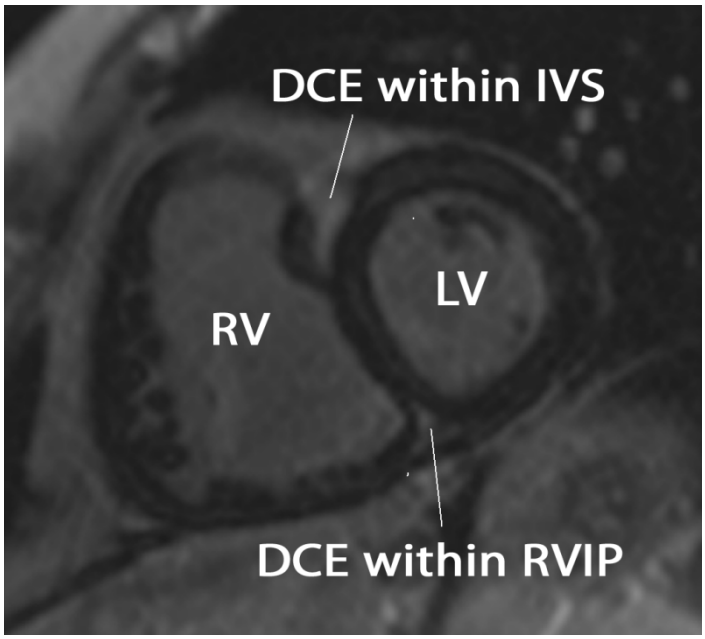

A contrast enhanced short axis cardiac MR cine image was acquired at a basal ventricular level. The delayed contrast enhancement pattern has a mid wall distribution involving the right ventricular insertion point (RVIP) and the IVS.

1.4.7 Stress CMR

Stress testing, by exercise or drug infusion, can be used to determine cardiac reserve. Physical exercise within the confines of the magnet is technically difficult and leads to image degradation. Holverda and colleagues, however, demonstrated that IPAH patients were unable to significantly increase SV from rest to exercise, using an MR compatible ergometer (99). Pharmacological CMR stress can be used in patients with congenital heart disease to detect early RV dysfunction. The physiological effects of exercise are imitated by a continuous infusion of a short acting agent such as dobutamine (a relatively selective beta-1-adrenoceptor agonist) (100). Dobutamine has a positive inotropic effect on RV contractility, which can be determined using MRI. During CMR, perfusion with adenosine stress in PH patients, biventricular vasoreactivity has been found to be diminished. The degree to which this occurs in both ventricles could be predicted from mPAP (101).

1.4.8 CMR flow measurements

Velocity encoded imaging is another CMR approach for the assessment of PH. In the setting of PH, the most important applications of flow analysis include measurement of cardiac output (CO) / stroke volume (SV) and pulmonary to systemic flow measurements in the estimation of right-to-left and left-to-right shunts. It has been suggested that measurement of SV/CO in PH patients should be made by aortic flow analysis during CMR imaging (102). The aorta is smaller, has more coherent flow patterns and less translational movement than the main pulmonary artery. RV SV can be calculated as the difference of end-diastolic and end-systolic RV volumes, or by the measurement of volumetric flow in the main pulmonary artery employing phase contrast velocity mapping. SV, calculated from flow measurements in the pulmonary artery, and from volumetric measurements of the RV correspond well in healthy controls, and show little divergence in patients with mild TR. However, with considerable tricuspid regurgitation (TR) (e.g. PH patients), the volumetric SV overestimates the actual SV (69) because it is impossible to differentiate between the volume that moves back through the tricuspid valve and forward though the pulmonary valve.

The analysis of these images enables us to describe changes or irregularities of pulmonary blood flow in PH. Previous studies using this technique have found highly inhomogeneous velocity profiles, a large volume of retrograde flow, and decreased distensibility of the main pulmonary artery in patients with PH (103, 104). From the quantitative analysis of the pulmonary flow profile, non-invasive indexes (e.g. acceleration time [defined as time from onset of flow to the peak velocity] and acceleration volume) have been derived for the assessment of pulmonary vascular resistance (105). Peak blood flow velocity in the main pulmonary artery (MPA) is lower in patients with PH and shows inverse correlation with mean PAP and PVR. When examined in patients with CTEPH, values after pulmonary endarterectomy were significantly higher than before surgical intervention, but did not reach normal range (106). A significant reduction of peak velocity in both right and left pulmonary arteries was observed in patients with PH secondary to cystic fibrosis (107). As the study revealed no change in the flow of the main pulmonary artery, it was concluded, that early and subtle changes of pulmonary haemodynamics are first noticeable in the periphery of the pulmonary arterial system. CMR could, therefore, be the

method of choice for detection of early haemodynamic change before RV function is altered.

CMR derived flow in the mPA has also been used to gauge haemodynamics e.g. pulmonary pressures were shown to be inversely correlated with average blood velocity in the mPA (108). In addition, total pulmonary resistance has been estimated by determining the percentage of regurgitant flow and cross sectional area of the MPA (104), or calculating the ratio of the maximal change in flow rate during ejection to the acceleration volume (105). Finally, the use of four dimensional flow (109) has built on early work in two dimensional flow (110), to show that in patients with PH, a vortex can be detected in the primary flow direction whose duration correlates well with mPAP.

1.4.9 Distensibility of Pulmonary Artery

Pulmonary artery distensibility measured by CMR was found to be significantly lower (8%) in PH patients than it was in normal subjects (23%) (103). A pilot study performed by Jardim and colleagues (111) indicated that the non-invasive assessment of pulmonary artery distensibility by MR reflected the acute response pattern in IPAH patients. Pulmonary artery distensibility was significantly higher in responders to an acute vasodilator test during invasive haemodynamic evaluation. Gan and colleagues (112) have recently demonstrated that proximal pulmonary artery stiffness (in terms of area distensibility and noninvasively assessed relative area change [RAC] by CMR) predicted mortality in patients with PH. It has been shown that a fractional change in the cross-sectional area of the mPA of less than 40% has a high sensitivity for detecting elevated mPAP (113). Additionally, compliance has been calculated by combining velocity-encoded data and cross-sectional area change of the mPA and deriving pulse pressure through an iterative process (114). From this, pulse wave velocity (PWV – a measure of vessel stiffness) was derived which had a reliability percentage of 87% for framing the actual mPAP. PWV can be calculated directly using the transit time technique by determining flow wave arrival time at two points in the proximal PAs using a high-temporal resolution flow mapping sequence and dividing the difference between them (115). This calculation does not depend on a prior knowledge of PA pressure and raises the possibility of entirely non-invasive assessment of PA stiffness.

1.4.10 CMR Pulmonary Angiography

The typical findings of CTEPH (intraluminal webs and bands, vessel cut-offs, and organised thrombus) are well demonstrated by pulmonary MRA and can be seen in vessels to segmental level. Beyond the segmental level, the higher spatial resolution of conventional angiography makes it superior. Surgical intervention is largely limited to proximal and segmental vessels, and in a study by Kreitner and colleagues (106), ceMRA correctly predicted surgical success in 33 out of 34 patients. The study demonstrated that 3D contrast enhanced MRA performed equally as well as X-ray pulmonary angiography for the visualisation of segmental pulmonary vessels, was slightly worse for subsegmental vessels but was superior for the depiction of the central origin of thromboembolic material. Pulmonary MRA may be combined in the same examination with a variety of cine techniques to gauge cardiac function and flow. Contrast enhanced MRA should identify patients with CTEPH that delineate typical findings and are potential candidates for surgery.

1.4.11 CMR Pulmonary Perfusion Imaging

Ohno and colleagues have demonstrated that 3D dynamic contrast-enhanced MRI has the potential for assessment of disease severity in PH patients (116). This technique showed significant differences in pulmonary blood flow and mean transit time between healthy and PH subjects.

1.4.12 Pulmonary Artery Pressure Estimation by CMR

Repeated measurements of pulmonary artery pressure (PAP) are sometimes used to assess disease progression in PH. Echocardiography (117) is safe and widely available, but has limitations as previously discussed. MRI has been proposed as an accurate alternative for echocardiography in estimating PAP. Investigators have attempted to use CMR as a non-invasive means of estimating mean PAP but none have reported any advantages over echocardiography. Several estimators based on different MRI techniques have been described in recent years including acceleration time (AT: the time of onset of forward flow to the moment of maximum flow velocity in the MPA), AT/ejection time (ET) ratio, pulse wave

velocity, cross-sectional area of MPA and ventricular mass index. RV end-diastolic wall thickness has been shown to correlate well with mean PAP in IPAH and some cases of secondary PH (118, 119). A linear relationship between RVM and mean PAP has been described for IPAH (51). The ratio of the MPA diameter over descending aortic diameter has also been shown to correlate with mean PAP in PH. A computed method for the non-invasive MR assessment of PH has been elaborated (120, 121), where a combination of physical parameters including mPA blood flow velocity at peak systole, maximal systolic mPA cross sectional area and biophysical parameters including patient height, weight and heart rate were used to estimate pulmonary artery pressure The *ventricular mass index* was found to be the best among five different CMR-based methods for the estimation of PAP and similar to echocardiography (r=0.55 using the modified Bernoulli equation and peak tricuspid regurgitation velocity), but not accurate enough to replace RHC in clinical practice (76). Based on recent results, the degree of septal displacement may be a more promising measure (78).

1.4.13 NMR Spectroscopy

Despite its potential, nuclear magnetic resonance (NMR) spectroscopy remains relatively unexplored in PH. An isolated case report using 31P-NMR spectroscopy offers a unique insight into the failing RV by showing how RV energetics are disturbed in PAH but improve with bosentan treatment (122).

1.4.14 Summary of CMR

CMR imaging has a number of advantages over other techniques (123, 124). It is non-invasive, employs nontoxic contrast agents and does not use ionizing radiation. CMR imaging provides high resolution, 3-dimensional images that avoid the need for geometric assumptions that are required for some calculations in echocardiography. Images can be obtained from every plane, allowing accurate volume measurement. Cardiac gating can permit the acquisition of scans in a single brief breath hold, which limits respiratory motion artifacts. CMR imaging can show soft tissue and is able to identify early changes in cardiac structure and function. But CMR imaging is less suitable for dynamic measurements than echo because temporal resolution is more limited. It is less widely available,

incompatibility with ferrous objects and long scan times limit its usefulness in some patients. Despite these limitations, given the relevance of the RV in PAH, CMR imaging is likely to increase in importance as the optimal method for assessment of structural and functional parameters in the evaluation of patients where PAH is established.

1.5 Inert gas rebreathing

The functional consequence of a raised pulmonary vascular resistance is a decrease in exercise capacity and a low cardiac output. In patients with PH, the CO is directly related to the clinical severity of the disease and is one of the most important prognostic factors. The evaluation of treatment efficacy in PH would benefit from non-invasive tools to monitor haemodynamic changes.

Inert gas rebreathing is a physiological technique, which measures pulmonary blood flow (PBF), which is equivalent to CO in the absence of intracardiac and intrapulmonary shunts (125). Inert gas rebreathing is an old technique which was introduced by August Krogh in 1912 and has been widely validated (126-129). Acetylene rebreathing method using a mass spectrometer has been shown to provide an accurate estimate of CO compared with TD and the Fick method in PH patients.

The IGR method measures PBF during rebreathing of an oxygen enriched mixture of blood soluble and blood insoluble gases. As inert gases are non-physiological, their serum concentration in systemic venous blood can be assumed to be zero. As the subject re-breathes through a respiratory apparatus from a bag prefilled with the gas mixture for about 30 seconds, the blood soluble gas dissolves rapidly in the pulmonary capillary blood, and its rate of disappearance from the alveoli is proportional to the effective PBF. The blood-insoluble gas is not taken up in the pulmonary capillary blood, and remains in the alveoli to correct for changes in total alveolar volume during the rebreathing manoeuvre. Cardiac output is equivalent to PBF in the absence of significant intrapulmonary or intracardiac shunts.

Inert gas rebreathing, with continuous analysis of ventilatory gas concentrations, is an easy, safe and well-established method for non-invasive measurements of

effective PBF or CO. However, IGR measurements have traditionally required the use of mass spectrometers, which are bulky, difficult to operate and need frequent calibration and maintenance. These factors have significantly limited the clinical application of measurements of PBF/CO by the inert gas rebreathing technique.

More recently, a metabolic system (Innocor, Innovision, Odense, Denmark), using rebreathing of nitrous oxide (N_2O) and sulphur hexafluoride (SF_6), has been introduced. This device (Innocor®), which is employed in this thesis, uses rapid photoacoustic analysis of gas concentrations. It was validated against the direct Fick and thermodilution methods in a cohort of patients with stable heart failure (130) and in patients pre and post cardiac surgery (131). Compared with conventional mass spectrometers, this analyser is more portable and easier to maintain, which markedly facilitates clinical use. Please refer to the materials and methods section of this thesis for physiological principles and operational detail.

1.6 Evaluation of Pulmonary Hypertension

The evaluation process of a patient with suspected PH requires a series of investigations intended to:

i. confirm the diagnosis
ii. clarify the clinical group of PH and the specific aetiology within the PAH group
iii. evaluate the functional and haemodynamic impairment
iv. consider the prognosis

An accurate diagnostic assessment is imperative for the appropriate management of the patient with a new diagnosis of PH.

1. Clinical evaluation

Precise history taking and physical examination are essential. Although the symptoms PH are nonspecific, the New York Heart Association (NYHA) functional classification for heart failure has been adapted for PH as the WHO functional class. It is a four point scale to rate the impact of breathlessness and fatigue

according to daily activity. Despite large interobserver variation in the measurement, WHO functional class remains a powerful predictor of survival. In untreated patients with IPAH or heritable PAH, historical data showed a median survival of 6 months for WHO-FC IV, 2.5 years for WHO-FC III, and 6 years for WHO-FC I and II (4). It can be confounded by comorbidities e.g. obesity, and by coexisting/underlying diseases e.g. patients with systemic sclerosis associated PAH may have their symptoms and exercise capacity limited by musculoskeletal factors (132). Extremes of age (<14 years or >65 years), falling exercise capacity, syncope, haemoptysis, and signs of RV failure also carry a poor prognosis in IPAH.

2. Electrocardiogram (ECG)

The ECG may provide suggestive or supportive evidence of PH by demonstrating RV hypertrophy and strain, and right atrial dilatation.

3. Chest radiograph (CXR)

In 90% of patients with IPAH the chest radiograph is abnormal at the time of diagnosis (25). Findings include central pulmonary arterial dilatation, which contrasts with 'pruning' (loss) of the peripheral blood vessels. Right atrium and RV enlargement may be seen in more advanced cases although the degree of PH does not correlate with the extent of radiographic abnormalities. The CXR allows associated moderate-to-severe lung diseases or pulmonary venous hypertension due to left heart disease to be reasonably excluded.

4. Blood tests and immunology

Routine biochemistry, haematology, and thyroid function tests are required. Serological testing is important to detect underlying CTD, HIV, and hepatitis. Thrombophilia screening should be performed in CTEPH.

5. Biomarkers

- Serum uric acid is a marker of impaired oxidative metabolism of ischaemic peripheral tissue and high levels are found to relate to poor survival in patients with IPAH (133).
- Brain natriuretic peptide (BNP) induces vasodilatation and natriuresis and is released from the myocardium in response to wall stress. The final step

of BNP synthesis consists of a high molecular weight precursor, proBNP cleaved into biologically inactive N-terminal segment (NT-proBNP) and the proper low molecular weight BNP. NT-proBNP has a longer half-life and a better stability both in circulating blood and after sampling. RV failure is the main cause of death in PAH, and BNP/NT-proBNP levels reflect the severity of RV dysfunction. Nagaya *et al*. (134) showed that the baseline median value of BNP (150 pg/mL) distinguished patients with a good or bad prognosis. In a trial involving 68 patients with PAH associated with scleroderma, NT-proBNP below a median of 553 pg/mL was related to better 6-month and 1-year survival (135). Using receiver operating characteristic (ROC) analysis, an NT-proBNP cut-off point at 1400 pg/mL was predictive of a 3-year outcome in 55 patients with severe precapillary PH (136). Serum NT-proBNP below 1400 pg/mL seemed particularly useful for identification of patients with good prognosis, who would not need escalation of treatment in the immediate future, and this has been independently confirmed (137). Larger outcome trials are still required to verify the suggested cut-off levels for NT-proBNP.

- Elevated plasma levels of cardiac troponin T and troponin I are established specific markers of myocardial damage and are prognostic indicators in acute coronary syndromes and acute pulmonary embolism. Elevated cardiac troponin T was an independent predictor of fatal outcome during 2-year follow-up in a single trial on 51 patients with PAH and five with CTEPH (138).

6. Pulmonary function tests (PFTs) and arterial blood gases (ABGs)

PFTs and ABGs will identify the contribution of underlying airway or parenchymal lung disease. Patients with PAH usually have decreased lung diffusion capacity for carbon monoxide (DLCO) and mild to moderate reduction of lung volumes. Arterial oxygen tension is normal or only slightly lower than normal at rest and arterial carbon dioxide tension is decreased because of alveolar hyperventilation.

7. Exercise testing

For objective assessment of exercise capacity, the 6-minute walk test (6MWT) and cardiopulmonary exercise (CPET) testing are commonly used in patients with PAH.

- The 6MWT is a submaximal exercise test, which can be performed by patients who are incapable of tolerating maximal exercise testing. The 6MWT is technically simple, inexpensive, reproducible, and well standardized (139). Distance walked, dyspnoea on exertion (Borg scale) and finger O_2 saturation are recorded. The 6MWT correlates fairly well with peak aerobic capacity (140) and has prognostic significance in PAH (141).

- CPET measures metabolic gas exchange at rest and during exercise. It quantitates aerobic capacity and ventilatory inefficiency in order to determine the severity of PAH (142) and might provide a more sensitive exercise assessment than 6MWT early in the course of the disease (143). In PAH, O_2 uptake at the anaerobic threshold and peak exercise are reduced in relation to disease severity, as are peak work rate, peak heart rate, O_2 pulse, and ventilatory efficiency (144). Following multivariate analysis of clinical, haemodynamic, and exercise parameters peak O_2 uptake (<10.4 ml O_2/kg/min) and peak systolic arterial pressure during exercise (<120 mmHg) independently predicted a worse prognosis in IPAH patients (145).

8. Echocardiography

Transthoracic echocardiography (TTE) provides several measurements which correlate with right heart haemodynamics including pulmonary artery pressure (PAP). The estimation of PAP is based on the peak velocity of the tricuspid regurgitation (TR) jet. Other TTE measurements suggestive of PH include increased velocity of pulmonary valve regurgitation and a short acceleration time of RV ejection into the PA. Increased dimensions of right heart chambers, abnormal shape and function of the interventricular septum, increased RV wall thickness, and dilated main PA are suggestive of PH, but tend to occur later in

the course of the disease. Echocardiography can be helpful in detecting the cause of suspected or confirmed PH e.g. identification of congenital heart disease (CHD).

Echocardiography generates many indices, and those with the best prognostic value identified by multivariate analysis are pericardial effusion (6, 90), indexed right atrium area, LV eccentricity index (90) and the RV Doppler index (83, 146). Estimated systolic PAP derived from TR jet velocity is not prognostic (90). Normal RV function is highly dependent on longitudinal shortening and this can be assessed by placing an M-mode cursor on the tricuspid valve annulus in the 2D four-chamber view to measure the annular displacement in the longitudinal direction. A normal tricuspid annular plane systolic excursion (TAPSE) should be higher than 1.5cm in adults. The TAPSE has been reported to be of prognostic value in patients with PH (147).

Although there is substantial interest in exercise stress echocardiography, particularly in early disease, this study is difficult to perform and interpret. Similarly, although 3-D echo might improve our understanding of the pathophysiology of RV failure in PAH, it has been minimally evaluated in PAH.

9. Ventilation/perfusion (V/Q) scan

The V/Q scan should be performed in patients with suspected PH to look for potentially treatable CTEPH. This is the screening method of choice for CTEPH because of its higher sensitivity than CT (148). A normal or low probability V/Q scan effectively excludes CTEPH with a sensitivity of 90–100% and a specificity of 94–100%. While in PAH the V/Q scan may be normal, it may also show small peripheral unmatched and non-segmental defects in perfusion. Contrast-enhanced CT may be used as a complementary investigation but does not replace the V/Q scan or traditional pulmonary angiogram.

10. High-resolution computed tomography (HRCT) and CT pulmonary angiography (CTPA)

HRCT provides detailed views of the lung parenchyma and facilitates the diagnosis of interstitial lung disease and emphysema. HRCT may be very helpful where there is a clinical suspicion of PVOD or PCH. CTPA is helpful in

determining whether there is evidence of surgically accessible CTEPH. It can delineate the typical angiographic findings in CTEPH such as complete obstruction, bands and webs, and intimal irregularities as accurately and reliably as digital subtraction angiography (149, 150).

11. Cardiac magnetic resonance (CMR) imaging

CMR is increasingly used in patients with PH for the evaluation of pathological and functional changes in the heart and pulmonary circulation. It provides a direct evaluation of right ventricular size, mass, morphology and function (151). Normal ranges of cardiac measurements have been established (51, 104). CMR findings in PH include RV dilatation, tricuspid regurgitation, RV hypertrophy, interventricular septal flattening or paradoxical motion, and change in chamber morphology from a normal crescent shape to a more concentric form. Non-invasive assessments of blood flow, including stroke volume and cardiac output, and distensibility in the pulmonary arteries can be made (152-154). There is good correlation between RHC and MR suggesting that MR data could be used as a surrogate of right heart haemodynamics (153). CMR has also been used to determine which patients with IPAH might benefit from long term CCBs by assessing mPA distensibility (155). Baseline CMR measurements in PAH associated with a poor prognosis include a decreased stroke volume, an increased RV end-diastolic volume, and a decreased LV end-diastolic volume (73). More recently, RVEF has been confirmed to be a prognostic marker in PAH (156). CMR parameters of PA stiffness are also relevant to prognosis (112).

12. Abdominal ultrasound scan

Liver cirrhosis and/or portal hypertension can be reliably excluded by the use of abdominal ultrasound.

13. Right heart catheterisation, vasoreactivity and pulmonary angiography

RHC is required to confirm the diagnosis of PH, to assess the severity of the haemodynamic impairment, and to test the vasoreactivity of the pulmonary circulation. When performed at experienced centres, RHC procedures have low morbidity (1.1%) and mortality (0.055%) rates (21). The following measurements must be recorded during RHC: PAP (systolic, diastolic, and mean), right atrial pressure, PWP, and RV pressure. CO must be measured in triplicate preferably

by thermodilution or by the Fick method. Superior vena cava, PA, and systemic arterial blood oxygen saturations should also be determined. Adequate recording of PWP is required for the differential diagnosis of PH due to left heart disease. Left heart catheterisation may be required for direct assessment of LV end-diastolic pressure. Coronary angiography may be required in the case of the presence of risk factors for coronary artery diseases and angina or in case of listing for double lung transplantation or pulmonary thromboendarterectomy (PEA) in patients with CTEPH.

In PAH, vasoreactivity testing should be performed at the time of diagnostic RHC to identify patients who may benefit from long-term therapy with calcium channel blockers (CCBs) (29, 30). Currently the agent most used in acute testing is nitric oxide (NO). A positive acute response (positive acute responder) is defined as a reduction of mean PAP ≥ 10 mmHg to reach an absolute value of mean PAP ≤ 40 mmHg with an increased or unchanged CO (29). Only approximately 10% of patients with IPAH will meet these criteria.

Traditional pulmonary angiography is still required in many centres for the work-up of CTEPH to identify patients who may benefit from PEA (22). Angiography can be performed safely by experienced staff in patients with severe PH using modern contrast media and selective injections. Angiography may also be useful in the evaluation of possible vasculitis or pulmonary arteriovenous malformations.

Resting haemodynamics measured at RHC predict prognosis (4). These include PA O_2 saturation, RAP, CO, PVR, and a marked vasoreactivity response. PAP is also prognostic but less reliable as it may fall towards the end stage of the disease as the RV fails. Some studies suggest that reduced arterial O_2 saturation, low systolic blood pressure, and increased heart rate carry a worse prognosis (145).

The clinical assessment of the patient has a pivotal role in the choice of initial treatment, the evaluation of the response to therapy, and the possible escalation of therapy.

1.7 Follow up assessment of PH patients

Treatments for PH are always expensive, sometimes invasive and carry significant side effects. In order to convince patients, treating physicians, funding agencies and regulatory bodies of the value of treatments it is, therefore, extremely important to be able to assess patients response to therapy with investigations of appropriate quality. It is essential that we can assess the progress of patients in a non-invasive manner. The importance of having clinically meaningful methods to assess the patient's response to treatment must be reinforced.

It has been suggested that characteristics for an ideal assessment tool / marker in PH might include (157).

i. it should be heart or lung specific
ii. it should be abnormal in PH
iii. sample collection should be simple
iv. the marker should be easy to measure
v. values should be reproducible
vi. values should follow the course of the disease (i.e. increasing if patients deteriorate and falling if patients improve)
vii. abnormal values should be indicative of a poor survival.

The current aim is for an early diagnosis of PAH followed by treatment with first-line monotherapy (26, 158). The importance of escalating therapy if a patient does not respond to initial treatment has been emphasised in the recently published clinical guidelines. Regular evaluation of patients enables early identification of an inadequate response to treatment and should focus on measurements with established prognostic significance. Both clinical and haemodynamic assessments provide prognostic information which guides clinical management. Prognosis is significantly affected by the aetiology of PH (159).

According to the guidelines, published jointly by the ESC and ERS, the clinical condition of a patient can be defined as stable and satisfactory, stable but not satisfactory, or unstable and deteriorating. The goal of therapy is to bring the patient into the stable and satisfactory group (160). Please refer to table 1.2.

Table 1-2: Definition of patient status as guided by the European Society of Cardiology / European Respiratory Society guidelines.

Definition of patient status (ESC/ERS Guidelines)	
Stable and satisfactory	Patients meet the criteria listed in the "green zone" of the table 1.3. The most important features are absence of clinical signs of RV failure, stable WHO functional class I or II, absence of syncope, a 6MWT distance > 400 to 500m depending on the individual patient, a peak oxygen uptake of > 15mL/min/kg, normal or near normal BNP/NT-pro-BNP levels, no pericardial effusion, TAPSE > 2.0cm, and RAP < 8mmHg and a CI > 2.5L/min/m^2.
Stable but not satisfactory	Patients are not deteriorating but have not achieved the status that the patient and treating physician would consider desirable. Some of the limits described above for a stable and satisfactory condition and included in the green zone in table 1.3 are not fulfilled. Re-evaluation and consideration for additional or different treatment is required.
Unstable and deteriorating	Some or all of the criteria listed in the "red zone" of table 1.3. Patients present with RV failure, progression of symptoms and signs, worsening of functional class, a 6MWT distance < 300m to 400m, a peak oxygen uptake < 12mL/min/kg, rising BNP/NT-pro-BNP plasma levels, evidence of a pericardial effusion, TAPSE < 1.5cm, a RAP > 15mmHg and rising, and a CI < 2.0L/min/m^2. Clinical warning signs are increasing oedema and escalation of diuretic therapy, new onset, or increasing frequency of angina. The presence of syncope requires immediate attention as it is a common manifestation of a low cardiac output.

Table adapted from ESC/ERS guidelines.

Table 1-3: Current measurements with established importance for assessing disease severity, stability and prognosis in pulmonary arterial hypertension.

Better prognosis	Determinants of prognosis	Worse prognosis
No	Clinical evidence of RV failure	Yes
Slow	Rate of progression of symptoms	Rapid
No	Syncope	Yes
I, II	WHO-FC	IV
Longer (>500 m)[a]	6MWT	Shorter (<300 m)
Peak O_2 consumption >15 mL/min/kg	Cardio-pulmonary exercise testing	Peak O_2 consumption <12 mL/min/kg
Normal or near-normal	BNP/NT-proBNP plasma levels	Very elevated and rising
No pericardial effusion TAPSE[b] >2.0 cm	Echocardiographic findings[b]	Pericardial effusion TAPSE[b] <1.5 cm
RAP <8 mmHg and CI ≥2.5 L/min/m^2	Haemodynamics	RAP >15 mmHg or CI ≤2.0 L/min/m^2

This table lists measurements of prognostic importance that are widely used as follow-up tools. Patients with better or worse prognosis are separated by an intermediate group for which prognostication is more difficult. Table adapted from McLaughlin *et al* (161).

Physicians currently rely on the WHO functional class, exercise testing (6MWT and CPET), biomarkers (Brain Natriuretic Peptide [BNP] levels), echocardiography and RHC to follow up patients with PH. These investigations have acknowledged limitations. The question of which end points are most relevant in the assessment of PH has been the topic of intense discussion at End Point Meetings. Many clinicians feel that the current end points used in clinical trials of PAH are not as relevant as they might be. This frustration has been articulated recently (162). What is clear, however, is that since the trials of currently licensed therapies mostly used combination of 6MWD, functional class, and haemodynamics, all new studies will likely require significant improvement in one or more of these variables before they will be approved. Any new end point would probably need to be tested alongside traditional end points and shown to be demonstrably better if it is to be considered a primary or first-level secondary end point in the future. The impact of a treatment on disease progression associated with PAH was be measured by time to clinical worsening (TTCW). This endpoint is viewed as clinically relevant by clinicians and regulatory agencies. This end point has been used in several clinical trials as a secondary, or a primary end point, in the recent past.

1.7.1 WHO Functional Class

The WHO functional class has been an important end point in clinical trials of PH, although the assignment of patients to categories is subject to the bias of investigators, which limits its usefulness as an end point.

1.7.2 Quality of life (QoL)

It has been suggested that QoL is an important method to measure the efficacy of drug therapy. Unfortunately, it has always been very difficult to objectify QoL measurements, and until recently, there had been no specific health-related QoL measures in PAH. Advantages of QoL include that it is easy, cheap and quick and it measures things of particular value to patients. Disadvantages of QoL as an assessment include until recently, tests were not specific to PAH. A specific test is now available – Cambridge Pulmonary Hypertension Outcome Review (CAMPHOR) (163) but not yet has proven efficacy, and must be adapted for different countries and languages.

1.7.3 Exercise Testing

Exercise capacity is one of the most important prognostic indicators in PAH (141, 164, 165). Several exercise protocols have been used in PAH including 6MWT, formal exercise testing (treadmill, cycle ergometry) and CPET. Of these, the 6MWT has been accepted by regulatory agencies and is the most commonly used primary end point in randomised controlled trials (166, 167). The 6MWT must be performed correctly using the appropriate guidelines (ATS Statement) (139).
With respect to treatment effects, absolute values >380 m following 3 months of i.v. epoprostenol correlated with improved survival in IPAH patients, while the increase from baseline did not (164).

Flaws have been highlighted in its performance. There are concerns (168) that the 6MWD is influenced by (but not corrected for) a number of factors other than PH including age, gender, height, weight, musculoskeletal conditioning and patient motivation. Furthermore, it has been shown that the 6MWD can improve considerably with rehabilitation measures alone (169). The test is not sufficiently validated in PAH subgroups (139). Within-subject variability has been

seen in the 6MWT, with repeat testing on the same day resulting in a 66-ft improvement in a study of patients with COPD (170), an 18m improvement on 2 successive days in post-MI patients (171), and a 4.2% change in patients with ILD after 1 week (172). In addition, the 6MWT may be less discerning in patients who are less ill (173). Drug effects on the 6MWT tend to be slow to manifest and modest (10-15%) and may not provide an accurate reflection on how the patient might feel.

Several questions, therefore, remain regarding the 6MWT.

1. What is a clinically relevant improvement in 6MWT?
2. How should variables that are known to affect the 6MWT, such as age and height, be factored into this endpoint/assessment?
3. Is the 6MWT still a sensitive exercise test as we study patients earlier in the course of the disease?

Despite detailed recommendations (174, 175), a generally accepted standardisation of cardiopulmonary exercise testing with respect to data acquisition and analysis in PAH is lacking. The CPET is expensive and has proven technically difficult to perform and interpret in the setting of a multicentre RCT. While the results of both the 6MWT and CPET do correlate in PAH, CPET exercise testing failed to confirm improvements observed with 6MWT in RCTs (166, 167). Although lack of standardisation and insufficient expertise in performing cardiopulmonary exercise testing were identified as the main reasons explaining this discrepancy (144, 176), the 6MWT remains until now the only Food and Drug Administration- and European Agency for the Evaluation of Medicinal Products-accepted exercise endpoint for studies evaluating treatment effects in PAH.

1.7.4 Echocardiography

Echocardiography is the most well established and accessible imaging technique for screening and diagnosis of PH (177). As an imaging modality, it has the advantage of being widely available, inexpensive and safe. Echocardiography is routinely used for assessing RV size and function and severity of PH. In one RCT (32), advanced PAH therapy improved many echo variables, including LV area, systolic eccentricity index, RV/LV diastolic area ratios, pericardial effusion score, RV ejection time, Doppler RV index, LVSV and CO, and parameters of LV

filling. Thus, this technique is sufficiently sensitive to clinical changes to be used as a reinforcing end point. Standardising of echo measurements (some of which are highly technical) would be necessary to consider this as an end point in clinical trials. Two indexes that might be considered are the Tei Index and TAPSE (147, 178).

Doppler echocardiography is suitable for serial assessments although has some limitations. This investigation relies upon geometric assumptions which can be difficult to adopt for the complex shaped RV. Limiting factors include operator dependence and influence by prevailing conditions such as heart rate and body habitus. Most studies report a high correlation (0.57-0.93) between echocardiography and right heart catheterisation (RHC) measurements of PASP (179) although Arcasoy and colleagues concluded that estimation of PASP by echocardiography is frequently inaccurate in patients with advanced lung disease (180).

1.7.5 Biomarkers

Biochemical markers are a non-invasive tool for assessment and monitoring of RV dysfunction in patients with PH. RV failure is the main cause of death in PAH, and BNP/NT-proBNP levels reflect the severity of RV dysfunction. Nagaya *et al*. (134) showed that the baseline median value of BNP (150 pg/mL) distinguished patients with a good or bad prognosis. In 49 out of 60 patients, BNP measurement was repeated after 3 months of targeted therapy and the supramedian level (>180 pg/mL) was related to worse long-term outcome. Plasma BNP significantly decreased in survivors but increased in non-survivors despite treatment. Larger outcome trials are still required to verify the suggested cut-off levels for NT-proBNP. Increases in NT-proBNP plasma levels on follow-up have been associated with worse prognosis (135). Several recent trials assessing new drugs in PAH or CTEPH reported a significant decrease in NT-proBNP in the actively treated vs. placebo patients.

Serial measurement of plasma NT-proBNP has great attractions as an end point. Its presence in the blood is related to RV dysfunction, the test is non-invasive, it is simple to measure and relatively inexpensive. Some remarkable relationships between plasma BNP/NT-proBNP and various elements of RV dysfunction have

been shown (96, 181, 182). It would appear that BNP/NT-proBNP measurement is a dynamic measurement reflecting the current state of the RV. An increase in NT-proBNP over time reflects RV dilatation concomitant to hypertrophy and deterioration of systolic function (182). We await the results of large scale studies to determine the role of BNP in the assessment and management of patients with PH.

Elevated plasma levels of cardiac troponin T and troponin I are established specific markers of myocardial damage and are prognostic indicators in acute coronary syndromes and acute pulmonary embolism. Elevated cardiac troponin T was an independent predictor of fatal outcome during 2-year follow-up in a single trial on 51 patients with PAH and five with CTEPH (138). In some patients cardiac troponin T disappeared from plasma either temporarily or permanently after introduction of treatment. The value of monitoring of the cardiac troponin T level in patients with PH still requires confirmation in future studies. Other biomarkers are currently under investigation (183, 184).

Several circulating biomarkers convey prognostic information in patients with PAH, but their value in everyday clinical practice is still not established. BNP/NT-proBNP plasma levels should be recommended for initial risk stratification and may be considered for monitoring the effects of treatment, in view of their prognostic implications. Low and stable or decreasing BNP/NT-proBNP may be a useful marker of successful disease control in PAH.

1.7.6 Haemodynamics

The normalisation of measures of cardiovascular haemodynamics would be an ideal end point. However, resting haemodynamics improve only marginally in most patients, even when the clinical response appears to be excellent (185), and do not reflect changes that may occur with exercise. Clinical improvement, therefore, is only partly related to a modification of resting haemodynamics in most patients. The magnitude of the mPAP correlates poorly with symptoms and outcome as it is determined not only by the degree of PVR increase but also by the performance of the RV. Thus, the PAP alone should not be used for therapeutic decision making. In patients with PAH, CO is directly related to the clinical severity of the disease and is an important prognostic factor (1, 4). It has

been suggested that monitoring SV could be a meaningful outcome measure in PAH patients. Van de Veerdonk and colleagues recently demonstrated that PVR decreased after 12 months of medical therapy in 68% of patients (156). Although, 25% of those patients with a decreased PVR showed deterioration in RV function (as determined by CMR) and had a poor prognosis.

There are disadvantages to this procedure, but most important are the significant risks to the patient. A recent study by Hoeper and colleagues assessed the risks associated with RHC (7218 procedures) in patients with PH (21). It was concluded that when performed in experienced centres, RHC in this patient group was associated with low morbidity and mortality rates (76 serious adverse events). 4 fatal events were recorded in association with any of the catheter procedures, resulting in an overall procedure-related mortality of 0.055% (95% confidence interval 0.01% to 0.099%). RHC, therefore, is an invasive procedure that is not ideal for serial evaluation due to the associated risks. Apart from the risks, hospital admission is usual procedure which may be inconvenient for patients. Some units, however, use RHC to determine success or response to treatment.

1.7.7 Cardiac Magnetic Resonance Imaging

CMR is well suited to longitudinal follow up as it is non-invasive and non-ionising. CMR findings in PH include RV dilatation, tricuspid regurgitation, RV hypertrophy, interventricular septal flattening or paradoxical motion, and change in chamber morphology from a normal crescent shape to a more concentric form. Prognosis of patients with PH remains poor despite the improvements in PVR or 6MWD seen during therapy. It has been suggested that RV function may be continuing to deteriorate despite the encouraging haemodynamic or functional signs e.g. van de Veerdonk and colleagues demonstrated that 25% of patients with reduced PVR following 12 months of therapy had deteriorating RV function (assessed by RVEF) during this period and that these patients had a poor outcome (156). It is imperative, therefore, that we can monitor RV function accurately.

CMR imaging fulfils the stated characteristics of an ideal marker. Modern CMR protocols provides abundant information regarding the ventricular myocardium

and pulmonary vasculature. RV volumes, muscle mass and functional parameters including stroke volume, ejection fraction and cardiac output differ significantly in PH compared to healthy subjects. CMR imaging is easily performed by trained MR technicians/physicians although is technically demanding. The majority of patients tolerate this non-invasive investigation well. Manual planimetry of the myocardium and flow analysis is simple to perform and reproducible although time consuming at present. Sequential MRI is the optimal tool to monitor therapeutic effects on vascular remodelling and right heart performance. CMR derived RV functional parameters correlate well with established haemodynamic parameters of prognostic significance. Although RHC remains the definitive assessment of pulmonary hypertension at present, the non-invasive evaluation of cardiac morphology and function and of the pulmonary circulation is a new and promising application for CMR imaging.

Figure 1-7: Pre (A) and post (B) treatment cardiac magnetic resonance images.

Figure A

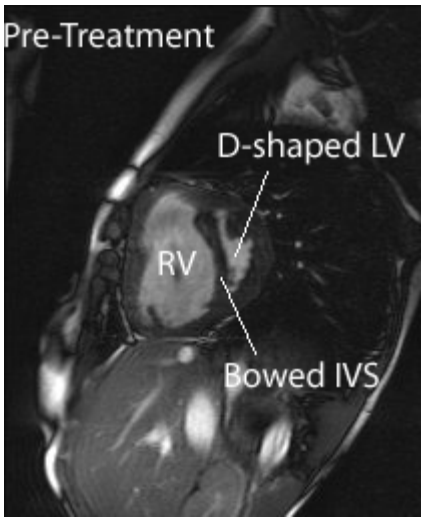

Figure B

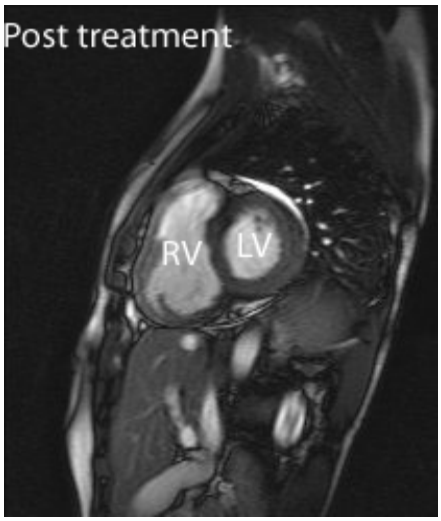

A fourteen year old male presented with dyspnoea and exertional syncope. Idiopathic pulmonary arterial hypertension was diagnosed. Figure A is the baseline short axis mid ventricular CMR image demonstrating a grossly dilated right ventricle with pronounced bowing of the interventricular septum compromising the left ventricle. Oral bosentan and anticoagulation therapy were commenced. There was considerable functional improvement. Figure B is the interval short axis mid ventricular CMR image at 6 months. A dramatic improvement in cardiac morphology is demonstrated.

CMR as an End Point

CMR is gaining a dominant role as the reference method for clinical trials assessing longitudinal changes in LV function after therapeutic interventions (186-188). The accuracy and reproducibility of CMR in assessing cardiac morphological and functional parameters leads to low interstudy variability, which translates into a significant reduction in sample sizes required to test the efficacy of therapeutic interventions (57, 68). It is expected that the number of clinical trials using CMR parameters as study end points will increase considerably in the future. Patient outcome is the relevant clinical issue and effort should be directed toward testing whether changes in cardiac variables as measured by CMR indeed translate into differences in patient outcome.

Several studies have reported the positive effects that medical (70, 189-191) and surgical (188, 192-195) therapies have on RV structure and function. Changes in RV mass, function and pulmonary artery blood flow have been demonstrated by CMR following lung transplantation in several studies (188, 192, 196). The functional and morphologic effects of pulmonary endarterectomy in patients with CTEPH was assessed by Kreitner *et al* using a combination of three-dimensional (3D) gadolinium-contrast enhanced MR angiography, cine-CMR and velocity encoded CMR (106). In 2003, Michelakis and colleagues (189) performed a small non-randomised, pilot study of 5 patients with PH to investigate the effect of sildenafil 50mg tid. RVM was utilised as an endpoint. Sildenafil significantly reduced RVM and increased the RVSV as measured by CMR. The pathological septal shift towards the LV was reversed by long-term sildenafil therapy. In a prospective study of PH patients with prostacyclin therapy, the significant increase in RVSV (PA flow analysis) corresponded well with functional improvement (WHO functional class, 6MWT) (70). In a comparison study between sildenafil and bosentan, RV mass (measured by CMR) did not change after 3 months of bosentan treatment, whereas sildenafil reduced RV mass (191). It was demonstrated by CMR that the addition of sildenafil reversed RV dilatation and hypertrophy in patients receiving treatment (190). More recently, 16 patients with PAH were assessed by CMR at baseline and after 12 months treatment with bosentan (197). After treatment cardiac index, PVR and 6MWT distance increased. There was a trend towards improvement in RV SV ($p=0.08$) although there was no change in RV ejection fraction or RVEDV as determined by CMR. To

date, two trials (191, 198) have used CMR-derived RVM as an end-point. This particular surrogate remains unvalidated and may not be the best end point since it is not known whether a reduction in RVM is beneficial or harmful to patients.

Deterioration of RV function at follow up examinations indicates an unfavourable prognosis because functional impairment of the RV is the major factor in disease progression and decline in life expectancy (164). Medical therapies or surgical interventions may stop, or even reverse this process, and the improvement of RV function could be detected by CMR.

Baseline CMR measurements in PAH associated with a poor prognosis include a decreased stroke volume, an increased RV end-diastolic volume, and a decreased LV end-diastolic volume (73). Van Wolferen *et al* performed a longitudinal CMR study which confirmed RV dilatation and a decrease in SV and LV diastolic volume are strong predictors of treatment failure and death at follow up (73). A recent cardiac magnetic resonance (CMR) study (73) confirmed that a low baseline stroke volume index (SVI) was predictive of a poor survival whereas cardiac index (CI) was not. A further reduction in SV at 1 year follow up predicted treatment failure and a poor long term outcome. SV directly reflects RV function in response to its load, without the correlation of compensatory increased HR as is the case for CO. SV, therefore, is an important haemodynamic parameter to monitor during treatment. A recent CMRI based study confirmed that a 10ml change in SV during follow up should be considered as clinically relevant. This value can be used to interpret changes in SV during clinical follow up in PH (199). The first outcome study to be reported with CMR (73) demonstrated the importance of indexed biventricular dimensions; a relationship that had not been hitherto revealed by echo studies. Indexed RVEDV was prognostic both at baseline and at 1 year as were indexed SV and LVEDV. These data have recently been extended to include RVEF (200).

CMR imaging enables a unique combination of morphological and functional assessment of the right ventricle and pulmonary circulation. CMR has emerged over recent years as the gold standard for a detailed study of the RV and has become an established modality for the physiological assessment of PH patients

in cross-sectional studies, longitudinal follow up studies and clinical trials of therapy. We anticipate that MR imaging will increasingly be utilised as the primary modality for combined anatomic and functional assessments that enable more complete and efficient evaluation of patients with PH.

1.8 Hypotheses and Aims

Pulmonary hypertension is a rare disease that is characterised by increased pulmonary vascular resistance leading to chronic right ventricular pressure overload. On the strength of available evidence, the adaptation of the right ventricle is the major prognostic influence in pulmonary hypertension. The right ventricle is difficult to assess. As discussed in the introduction, the currents methods of assessment are suboptimal. Modern drug therapy leads to a significant improvement in patients' symptomatic status and a slower rate of clinical deterioration. With the advent of multiple new disease-targeted therapies for pulmonary hypertension, it is increasingly important that we can assess the progress of patients in a non-invasive manner.

CMR will be used as the primary imaging modality in this thesis, as it represents the current gold standard method to measure ventricular volumes, mass and function. This study intends to provide a comprehensive evaluation of the use of CMR imaging in patients with PH.

The hypotheses and aims of the study are as follows:

Chapter 3

Non-invasive assessment of patients with PH is imperative. Measurement of stroke volume (SV) non-invasively is a promising method to monitor disease progression in PH. We aim to determine the accuracy of SV measurement by CMR imaging and by inert gas rebreathing using photoacoustic analysis compared with thermodilution technique (current gold standard) during right heart catheterisation in patients with suspected PH.

Chapter 4

The prognosis of IPAH associated with connective tissue disease is much worse than IPAH. RV function is the main prognostic determinant of patients with PH. Can CMR identify any differences in RV adaptation between these two groups? We hypothesise that RV adaptation (as assessed by CMR) to high pulmonary artery pressures may differ between the IPAH and CTDPH patient groups.

Chapter 5

Cardiac magnetic resonance imaging is proposed as a method to noninvasively assess the right ventricle in patients with PH. The clinical utility of CMR imaging in patients with PH requires confirmation. By evaluating CMR along with established methods of assessment, we hope the use of CMR will be clarified. Ultimately this study endeavours to determine if CMR imaging has a role in the continuing assessment of patients with PH. Can cardiac magnetic resonance imaging be used as a non-invasive, accurate, patient friendly method to follow up patients with pulmonary hypertension? This thesis was the starting point for the EURO-MR study. This was a prospective, longitudinal study conducted in four European centres.

Chapter 2

Materials and Methods

2 Materials and Methods

2.1 Introduction

The principle technique used for this thesis was cardiac magnetic resonance (CMR) imaging. This technique was supplemented by assessment of WHO functional class, six minute walk test, right heart catheterisation and inert gas rebreathing. In this chapter, the background, methods, apparatus and protocols used for these techniques will be outlined.

The Scottish Pulmonary Vascular Unit

The Scottish Pulmonary Vascular Unit (SPVU) provides a tertiary service for the population in Scotland. An epidemiology study performed in 2007 estimated the incidence of PAH in Scotland to be 7.6 cases per million per annum and the prevalence 26 cases per million (9).

Patient Recruitment

Newly referred treatment-naïve patients undergo a comprehensive diagnostic evaluation at the SPVU. The patients involved in the studies for this thesis were recruited during the course of their routine diagnostic assessment for suspected PH at the Western Infirmary / Golden Jubilee National Hospital, Glasgow, UK. All patients had undergone an initial assessment at an outpatient pulmonary vascular clinic; those in whom a diagnosis of PH was suspected were offered a one-week elective admission for further investigation. All subjects were asked to participate in the studies on the Monday of their admission. The patients, who agreed, gave informed written consent to a study protocol that had been approved by the ethics committee of West Glasgow University NHS Trust. The studies included in this thesis did not interfere with in-patient management in any way.

Definition of pulmonary hypertension

The diagnosis of PH is based on RHC in accordance with contemporary guidelines (7). PH was defined as an increase in mean pulmonary arterial pressure (mPAP) ≥ 25mmHg at rest, with a PCWP ≤ 15mmHg and PVR > 3 Wood units. The term

"PAH" is used specifically for WHO group I disease whereas "PH" is used as a general term to describe any group. Positive acute vasodilator response is defined as a drop in mPAP to < 40mmHg and by > 10mmHg with maintained or increased CO.

Table 2-1: Baseline diagnostic investigations at the Scottish Pulmonary Vascular Unit.

SPVU: Baseline diagnostic investigations
• Full clinical history
• Full physical examination – including height and weight
• WHO functional class status
• Routine blood sampling / ABGs
• NT-proBNP
• ECG
• CXR
• Transthoracic echocardiogram
• 6MWT
• CPET
• Inert gas rebreathing (subgroup of patients)
• V/Q scan
• HRCT / CTPA
• Cardiac magnetic resonance imaging
• Right heart catheterisation ± pulmonary angiography ± vasodilator studies

Figure 2-1: Flow chart of patient journey at the Scottish Pulmonary Vascular Unit.

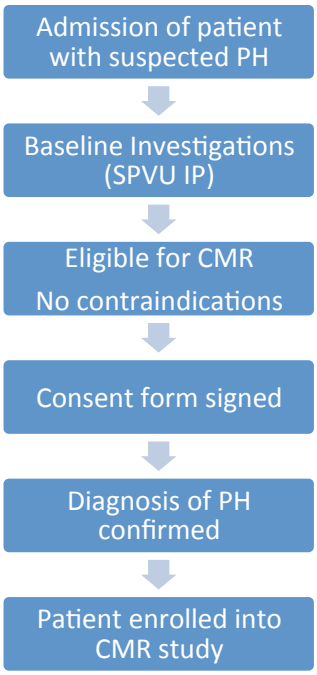

SPVU; Scottish Pulmonary Vascular Unit. PH; pulmonary hypertension. IP; inpatient. CMR; cardiac magnetic resonance imaging.

This thesis includes three separate studies as identified in the subsequent chapters. Baseline investigations were performed for all patients during their diagnostic evaluation at the SPVU. All patients underwent CMR imaging. A subgroup of 33 patients underwent inert gas rebreathing. Cross-sectional data obtained at baseline assessment was utilised in two of the studies (chapters 3 and 4) in this thesis. Chapter 5 details the longitudinal project performed. This study was performed as part of the multinational Framework 6 project EURO-MR.

Table 2-2: Inclusion and exclusion criteria for entry into cardiac magnetic resonance studies at Scottish Pulmonary Vascular Unit.

Criteria for enrolment into cardiac magnetic resonance studies
Inclusion criteria: 1. **Diagnosis of pulmonary hypertension confirmed** 2. **Ability to give informed consent** 3. **Patient ≥ 18 years**
Exclusion criteria: 1. **Severe or significant co-morbidity** 2. **MRI-incompatible (ferrous) prosthesis** 3. **Inability to complete CMR scanning e.g. orthopnoea** 4. **Claustrophobia causing inability to tolerate CMR** 5. **Pregnancy**

Figure 2.2 presents the consent form utilised for the studies in this thesis.

Please refer to Figure 2.3 for the patient information sheet.

Figure 2-2: Consent form for CMR clinical research project.

WEST ETHICS COMMITTEE

FORM OF CONSENT FOR PATIENTS/VOLUNTEERS IN CLINICAL RESEARCH PROJECT

Title of Project: **The Assessment of Pulmonary Hypertension using Cardiac MRI**

By signing this form you give consent to your participation in the project whose title is at the top of the page. You should have been given a complete explanation of the project to your satisfaction and have been given the opportunity to ask questions. You should also have been given a copy of the patient information sheet approved by the West Ethics Committee to read and to keep. Even though you have agreed to take part in the research procedures you may withdraw this consent at any time without the need to explain why and without any prejudice to your care.

Consent:

……(PRINT)

of ……

give my consent to the research procedures above, the nature, purpose and possible consequences of which have been described to me

by ……

Patient's signature ……..Date……

Doctor's signature ……..

Figure 2-3: Patient information sheet.

Brief Title of Project

The Assessment of Pulmonary Hypertension using Cardiac MRI

Patient's Summary (Purpose of study, nature of procedure, discomfort and possible risks in terms which the patient or volunteer can understand).

Background

Pulmonary Hypertension is a rare and potentially serious condition. It is often difficult to diagnose and to treat. The major problem in Pulmonary Hypertension is high blood pressure in the lungs; this often leads to excessive stress being exerted on the right hand side of the heart. Sometimes, as a result of this, the right side of the heart becomes unable to pump blood into the lungs, as it should. This obviously can make the patient feel very unwell.

We usually make the diagnosis after a number of tests have been carried out; the most important of these currently is a Right Heart Catheter. This involves passing a plastic catheter into the heart through a vein in the neck or groin. Through this catheter we can measure the blood pressure in the lungs and assess how well the heart is pumping. We can also assess how likely the patient is to respond to treatment.

This test is very useful and generally safe, but some patients find it unpleasant and there are some risks involved. We therefore do not tend to repeat it to see how well or badly a patient is doing unless it is absolutely necessary. Instead, we use a test that measures how far a patient can walk in six minutes. We then compare this measurement to the last one to say whether they are better or worse. This test is useful but can sometimes be misleading.

The Study

We are conducting a study looking at new ways to diagnose and monitor patients with Pulmonary Hypertension. We would like to invite you to take part. The study involves the use of a relatively new scanning technique called MRI (Magnetic Resonance Imaging).

MRI allows us to get a lot of useful information about Pulmonary Hypertension. It does not use any X-rays or radiation, but instead uses magnets to acquire detailed images of pulmonary blood vessels and the heart. It is therefore very safe. We can get a lot of the same information using MRI that we get at right heart catheterisation. Gadolinium is a clear fluid like water. It is used in MRI scanning as it accumulates for a short time in abnormal tissue and lights up that area so that the scanner can detect this part of the body. It is therefore useful in telling us which part of the blood vessels and heart are affected. After a short while Gadolinium fades away and is removed from your body (within a few hours).

Compared with right heart catheterisation, MRI is safer, and patients tend to fine it less unpleasant. This means not only could MRI be used in the diagnosis of Pulmonary Hypertension, we would be happier to repeat it in the future. This may allow us to better identify changes in the illness over time and so allow better tailoring of your treatment.

In addition to the MRI we would like to measure certain proteins in your bloodstream that may go up and down depending on how well you are.

What the study involves

During your 5-day stay at the Western Infirmary you will have a number of tests, including blood samples and x-rays. On the Thursday you will have your right heart catheterisation. We would propose doing an MRI scan at some time during this week. The scan would take around $1^1/_2$ hours and would not prolong your stay in hospital. We will take some extra blood samples in addition (around one tablespoon in total). These samples will be taken off at the same time as your routine bloods and will not involve any extra needles. We normally see patients about 3 months after their discharge in clinic and repeat the six-minute walking test. You will follow this normal routine. **As part of the study you will also have further MRI scans 4 months and 12 months later**, to assess your progress. If required, we will be able to organise for a taxi to pick you up and take you home free of charge.

What does the MRI involve?

On arrival at the Clinical Research Initiative (CRI) a radiographer will go through a safety checklist and make sure that all magnetic objects (e.g. jewellery and bankcards) have been removed. Following this you will be asked to sign the consent form. Once you have changed into a hospital gown you will then be asked to lie flat on the bed that will move into the scanner. The scanner is basically tunnel shaped, like a large "polo" mint. You are slid into the centre of the "polo" on an electric bed and the scans are acquired. Some patients find it a little enclosing, but you can come out at any time.

Before you go into the scanner a small plastic cannula (similar to that used when putting up a drip) will be inserted into a vein in your arm. This allows us to give you a harmless dye called Gadolinium. A doctor will insert the cannula. During the scan we will inject some Gadolinium dye into the cannula in your arm, this will help light up your blood vessels and heart muscles on the pictures. A doctor will be in the control room throughout this procedure.

When you are in the scanner you will need to wear a pair of headphones, allowing you to listen to music of your choice (you are welcome to bring your own CD) and to allow us to communicate with you throughout the scan. The headphones are also necessary because of the loud knocking noise that occurs when the pictures are being taken. You will be given an emergency buzzer and you can very quickly be taken out the scanner should you feel it uncomfortable or if it is felt necessary. During the scan you will be asked to hold your breath at times to improve the quality of the pictures.

What are the risks?

◦ The MRI scanner is very safe as long as you have no metal implants in your body.

◦ The dye used is called Gadolinium. It is generally harmless and will be washed out of your system by your kidneys. Rarely, it can cause headaches.

NB • You should not take part in this study if you are pregnant.

• If you wish to take part in this study, your General Practitioner will be advised of your participation and the clinical management that you will undergo.

• If you do not wish to participate in this study, or wish to withdraw at any time your care will not, in any way, be affected.

If you have any questions regarding the study please contact **DR LINDSEY MCLURE** at 0141 211 1812.

2.2 Cardiac Magnetic Resonance Imaging

2.2.1 CMR protocol

All scans were performed on a 1.5 Tesla Siemens Sonata whole body MR scanner (Siemens Medical Solutions, Erlangen, Germany). The CMR scans completed for the purpose of these studies were performed by myself (after completion of the Magnetic Resonance Imaging Basic Competencies course run by the Institute of Physics and Engineering in Medicine) or by Ms Tracey Steedman, Cardiac MR Radiographer, Western Infirmary. I was present throughout all the scans to provide constant medical cover. The importance of keeping as motionless as possible, and maintaining adequate breath-holds, was reinforced verbally prior to commencement of the scan. End-expiration is optimal for consistent breath holding and was preferred.

2.2.2 Preparation of patient for CMR scan.

The following steps were performed in all cases:

- Prior to entering the controlled zone, an MRI safety checklist was performed and signed by both patient and qualified MRI personnel.
- Before entry into the MR scanning room the patient was asked to complete and sign a safety questionnaire. If the patient reported any previous injuries involving metal fragments, especially any to the eyes, appropriate plain radiographs were requested to ensure that no fragments remained.
- Patient demographic details entered on scanner database.
- Patient placed on MR table.
- Siemens active Brooker electrodes placed on patient's anterior chest wall, and position varied to obtain an optimal R wave
- The phased-array chest coil (Siemens CP body array flex) was applied and aligned
- Patient, wearing ear protectors or headphones, enters scanner.

2.2.3 Cardiovascular Magnetic Resonance Imaging

The patient was asked to lie supine on the examination table, which had been remotely removed from inside the bore of the magnet, to a more accessible position (see Figure 2.4). Adhesive monitoring pads for the 3-lead ECG were connected, and the phase array chest coil was placed on the patient's chest and secured in position with a loose fitting Velcro strap. The patient was then supplied with an emergency buzzer and protective ear defenders. Immediately before movement of the patient inside bore of the magnet, the centre of the chest coil, approximating the position of the heart, was defined by a laser pointer attached at the 12 o'clock position of the magnet's inner circumference. This point of reference was used to move the patient to a precise point within the bore of the magnet which ensured their heart was at the centre of the main magnetic field. Once the patient was inside the bore of the magnet, the door of the scanning room was sealed and staff performing the scan moved to the control room. Proper functioning of the microphones and headphones that allow direct communication between patient and operator was verified before image acquisition was initiated.

Figure 2-4: Cardiac magnetic resonance imaging at the Scottish Pulmonary Vascular Unit.

Tracey Steedman (Cardiac MR Radiographer) positioning a patient before a scan using the Siemens Sonata 1.5 Tesla system at the Western Infirmary, Glasgow. The examination table is extended and the phased-array chest coil has been secured over the patient's chest using velcro straps.

2.2.4 CMR image acquisition and analysis

RV/LV structure and function

All CMR scans commenced with a multi-slice breath hold localiser. Each of the localisers described in this section used the same protocol:

Protocol: Multislice single-shot breath-hold true fast imaging with steady state precession (trueFISP) localiser with transverse, sagittal and coronal slices. Settings: field of view = 360mm, field of view phase = 81.3%, slice thickness = 6mm, repetition time (TR) = 3.41ms, echo time (TE) = 1.71ms, flip angle = 60%, averages = 1, phase resolution = 80%, phase oversampling = 0%.

Figure 2-5: Typical orthogonal scout images used to localise the heart within the thoracic cavity.

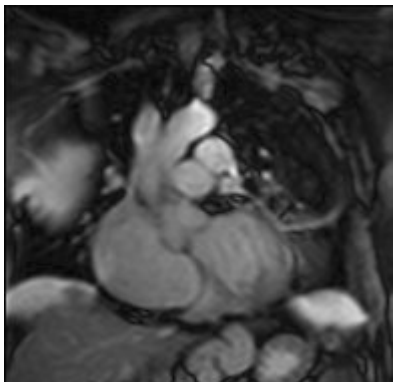

Coronal Scout Image

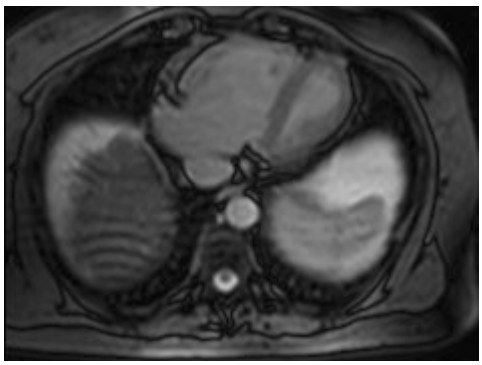

Transverse Scout Image

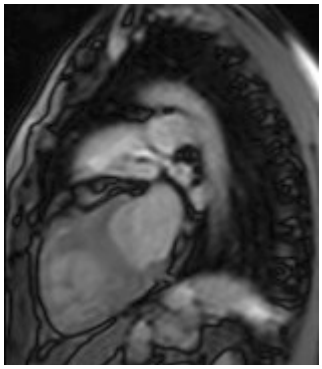

Sagittal Scout Image

Typical orthogonal scout images used to localise the heart within the thoracic cavity during CMR imaging of a patient with pulmonary hypertension. Note the low definition images of these preliminary Fast imaging with steady state precession (TrueFISP) scout images.

From these images, the best axial image depicting the LV and septum was selected. If no suitable image was produced by the initial localiser, a second axial localiser was performed using the coronal images until the closest match to Figure 2.6 (A) was obtained. This was used to plan 3 vertical long axis (VLA) parallel localisers along the long axis of the LV from the mid-point of the mitral valve to the apex.

From the resulting VLA scan, 3 horizontal long axis (HLA) localisers were then planned, using the mid-point of the mitral valve and the LV apex to prescribe the orientation (Figure 2.6 (B)). This resulted in 3 HLA slices (Figure 2.6 (C)). Using the atrioventricular groove as a landmark, 3 short axis (SA) localiser slices were planned, with the most basal slice positioned in the atria to depict the left ventricular outflow (Figure 2.6 (C)). From the resulting SA images, 3 long axis views can be prescribed – the 4-chamber, the 2-chamber and the left ventricular outflow tract (LVOT) (Figure 2.6 (D)).

Cinematographic (cine) imaging:
Having thus acquired 3 orthogonal long axis views, cine studies were acquired in each of these 3 orientations, as follows:
Protocol: trueFISP breath-hold cine. Settings: field of view = 360mm, field of view phase 81.3%, slice thickness = 8mm, TR = 47.4ms, TE = 1.58ms, flip angle = 60°, averages = 1, measurements = 1, phase resolution = 65%, phase oversampling = 20%, segments = 15.
These images were used for visual analysis of structure and long axis function.

Short axis cine stack:
Quantitative volumetric assessment of ventricular function requires that the LV/RV be divided into a stack of SA slices from base to apex. Measurements from each slice are then summed to provide overall ventricular mass and volumes. The SA stack was prescribed from 4-chamber HLA cine already acquired. Using the end-diastolic image from this view, the cursor was positioned in an orientation across the mitral valve plane through the atrioventricular groove (as a marker of the most basal SA slice) as in Figure 2.6 (E). The most basal slice that results is depicted in Figure 2.6 (F). The slice position was then incremented by 10mm moving towards the apex of the LV/RV and repeated until

the LV/RV were completely covered; interslice gaps of 2mm were used. A representation of the final SA cine stack is shown in Figure 2.6 (G). The same protocol was used for all SA cine slices:

Protocol: trueFISP breath-hold cine. Settings: field of view = 340mm, field of view phase = 81.3%, slice thickness = 8mm, interslice gap = 2mm, TR = 47.4ms, TE = 1.58ms, flip angle = 60°, averages =1, measurements = 1, phase resolution = 65%, phase oversampling = 20%, segments =15.

Figure 2-6: Planning of cine cardiac magnetic resonance image acquisition.

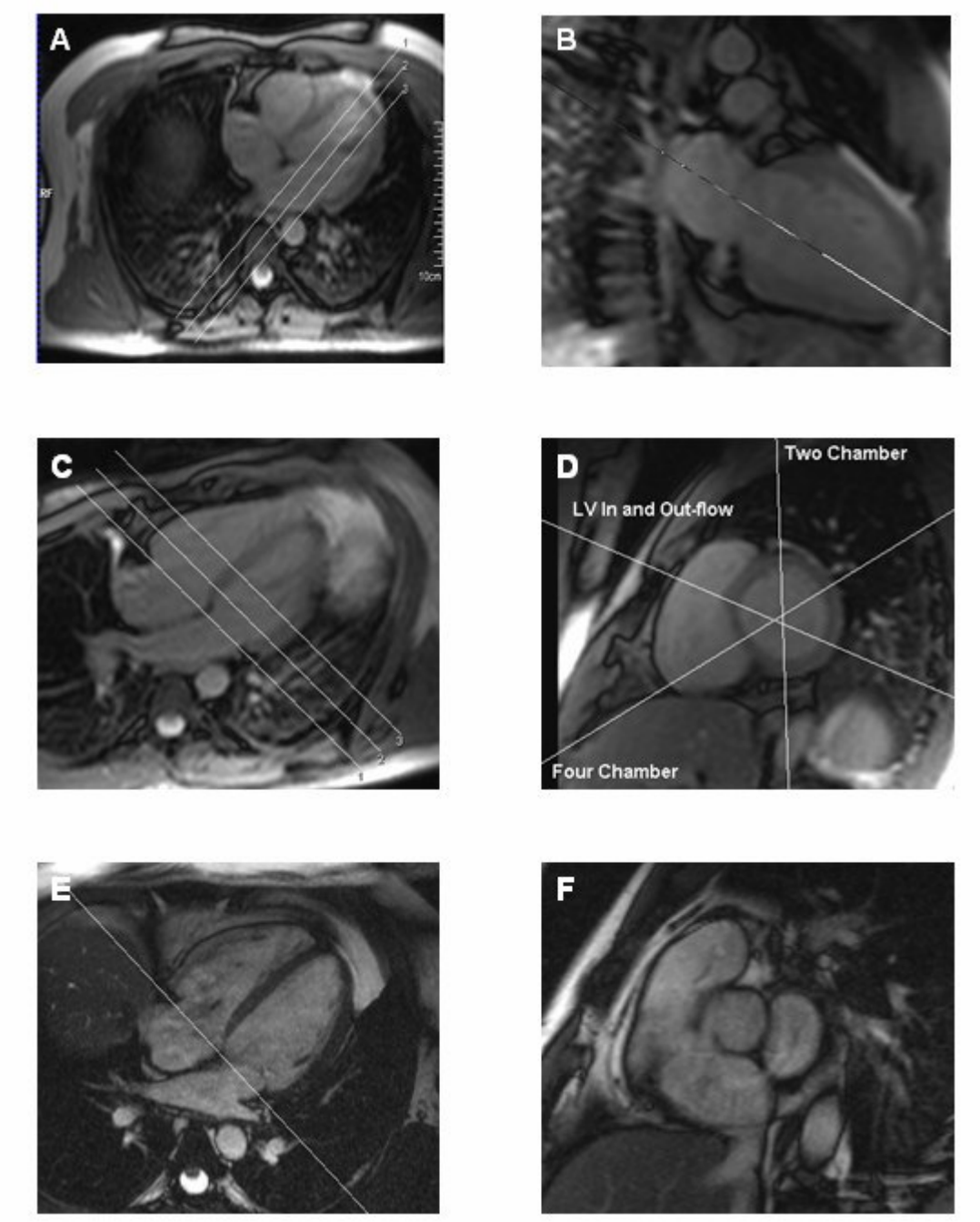

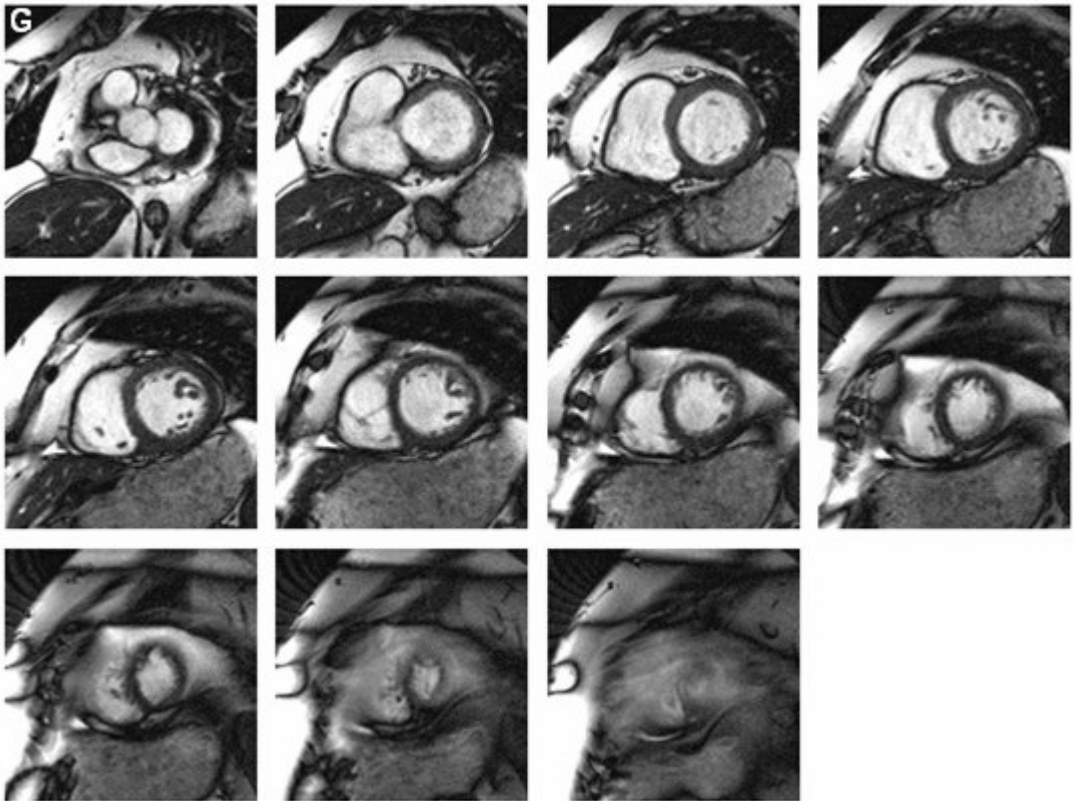

Planning of cine CMR image acquisition. From coronal, transverse and sagittal scout images, the best image depicting the LV and septum is selected (A) and utilised to produce a vertical long axis (VLA) localiser (B). Prescribing an orientation through the apex and mid-point of the mitral valve (B – orientation line) creates a horizontal long axis (HLA) localiser (C). Using the atrioventricular grooves as landmarks (C), a perpendicular plane to this HLA localiser is prescribed (D), based on which three orthogonal long axis planes can be planned (2-chamber, 4-chamber and LV outflow tract views). Cine images are acquired for each of these three long-axis orientations. Finally a short axis cine stack is planned on the 4-chamber HLA cine image (E). A short axis image is acquired of the base of the LV (F), from which slice position is advanced at 10mm intervals from base to apex, creating a short-axis cine stack (G).

Flow Analysis

Right ventricular stroke volume (SV) was measured using MR phase-contrast flow quantification in an image plane positioned perpendicular to the main pulmonary artery, at least 1cm distal to the pulmonary valve. Left ventricular SV (aortic flow) was also measured, approximately 2 - 4cm above the aortic valve and distal to the coronary arterial ostia. A velocity encoded k-space segmented gradient-echo sequence was used (imaging parameters: echo time / repetition time / flip angle / slice thickness / temporal resolution / image matrix / field of view / in-plane resolution / velocity encoding range = 3.1ms / 16ms / 15° / 6mm / limited by TR / 256 / 380mm / 1.9x1.5mm / 150cm per second) to generate 45 matched pairs of anatomical and velocity images. Retrospective ECG-gating was used to ensure coverage of the complete cardiac cycle. Patients were instructed to breath freely throughout this section of the protocol and the average time of acquisition was 2-3 minutes depending on the patient's heart rate.

2.2.5 Analysis of CMR images

CMR analysis methodology

All CMR images were analysed by a single operator (L.M.) on a satellite workstation attached to the main MR scanner using the Argus analysis software (Siemens, Erlangen, Germany). At the time of analysis, I was blinded to the haemodynamic results of any given patient. Although the name of the patient was visible in the corner of each MR image, each analysis was performed some time after their invasive assessment and I was unaware of their haemodynamic results at the time of MR analysis.

The images for each patient were loaded into the Argus program from each compact disc (CD). Argus automatically identified the images within each SA cine loop that had the largest and the smallest blood volumes and defined these as end-diastole and end systole, respectively. The number of slices required to cover the RV/LV in end-diastole and end-systole varied from scan to scan dependent on the long axis diameter of the RV/LV. An example of a complete image series with these images defined is provided (Figure 2.7). The end-diastolic image was usually the first image acquired after R-wave deflection.

Using a trackball cursor the endocardial and epicardial borders of the end-diastolic and end-systolic images at each slice position within the SA stack were then defined by manual planimetry. These methods are standard in clinical MR practice and have been published before. Particular points of note regarding the planimetry used herein include the deliberate inclusion of trabeculations ad papillary muscles in all analyses. This has been shown by previous authors to be a more accurate, but more time consuming method (201). By multiplying the individual slice areas by slice thickness (8mm) plus the inter-slice gap (2mm) and applying Simpson's Rule, the Argus software automatically calculated RVEDV, RVESV, LVEDV and LVESV. Right and left ventricular stroke volumes (RVSV and LVSV) were determined as RVEDV – RVESV and LVEDV –LVESV. Ejection fraction was determined as a percentage (%) as (RV or LV SV/EDV) x 100) using this planimetry derived SV measurement.

Velocity encoded flow mapping was used to determine precise, forward stroke volumes for each ventricle. The measurements of SV yielded by this technique were used to calculate RV and LV EF. The flow mapping technique circumvents the predictable measurement error in planimetry derived SV resulting from tricuspid valve regurgitation. However, both methods are established and commonly used tools for the assessment of SV and EF in clinical practice. Please refer to Figure 2.8.

RV and LV mass (RVM and LVM) were determined as the product of the difference between the end-diastolic and end-systolic volume for each ventricle and the quoted density of cardiac muscle (1.05g/cm^3). RVM was determined as RV free wall mass, with the interventricular septum (IVS) considered part of the LV. These methods are again, common in clinical CMR practice and have been published before (151, 201). Ventricular mass index (VMI) was determined as RVM/LVM as previously shown (75). Throughout this thesis, all ventricular volumes are corrected for body surface area (BSA) and are reported as indexed measurements.

Table 2-3: Measurements obtained from cardiac magnetic resonance imaging for this thesis.

Measurements from CMR imaging
• RV/LV end diastolic volume index (RV/LVEDVI)
• RV/LV end systolic volume index (RV/LVESVI)
• RV/LV ejection fraction (RV/LVEF)
• RV/LV mass index (RV/LVMI)
• Ventricular mass index (VMI)
• Pulmonary artery flow analysis (SVI)
• Aortic flow analysis (SVI)

Figure 2-7: Planimetry analysis of the right ventricle.

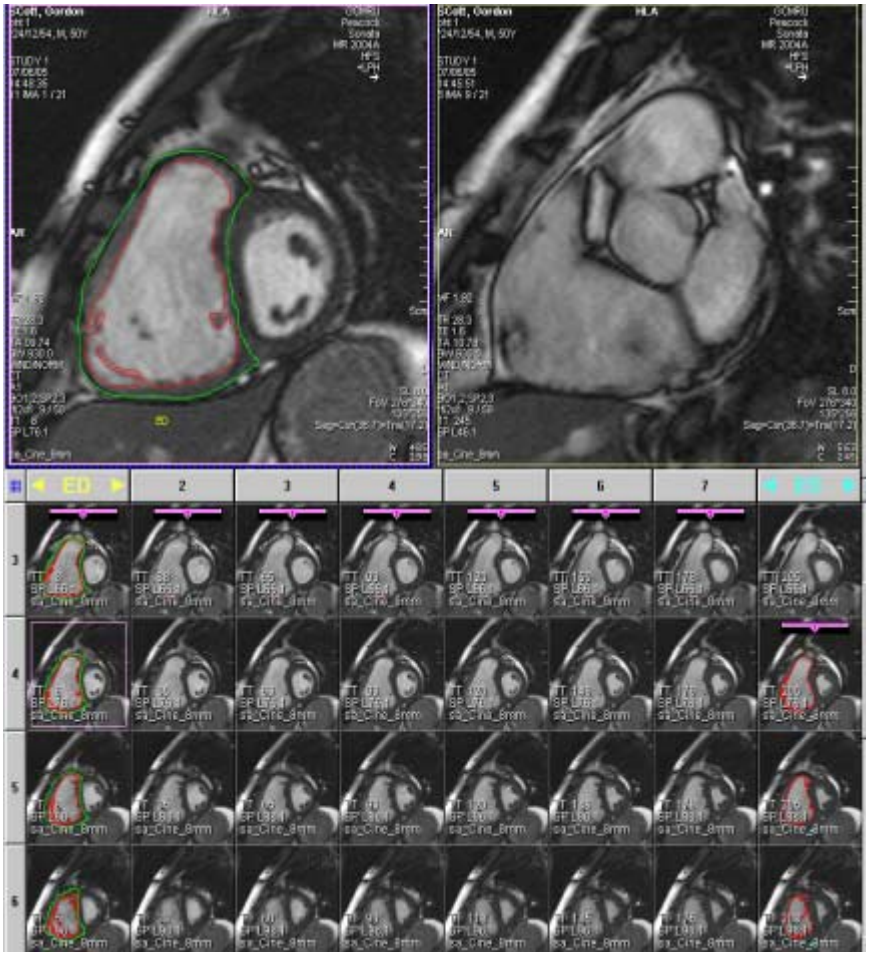

An example of planimetry analysis of right ventricular volumes and mass using the Argus analysis software. Each row of short axis images represents a loop of cine images acquired during one cardiac cycle at consecutive slice positions, beginning at the base of the heart, moving apically to cover both ventricles. The first images within each row (or slice position) were acquired immediately after R-wave deflection. They are therefore defined by the Argus software as the end-diastolic images (indicated by the yellow ED at the top of the left-hand column) and have the greatest total ventricular blood volume. The end-systolic images were defined automatically by the Argus software as the column of images with the smallest total ventricular blood volume and verified visually. A trackball mouse and cursor was used to define the endocardial (in red) and epicardial (in green) surfaces of the RV at end-diastole and the endocardial surface only at end-systole (in red). This allowed computation of RV end-diastolic and endsystolic volumes and RV mass.

Figure 2-8: Velocity encoded flow maps of the pulmonary artery to determine stroke volume.

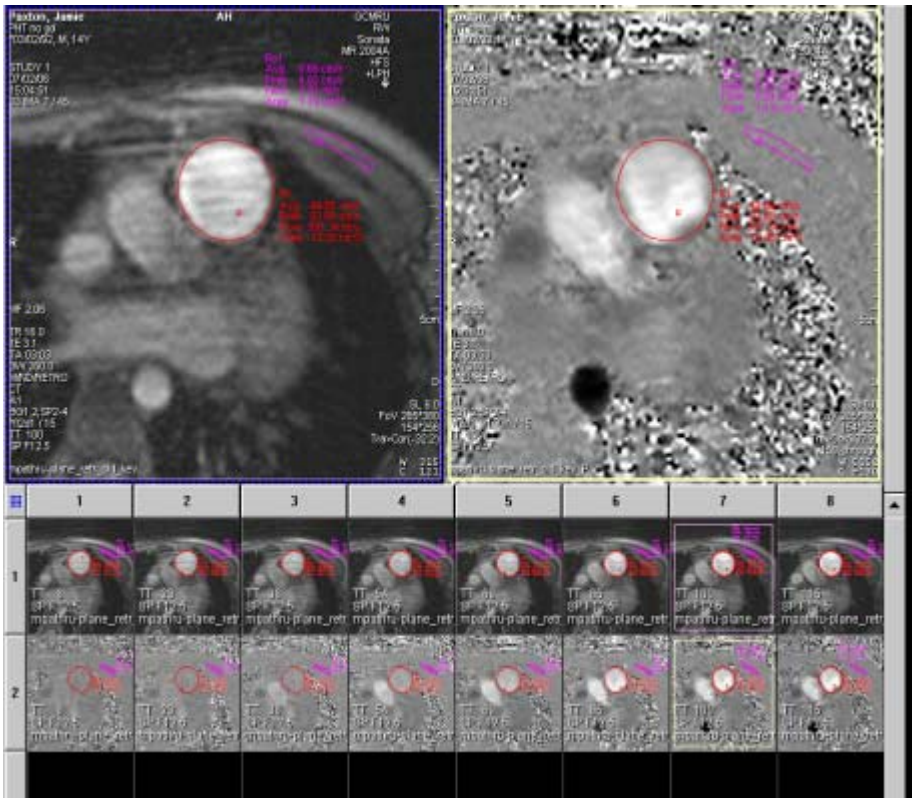

Velocity encoded flow maps were used to determine RVSV and LVSV at rest; two flow maps were therefore analysed for each patient, each containing 90 images. The resting main pulmonary artery flow map from a patient with PH is shown below. The anatomical image is shown on the left with the corresponding velocity-encoded image, from the same time point in the cardiac cycle on the right. A region of interest (ROI) was drawn around the interior surface of the target vessel on the first anatomical image. This ROI was propagated throughout the 45 anatomical images using a semi-automatic function within the Argus software. The propagated ROIs were then checked visually and modified using the nudge function within Argus to approximate the interior surface of the target vessel throughout the set. These modifications were then copied onto the corresponding 45 velocity images. The final contours that resulted are shown overleaf in red. A second, reference ROI (shown in purple) was then drawn on the first anatomical image and copied directly onto all of the other images. This was defined within the soft tissue of the chest wall as close as possible to the target vessel and was used to correct for background movement of the thoracic contents through the imaging plane during cardiac motion and normal respiration.

2.2.6 Intra-observer variability of CMR analysis in this thesis

Ten CMR examinations were randomly selected during this thesis to determine intra-observer variability. I reanalysed the CMR scans and was blinded to the initial results. End-diastolic and end-systolic volumes, stroke volume and mass were not indexed for body surface area during this analysis. Variability analyses were compared using Bland-Altman analysis and t tests. Please refer to Table 2.4 and Table 2.5.

These results demonstrate that variability was low in my CMR analysis. Intra-observer variability was higher in the right ventricular analysis compared with left ventricular measurements. This reflects the more challenging planimetry of the right ventricle compared to the left ventricle.

Table 2-4: Intra-observer variability data of CMR analysis.

CMR Measurement	Mean difference ± SD	Paired t-test	Correlation coefficient
Left heart			
LVEDV (ml)	0.33 ± 3.38	0.88	0.96
LVESV (ml)	-0.36 ± 1.78	0.53	0.97
LVM (g)	-2.27 ± 3.02	0.04	0.99
LVSV (Ao Flow) (ml)	-0.74 ± 2.83	0.43	0.99
Right heart			
RVEDV (ml)	-3.05 ± 7.45	0.23	0.99
RVESV (ml)	-5.9 ± 4.66	0.03	0.99
RVM (g)	5.14 ± 6.61	0.03	0.99
RVSV (PA flow) (ml)	-2.139 ± 3.39	0.07	0.99

LVEDV: left ventricular end-diastolic volume; LVESV: left ventricular end-systolic volume; LVM: left ventricular mass; LVSV (Ao flow): left ventricular stroke volume (aortic flow); RVEDV: right ventricular end-diastolic volume; RVESV: right ventricular end-systolic volume; RVM: right ventricular mass; RVSV (PA flow): right ventricular stroke volume (pulmonary artery flow).

Table 2-5: Summary of Bland-Altman analyses performed.

CMR Measurement	Bias	SD	95% Limits of Agreement	
			From	To
LVEDV (ml)	0.26	5.57	-10.67	11.19
LVESV (ml)	-0.36	1.78	-3.86	3.14
LVM (g)	-2.27	3.019	-8.19	3.65
LVSV (Ao) (ml)	-0.82	2.992	-6.09	5.04
RVEDV (ml)	-3.05	7.44	-17.63	11.53
RVESV (ml)	-5.90	4.66	-15.04	3.24
RVM (g)	5.14	6.61	-7.81	18.09
RVSV (PA) (ml)	-2.14	3.39	-8.79	4.509

LVEDV: left ventricular end-diastolic volume; LVESV: left ventricular end-systolic volume; LVM: left ventricular mass; LVSV (Ao flow): left ventricular stroke volume (aortic flow); RVEDV: right ventricular end-diastolic volume; RVESV: right ventricular end-systolic volume; RVM: right ventricular mass; RVSV (PA flow): right ventricular stroke volume (pulmonary artery flow).

2.3 WHO Functional Class (WHO FC)

Despite large inter-observer variation in the measurement, WHO FC remains a powerful predictor of survival. All patients had their WHO FC confirmed at baseline and at each follow up visit.

Table 2-6: World Health Organisation functional classification in pulmonary hypertension.

WHO FC	Description
Class I	Patients with PH but without resulting limitation of physical activity. Ordinary physical activity does not cause undue dyspnoea or fatigue, chest pain, or near syncope.
Class II	Patients with PH resulting in slight limitation of physical activity. They are comfortable at rest. Ordinary physical activity causes undue dyspnoea or fatigue, chest pain, or near syncope.
Class III	Patients with PH resulting in marked limitation of physical activity. They are comfortable at rest. Less than ordinary activity causes undue dyspnoea or fatigue, chest pain, or near syncope.
Class IV	Patients with PH with inability to carry out any physical activity without symptoms. These patients manifest signs of right heart failure. Dyspnoea and/or fatigue may even be present at rest. Discomfort is increased by any physical activity.

2.4 Six-minute walk test

2.4.1 Test protocol

The 6MWT was performed by a respiratory physiologist according to the American Thoracic Society guidelines (139). Testing was performed in a location where a rapid appropriate response to an emergency was possible and resuscitation equipment was available. The 6MWT was performed indoors, along a long, flat, straight, enclosed corridor with a hard surface that was seldom

travelled. The walking course was 20m in length. The turnaround points were marked with small, orange cones. A starting line, which marked the beginning and end of each 40m lap was marked on the floor. Measurements recorded included the 6MWT distance walked, dyspnoea on exertion (Borg scale) and finger O_2 saturation.

The performance of the six minute walk test was audited internally during these studies.

2.5 Right heart catheterisation

RHC was performed according to international recommendations (26). This investigation was required to confirm the diagnosis of PH, to assess the severity of the haemodynamic impairment, and to test the vasoreactivity of the pulmonary circulation. RHC was performed by SPVU physicians, in the catheterisation laboratory at the Western Infirmary (August 2005 – September 2007) and subsequently at the Golden Jubilee National Hospital (September 2007 - August 2008). Please see Figure 2.9.

Figure 2-9: Right heart catheterisation at the Scottish Pulmonary Vascular Unit.

A photograph of Dr Colin Church and Specialist Nurse Jim Mearns performing a right heart catheterisation on a patient under investigation for pulmonary hypertension.

Figure 2-10: Swan-Ganz Pulmonary Artery Catheter.

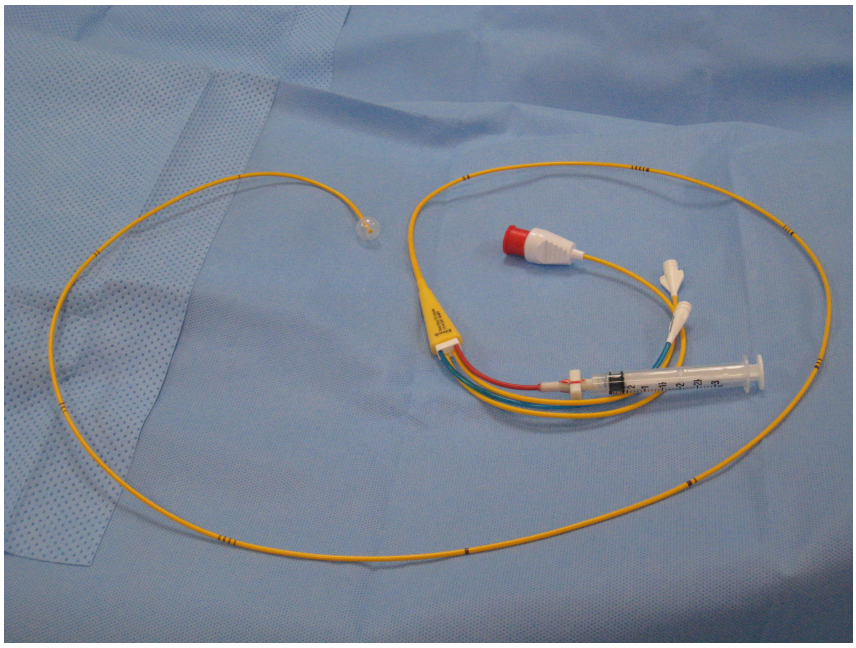

A photograph of a 7F triple-channel, balloon-tipped, flow directed thermodilution Swan Ganz catheter (Baxter Healthcare, Irvine, California, USA).

An 8F introducer sheath was inserted into the right internal jugular vein under ultrasound guidance prior to transfer to the catheterisation laboratory. If this was technically impossible, an 8F introducer sheath was inserted into the right femoral vein. Anxious patients were occasionally prescribed a short acting benzodiazepine, but in general no premedication was used.

A 7F triple-channel, balloon-tipped, flow directed thermodilution Swan Ganz catheter (see figure 2.10) (Baxter Healthcare, Irvine, California, USA) was advanced through an 8F introducer sheath inserted into the right internal jugular vein or the right femoral vein. All measurements were recorded with the patient in a supine position, at rest, breathing room air or supplemental oxygen if required. Measurements included mean right atrial pressure (RAP), right ventricular pressure and systolic and diastolic pulmonary artery pressures (PAP). Mean PAP was determined as the area under the PAP trace. Pulmonary capillary wedge pressure (PCWP) was recorded with the catheter in the wedge position and the balloon inflated. Mixed venous blood is sampled from the main

pulmonary artery to measure SvO_2. CO was measured by the thermodilution technique (202) following injection of 10ml of ice-cold, 0.9% saline through the proximal (right atrial) lumen of the catheter; the drop in temperature was measured at the distal thermistor. The final value is calculated by averaging three measurements with ≤ 10% variation. Cardiac output measurement allowed determination of pulmonary vascular resistance (PVR) by the following equation:

$$\mathrm{PVR} = \frac{(\mathrm{mPAP} - \mathrm{PCWP})}{\mathrm{CO}}$$

Cardiac index was determined as CO / body surface area.

An acute vasodilator study was performed using inhaled nitric oxide (40 parts per million) for 5 minutes to identify calcium channel blocker (CCB) responders. If, after review of the V/Q scan and CTPA prior to RHC, suspicion remained regarding the presence of thromboembolic disease, selective pulmonary angiography was also performed.

Table 2-7: Haemodynamic measurements performed during right heart catheterisation.

Routine measurements obtained during RHC
• RAP
• RVP
• Systolic, diastolic and mean PAP
• PCWP
• CO by thermodilution (CI as determined by BSA)
• PVR
• Mixed venous blood oxygen saturation
• ± Pulmonary angiography
• ± Vasodilator studies (inhaled nitric oxide) with repeat haemodynamic measurements

RAP; right atrial pressure. RVP; right ventricular pressure. PAP; pulmonary artery pressure. PCWP; pulmonary capillary wedge pressure. CO; cardiac output. CI; cardiac index. BSA; body surface area. PVR; pulmonary vascular resistance.

2.6 Inert gas rebreathing

2.6.1 Principles and operational detail

The rebreathing system (Innocor®) consists of a three-way respiratory valve with a mouthpiece and a rebreathing bag connected to an infrared photoacoustic gas analyser (AMIS 2001; Innovision A/S) (125). Pulmonary blood flow (PBF) was measured by rebreathing a gas mixture of 0.1% sulphur hexafluoride (SF_6) and 0.5% nitrous oxide (N_2O) through a mouthpiece with the nose occluded. Breath-by-breath respired gases were continuously sampled as patients breathed into the respiratory valve via a mouthpiece with the nose clipped. Gas concentrations were analysed using infrared photoacoustic gas analysers.

The rebreathing software calculated the pulmonary blood flow (PBF) from the rate of uptake of N_2O into the blood (slope of the regression line through the logarithmically transformed expiratory [i.e. alveolar] N_2O concentrations plotted against time) after correction for system volume changes using the SF_6 (blood insoluble gas) concentrations. PBF is equivalent to CO in the absence of significant intracardiac or intrapulmonary shunt. Right ventricular SV was derived by dividing PBF by heart rate. Repeatability of SV measurements by IGR (Innocor) was assessed by comparing the results from two IGR efforts.

Prior to each IGR measurement, a 3L Douglas bag was pre-filled with an oxygen enriched mixture containing two inert gases, N_2O and SF_6. This was obtained by mixing a bolus from a gas bottle containing 94% oxygen, 5% N_2O and 1% SF_6 with ambient air. The measurements were taken with the patient in the supine position. Patients were coached on how to perform the rebreathing manoeuvre and had 2-3 practices prior to testing. Duplicate measurements were made after 10 minutes of rest in the supine position. There was an interval of 5 minutes between duplicate measurements to ensure complete wash out of inert gases from the lungs.

Reproducibility of IGR measurements was tested on a subgroup of patients.

IGR measurements were initiated by the operator (L.M.) at the end of expiration. At this point, the respiratory valve was activated so that the patient rebreathed into the rebreathing bag in a closed circuit. The patient was

instructed to empty the bag during each inspiration and breathe at a rate of at least 20 breaths/min. N_2O, being highly blood-soluble and diffusion-independent, disappeared from the alveoli into the pulmonary capillary blood at a rate proportional to PBF. SF_6, being insoluble in blood, remained in the alveoli and served to determine the final lung volume from which N_2O was removed.

The total lung volume was calculated using the following formula:

$$V_L = \frac{[SF_6]_0}{[SF_6]_{eq}} . V_{RB}$$

V_L = total systemic volume (STDP)

V_{RB} = rebreathing bag volume

$[SF_6]_0$ = initial SF_6 concentration in the rebreathing bag

$[SF_6]_{eq}$ = SF_6 concentration after good mixing (back extrapolated to time zero)

After a few breaths, SF_6 was mixed in the lungs and its concentration stabilised. The difference between maximum and minimum SF_6 concentrations within a breath was continuously analysed. Calculation of PBF would start when this difference fell below a predefined level indicating good gas mixing (set at 15% of the average of maximum and minimum SF_6 concentrations) (Figure 2.11). It would usually be achieved after three breaths and calculation of PBF would take place over the subsequent three breaths. The rebreathing time should not exceed 30 seconds as re-circulation of N_2O may occur.

Figure 2-11: Sulphur hexafluoride concentration during rebreathing.

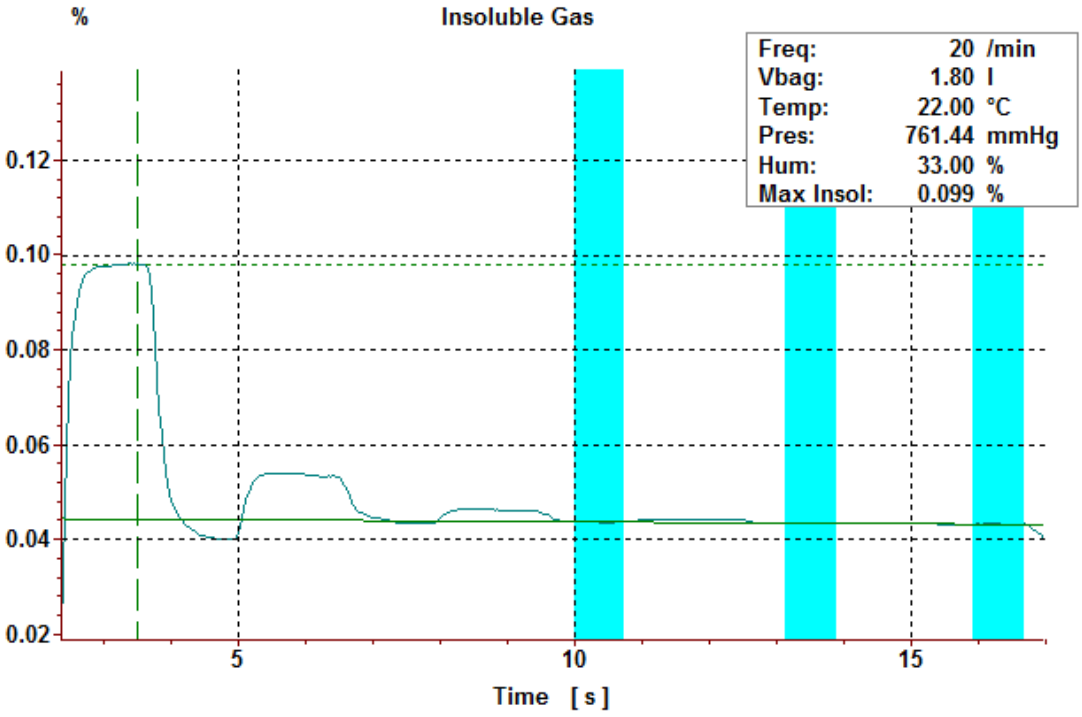

$[SF_6]_0$

Good gas mixing achieved and PBF calculation starts. 3 breaths are included in the calculation indicated by the blue bars.

During the rebreathing period, the lung volume varied slightly due to changes in the rate of carbon dioxide output relative to oxygen uptake. At the start, due to slight hyperventilation, more carbon dioxide entered the alveoli whereas oxygen uptake remained constant. The lung volume increased. As the alveolar carbon dioxide concentration increased, the diffusion gradient decreased. The rate of carbon dioxide output slowed and the lung volume shrunk. Alveolar N_2O concentration was normalised for changes in lung volume using SF_6 concentration before the start of each PBF calculation. As the rate of N_2O concentration decrease was proportional to PBF and N_2O concentration itself, N_2O concentration was a mono-exponentially decreasing function of time giving rise to a linear semi-logarithmic plot of normalised N_2O against time (Figure 2.12).

Figure 2-12: A semi-logarithmic plot of normalised nitrous oxide against time.

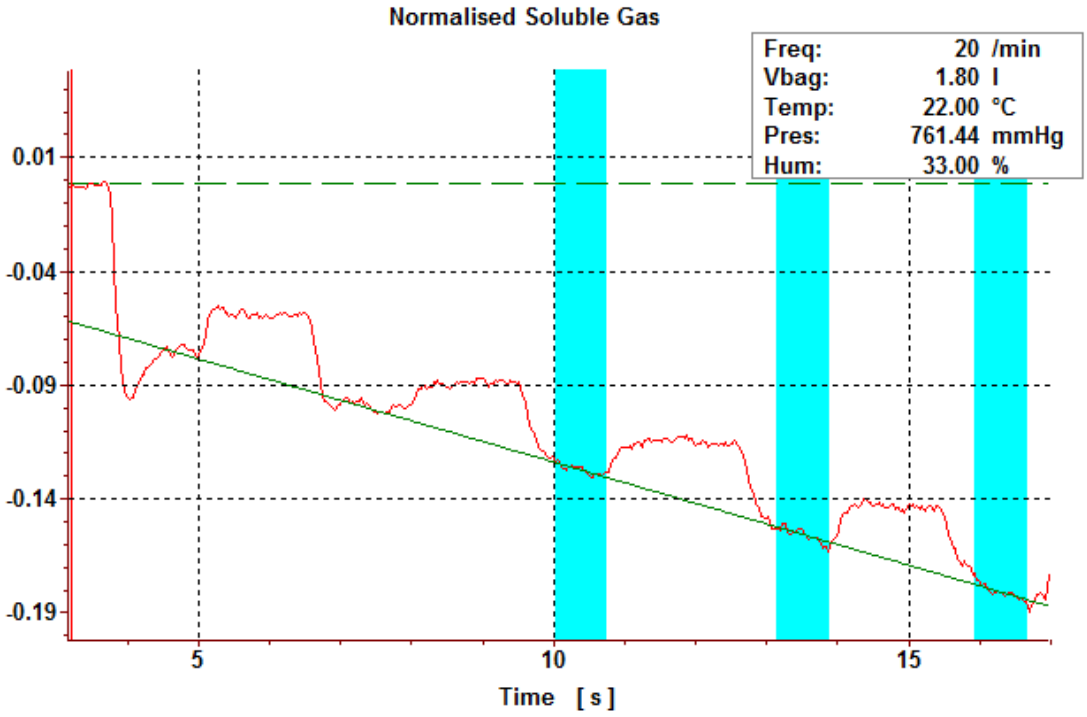

Regression line through the end-expiratory points of 3 breaths after good gas mixing. The slope of the line (β) is calculated directly from the plot.

PBF was calculated using the following formula:

$$\mathrm{PBF} = -\beta . \frac{V_L . C_1 . C_2}{\alpha_b}$$

β = slope of regression line

V_L = total systemic volume (STDP)

C_1 = 760 mmHg/(ambient pressure in mmHg – 47 mmHg)

C_2 = constant to account for absorption of N_2O into lung tissue

= Bunsen solubility coefficient of N_2O in tissue (0.407 STPD) x lung tissue volume (default 0.6 L)

α_b = Bunsen solubility coefficient of N_2O in blood (0.412 STPD)

Pulmonary blood flow (PBF) is equivalent to cardiac output (CO) in the absence of intracardiac or intrapulmonary shunt. SV was derived from PBF and HR.

$$\mathrm{SV} = \frac{\mathrm{PBF}}{\mathrm{HR}}$$

2.7 Statistical methods.

The statistical methodology pertaining to each study in this thesis is described separately, within the relevant chapters.

Chapter 3

Non-invasive stroke volume measurement by cardiac magnetic resonance imaging and inert gas rebreathing in pulmonary hypertension.

3 Non-invasive stroke volume measurement by cardiac magnetic resonance imaging and inert gas rebreathing in pulmonary hypertension.

3.1 Introduction

Pulmonary arterial hypertension (PAH) is a rare disease that is characterised by increased pulmonary vascular resistance leading to chronic right ventricular pressure overload. Without treatment patients have a poor prognosis and die of right heart failure. Although recent therapeutic advances have improved the short-to-medium term outlook of pulmonary hypertension patients, early death due to progressive right ventricular failure remains inevitable in many patients (164, 203).

The functional consequence of a raised pulmonary vascular resistance is a decrease in exercise capacity and a low cardiac output. In patients with PAH, the cardiac output (CO) is directly related to the clinical severity of the disease and is an important prognostic factor (1, 4). Stroke volume (SV) is highly variable in normal subjects and is increased during exercise. Patients with idiopathic PAH are unable to augment their SV in response to exercise due to an exercise induced increase in pulmonary arterial pressure resulting in further impairment of RV function and underfilling of the left vetricle (99). It has been suggested that monitoring SV rather than CO would be a more meaningful outcome measure in PAH patients. Physiologically, a reduction in resting SV can be compensated by an increase in resting heart rate (HR) leading to no or a small net change in CO. A recent cardiac magnetic resonance (CMR) study (73) confirmed that a low baseline stroke volume index (SVI) was predictive of a poor survival whereas cardiac index (CI) was not. In addition, a further reduction in SV at 1 year follow up predicted treatment failure and a poor long term outcome. A noninvasive, accurate measure of SV, therefore, could be beneficial to monitor disease progression in patients with PAH.

Several invasive and noninvasive techniques have been evaluated for the measurement of CO and SV in humans. The “gold standard” is the direct Fick

method, in which the CO is calculated as the quotient of oxygen uptake (VO_2) and the difference of the arterial and mixed venous oxygen content measured during right heart catheterisation (RHC). This method is rarely used in clinical practice, however, primarily because the bedside measurement of oxygen uptake is cumbersome and has been largely replaced by the thermodilution (TD) technique. TD is also performed during RHC and has been demonstrated to have reasonable accuracy in PAH (204). Noninvasive methods of monitoring SV and CO include cardiac magnetic resonance imaging (CMR) and inert gas rebreathing (IGR). CMR imaging is recognised as an accurate and reproducible means of measuring pulmonary arterial flow in patients with PAH (104, 105) despite their inhomogeneous velocity profile. However, a recent study by Mauritz and colleagues has suggested that CMR measurement of LV volumes and aortic flow are to be preferred for the measurement of SV in PAH patients (102). IGR, using the acetylene rebreathing technique, has been validated for measuring CO in PAH patients (204). A new rebreathing technique using rapid photoacoustic analysis of nitrous oxide has been introduced and validated in left heart failure. This technique has not yet been validated in patients with PAH.

The aim of this study was to determine the accuracy of SV measurement by CMR imaging and by IGR using photoacoustic analysis compared with the thermodilution technique measured during RHC in patients with suspected pulmonary hypertension.

3.2 Methods and Materials

3.2.1 Patients and Protocol

This was a cross-sectional study of thirty-three consecutive patients attending for assessment at the Scottish Pulmonary Vascular Unit (Glasgow, UK), with a provisional diagnosis of pulmonary hypertension determined by echocardiography. Patients had CO measured by (i) thermodilution technique during RHC, (ii) CMR imaging (pulmonary artery flow measurements), (iii) CMR imaging (aortic flow measurements) and (iv) IGR. These four techniques were performed within 48 hours of each other. The patients were supine during each technique and the measurements were performed after 5 minutes of rest. The

study protocol was approved by the Glasgow West Research Ethics Review Committee. All subjects gave informed written consent.

3.2.2 Right heart catheterisation and thermodilution measurements

A 7F gauge, balloon-tipped, flow directed Swan-Ganz catheter was advanced through an 8F introducer sheath inserted into the right internal jugular vein or the right femoral vein. CO was measured by the thermodilution technique (202) following injection of 10ml of ice-cold, 0.9% saline through the proximal (right atrial) lumen of the catheter. The drop in temperature was measured at the distal thermistor. The final value used was the average of three measurements agreeing within 10%.

3.2.3 CMR image acquisition and analysis

CMR imaging was performed on a 1.5T Sonata MRI scanner (Siemens Medical Solutions, Erlangen, Germany) with simultaneous ECG recording using a protocol that has been described in detail in the materials and methods section of this thesis. Right ventricular SV was measured using MR phase-contrast flow quantification in an image plane positioned perpendicular to the main pulmonary artery, at least 1cm distal to the pulmonary valve. Left ventricular SV (aortic flow) was also measured, approximately 2 - 4cm above the aortic valve and distal to the coronary arterial ostia. A velocity encoded k-space segmented gradient-echo sequence was used (imaging parameters: echo time / repetition time / flip angle / slice thickness / temporal resolution / image matrix / field of view / in-plane resolution / velocity encoding range = 3.1ms / 16ms / 15° / 6mm / limited by TR / 256 / 380mm / 1.9x1.5mm / 150cm per second) to generate 45 matched pairs of anatomical and velocity images. Retrospective ECG-gating was used to ensure coverage of the complete cardiac cycle. Patients were instructed to breath freely throughout this section of the protocol and the average time of acquisition was 2-3 minutes depending on the patient's heart rate.

All MR images were analysed by a single operator (L.M.) using the Argus analysis software (Siemens, Erlangen, Germany). Individual scans were coded by number

and analysed in batches by L.M. who was blinded to the haemodynamic and inert gas rebreathing results of any given subject at the time of analysis.

3.2.4 Inert Gas Rebreathing

The rebreathing system (Innocor®, Innovision A/S, Denmark) consisted of a three-way respiratory valve with a mouthpiece and a rebreathing bag connected to an infrared photoacoustic gas analyser (AMIS 2001; Innovision A/S) (125). Pulmonary blood flow (PBF) was measured by rebreathing a gas mixture of 0.1% sulphur hexafluoride (SF_6) and 0.5% nitrous oxide (N_2O) through a mouthpiece with nose occluded. Gas was sampled continuously from the mouthpiece for analysis by the infrared photoacoustic gas analyser. The rebreathing software calculated the PBF from the rate of uptake of N_2O into the blood (slope of the regression line through the logarithmically transformed end-expiratory [i.e. alveolar] N_2O concentrations plotted against time) after correction for system volume changes using the SF_6 (blood insoluble gas) concentrations. CO was assumed to be equivalent to PBF and right ventricular SV was derived by dividing PBF by heart rate. Repeatability of SV measurements by IGR was assessed by comparing the results from two IGR efforts.

3.2.5 Statistical Analysis

Data are given as mean ± SD unless otherwise specified. Correlation coefficients were calculated using the Pearson method. The agreement between the three techniques was analysed in a pairwise manner using the method described by Bland and Altman (205). All calculations were performed using GraphPad Prism (Version 4.00, GraphPad Software Inc, La Jolla, USA).

3.3 Results

Patient characteristics and haemodynamic variables are shown in Table 3.1. The results of the diagnostic evaluation are shown in Table 3.2. The presence of pulmonary hypertension was confirmed in 29 patients and 15 were diagnosed as having PAH. Four patients had no evidence of a raised mean pulmonary artery pressure (mPAP) as determined by RHC. Twelve patients had significant lung pathology (3 patients with chronic obstructive pulmonary disease [COPD]

[normal mPAP], 3 with pulmonary hypertension secondary to COPD and interstitial lung disease [ILD], 3 with PAH associated with connective tissue disease [CTD] and ILD, 1 with PAH secondary to sarcoidosis and 2 patients with pleural effusions secondary to left heart disease). Thirty-two patients provided satisfactory IGR measurements. This technique was unsuccessful in one patient with interstitial lung disease (sarcoidosis) due to severe destructive lung disease. Thirty patients completed CMR imaging and 30 patients underwent diagnostic RHC.

Table 3-1: Baseline characteristics of the subjects in the study.

Parameter	Value (mean ± SD)
Number of patients	**33**
Age	**55 ± 17 years**
Sex (male:female)	**17:16**
Echo PASP	**69 ± 25 mmHg**
mPAP	**39 ± 12 mmHg**
CI	**2.34 ± 0.52 L/min/m2**
PVRI	**4.50 ± 3.49 WU/m2**
6MWD	**327 ± 113 m**
FEV1	**2.11 ± 0.88 L/min**
FVC	**3.09 ± 1.33 L/min**

Data are expressed as mean ± standard deviation. 33 patients were enrolled into this study. PASP; pulmonary artery systolic pressure. mPAP; mean pulmonary artery pressure. CI; cardiac index. PVRI; pulmonary vascular resistance index. 6MWD; six minute walk distance. FEV1; forced expiratory volume in 1 second. FVC; forced vital capacity.

Table 3-2: Results of diagnostic evaluation.

Diagnosis	Number
No pulmonary hypertension	4
Pulmonary arterial hypertension	
- Idiopathic (IPAH)	9
- Familial (FPAH)	1
- Connective tissue disease	4
- HIV infection	1
Pulmonary hypertension associated with left heart disease	4
Pulmonary hypertension associated with lung disease/hypoxia	
- Chronic obstructive pulmonary disease	2
- Interstitial lung disease	1
Chronic thromboembolic pulmonary hypertension	
- Obstruction of proximal pulmonary arteries	2
- Obstruction of distal pulmonary arteries	4
Miscellaneous	
- Sarcoidosis	1

The average (± SD) SV values from the three techniques were as follows: CMR SV aortic flow 55.26 (± 23.67)ml, CMR SV pulmonary artery flow 61.77 (± 25.14) ml, TD SV 61.87 (± 22.90) ml and IGR SV 57.02 (± 25.01) ml. The reproducibility of the IGR SV measurements had a coefficient of variation of 6.9%. The correlation plots and Bland-Altman analyses for the 3 comparisons are shown in Figures 3.1, 3.2 and 3.3 and summarised in Table 3.3.

Figure 3-1: Correlation plot and Bland-Altman analysis comparing stroke volume measured by thermodilution and CMR (aortic flow).

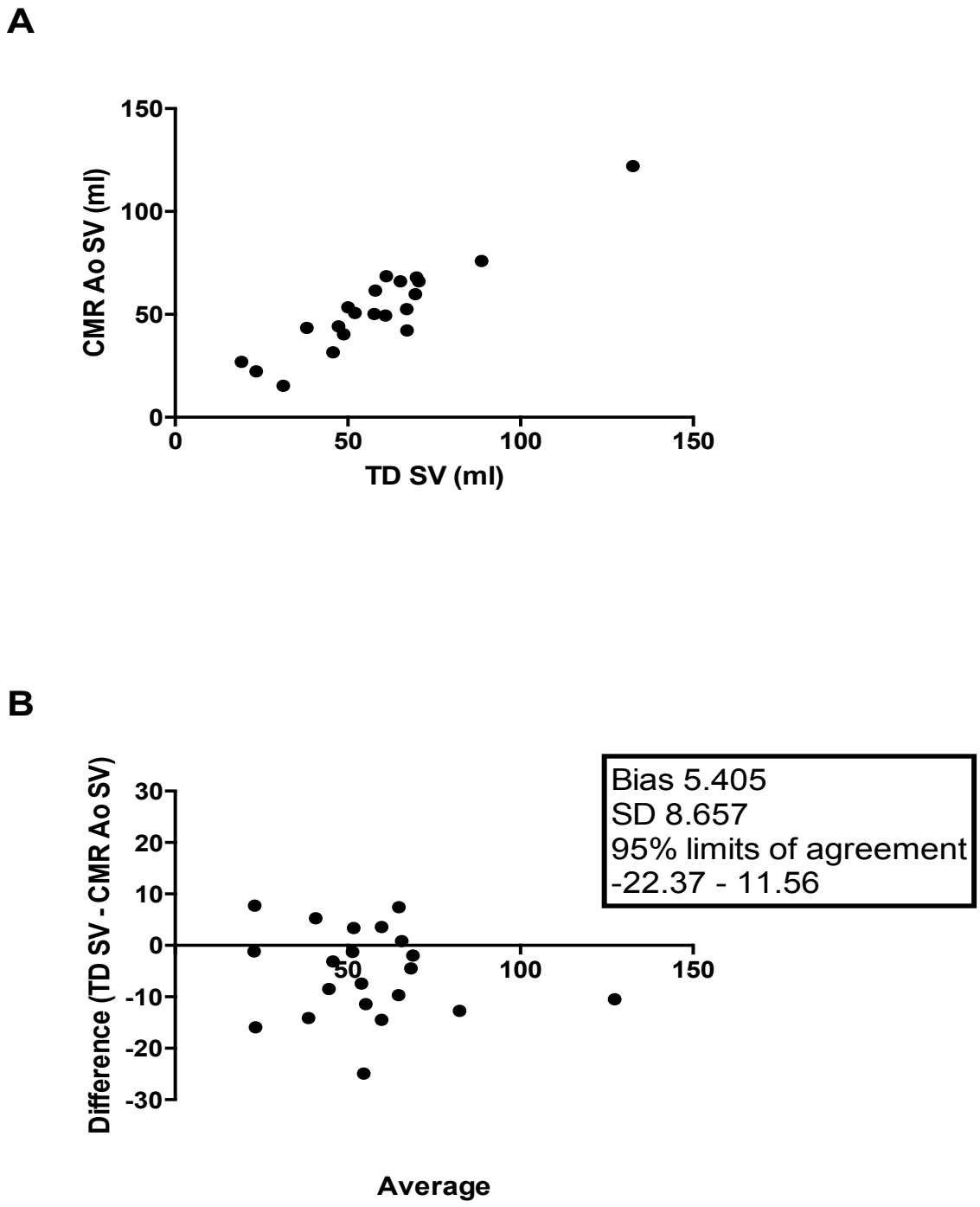

A: Correlation plot comparing SV measured by thermodilution and CMR aortic flow methods. n = 21, r = 0.9322, p < 0.0001.

B: Bland-Altman plot: Agreement between paired measurements of stroke volume measured by thermodilution and aortic flow by CMR.

SV: stroke volume. TD: thermodilution. Ao: aortic. CMR: cardiac magnetic resonance. n = number of patients. r = correlation coefficient.

Figure 3-2: Correlation plot and Bland-Altman analysis comparing stroke volume measured by thermodilution and CMR (pulmonary artery flow).

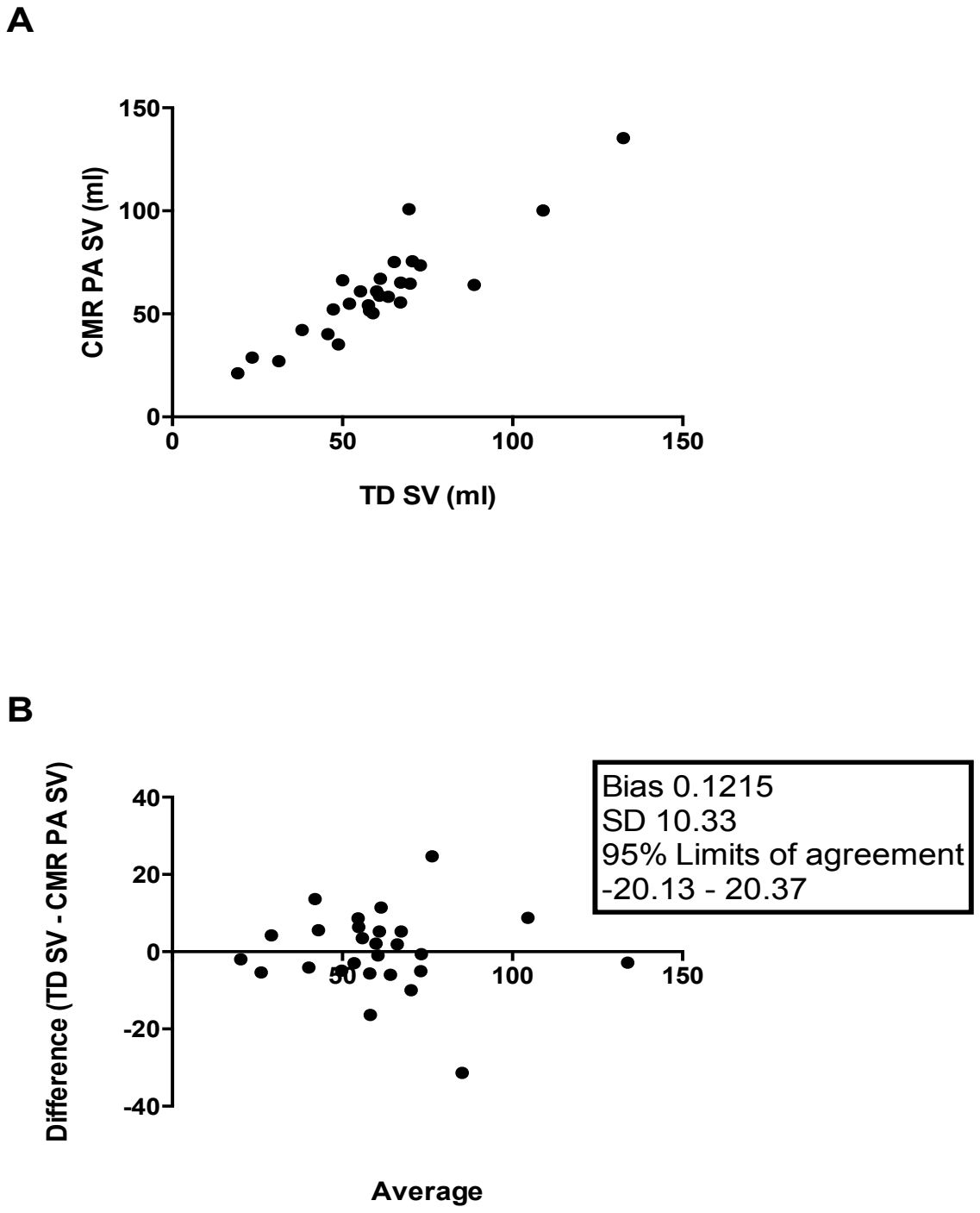

A: Correlation plot comparing stroke volume measured by thermodilution and cardiac magnetic resonance pulmonary artery flow. **n = 27, r = 0.9048, p < 0.0001.**

B: Bland-Altman plot; Agreement between paired measurements of stroke volume measured by thermodilution and cardiac magnetic resonance pulmonary artery flow methods.

n; number of patients. r; correlation coefficient. SV; stroke volume. TD; thermodilution. CMR; cardiac magnetic resonance. PA; pulmonary artery.

Figure 3-3: Correlation plot and Bland-Altman analysis comparing stroke volume measured by thermodilution and inert gas rebreathing.

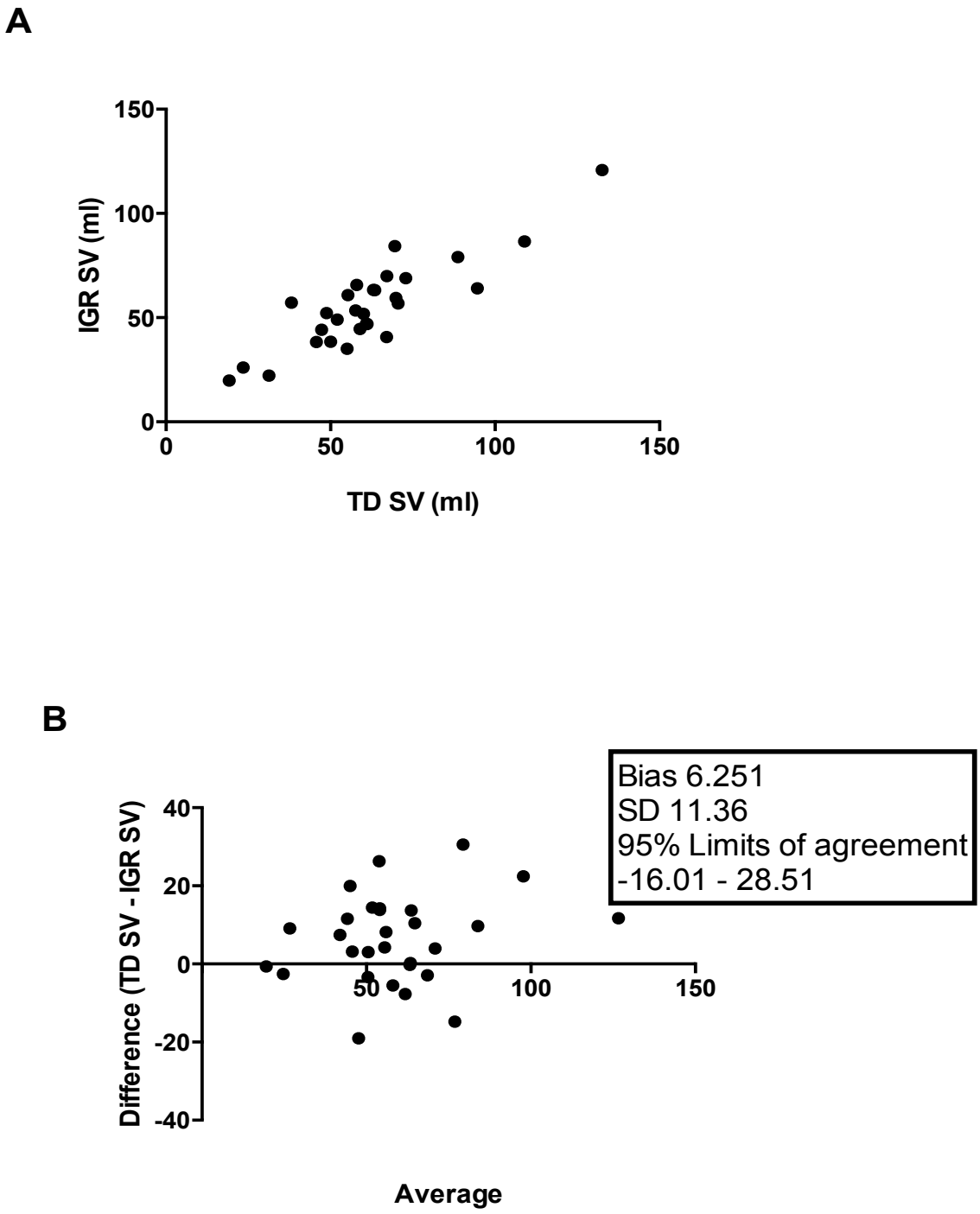

A: Correlation plot comparing stroke volume measured by thermodilution and inert gas rebreathing method. **n = 29, r = 0.8735, p < 0.0001.**

B: Bland-Altman plot; Agreement between paired measurements of stroke volume measured by thermodilution and inert gas rebreathing.

SV; stroke volume. TD; thermodilution. IGR; inert gas rebreathing. n; number of patients. r; correlation coefficient.

Table 3-3: Summary of Bland-Altman analyses performed.

Methods	Number	Correlation coefficient	Bias (ml)	95% Limits of Agreement (ml)	
				From	To
TD SV vs CMR Ao SV	21	0.9322	-5.405	-22.37	11.56
TD SV vs CMR PA SV	27	0.9048	0.1215	-20.13	20.37
TD SV vs IGR SV	29	0.8735	6.251	-16.01	28.51

TD; thermodilution. SV; stroke volume. CMR; cardiac magnetic resonance. Ao; aortic. PA; pulmonary artery. IGR; inert gas rebreathing. vs; versus.

The IGR technique is reported to be less accurate in the presence of parenchymal lung abnormalities (206). In our cohort, 12 patients had significant lung disease, as determined by high resolution computed tomography imaging and pulmonary function testing. The Bland-Altman analysis was repeated on both this subset and the whole cohort with this subset excluded and the results are shown in Table 3.4. As expected, the limits of agreement widen in the group with lung disease although the bias remains small.

Table 3-4: Results of Bland-Altman analyses performed in the presence and absence of lung disease.

Methods	Bias (ml)	95% Limits of Agreement (ml)	
		From	To
No lung disease			
IGR vs TD	-6.23	-25.47	13.02
Lung disease			
IGR vs TD	2.47	-27.88	32.81

IGR: inert gas rebreathing. TD; thermodilution.

3.4 Discussion

The aim of this study was to evaluate the performance of CMR imaging and inert gas rebreathing using a device based on photoacoustic analysis for the measurement of CO in patients with PAH. With the advent of multiple new disease targeted therapies for PAH it is increasingly important that we can assess the progress of patients in a non-invasive manner.

To evaluate these techniques, the results were compared with those from the widely accepted reference standard, thermodilution measured during right heart catheterisation. Bland-Altman analysis confirmed acceptable levels of agreement between the four techniques. Measurement of SV by aortic flow analysis during CMR imaging provided the most accurate results when compared to our reference standard. IGR was the least accurate of the techniques employed with increased 95% limits of agreement. The level of agreement, however, remained acceptable for this technique. The presence of parenchymal lung disease is a source of error in the IGR measurement of PBF and, as expected, caused a marginal impairment in the accuracy of the IGR results. It was still possible, however, to obtain reasonable results in this subgroup of patients. This study highlighted the ease with which IGR can be performed. The method was acceptable to all patients, even breathless patients with significant lung disease and the technique failed in only one subject who had severe

destructive lung disease (sarcoidosis). Reproducibility of the IGR technique was equivalent to that of the six minute walk test (8%) (139).

There have been many techniques, both invasive and noninvasive, proposed for the measurement of CO and these have had mixed success. These include the Fick (direct and indirect) method, indicator dilution techniques (including thermodilution), CMR imaging, IGR, echocardiography, electrical bioimpedance and pulse contour analysis. Since the introduction of the Swan-Ganz catheter in 1971 (202), the thermodilution technique (207) has been used extensively to measure CO in the clinical setting. It provides reliable results in healthy volunteers and in patients with cardiovascular disease (208) although there are concerns about its accuracy in patients with low CO or severe tricuspid regurgitation (209-213) which are both commonly present in patients with severe PAH. Hoeper *et al* (204) explored this question in detail and concluded that thermodilution provided a reliable assessment of CO in patients with pulmonary hypertension. One hundred and five CO measurements by the Fick method and thermodilution were compared in 35 patients with PAH. The mean difference ± 95% limit of agreement between thermodilution and the Fick method was + 0.01 ± 1.1L/min. As a consequence, the clinical evaluation of new methods is often done by comparison with the thermodilution method.

This study used CMR imaging to measure SV (214, 215). CMR imaging is recognised as an accurate and reproducible means of measuring pulmonary arterial flow in patients with PAH (104, 105) despite the inhomogeneous velocity profile. A recent study by Mauritz and colleagues has suggested that CMR measurement of LV volumes and aortic flow are to be preferred for the measurement of SV in PAH patients (102). Mauritz *et al* compared SV measurement by CMR and right heart catheterisation (Fick method). In a subset of 9 patients, the correlation of SV with CMR aortic flow (r=0.95) was stronger than with CMR pulmonary flow (r=0.76). In contrast, Bland-Altman analysis of our results confirmed that CMR aortic and pulmonary artery flow analysis provided very similar limits of agreement and minimal bias suggesting they could both be utilised for the measurement of SV in PAH patients.

IGR was introduced by August Krogh in 1912 and has been widely validated (126-129). This technique for CO measurement has been validated in PAH patients

using the acetylene rebreathing technique (204). It measures pulmonary blood flow (PBF), which is equivalent to cardiac output (CO) in the absence of intracardiac and intrapulmonary shunts (125). However, IGR measurements have traditionally required the use of mass spectrometers which are bulky, difficult to operate and require frequent calibration and maintenance. The new device employed in this study uses rapid photoacoustic analysis of gas concentrations. This device was recently validated against the direct Fick and thermodilution methods in a cohort of patients with stable heart failure (130) and in patients pre- and post-cardiac surgery (131). It has been successfully performed in patients with left heart failure during exercise combined with metabolic stress testing (216). So far only 3 patients with PAH have been evaluated using the Innocor device prior to this study (125). This device is of interest because of its ease of use and flexibility, as it can be used in both resting and exercise settings.

IGR becomes less accurate in conditions that affect the intra-alveolar distribution of gas such as in the presence of severe interstitial or obstructive lung disease (206). Kallay *et al* (217), using a mass spectrometer observed good agreement between PBF determined by rebreathing and CO determined by indicator dilution techniques in a group of patients with various cardiopulmonary diseases with preserved pulmonary function. However, the agreement was weakened when patients exhibited either restrictive or combined restrictive and obstructive pulmonary disease. Twelve patients in our study had significant lung disease. Analysis of the IGR technique in this patient subgroup demonstrated a reduction in accuracy with increased 95% limits of agreements. However, the level of agreement remained acceptable and IGR may still prove to be useful in this patient group.

The evaluation of treatment efficacy of pulmonary vascular disease would benefit from noninvasive tools to monitor haemodynamic changes. Although CMR is noninvasive, it is an expensive, inflexible and technically demanding alternative to measure SV. IGR measured by the Innocor® device could easily be performed in the outpatient setting as it is quick and readily tolerated and could have several applications such as:-

- serial, longitudinal measurements in PAH patients on medication to demonstrate treatment efficacy
- estimation of exercise stroke volume as this may be more sensitive to changes in the underlying pathology of the disorder than resting measurements

Our study was limited by the small number of patients recruited. Also, the four techniques were not completed by all patients making the population for analysis within each group different (eleven patients could not complete CMR imaging, IGR was unsuccessful in one patient and three patients did not proceed to RHC). The techniques to measure PBF in this study were not contemporaneous but performed within 48 hours of each other. Further investigation, however, indicated there was no significant variation in heart rate between each of the measurements. A potential source of error in the determination of CO by rebreathing is the presence of shunted blood through areas without gas exchange. In this study, we assumed PBF was equivalent to CO and did not investigate further for the presence of shunted blood flow.

This study has demonstrated that both cardiac magnetic resonance imaging and inert gas rebreathing using photoacoustic analysis can provide non-invasive measurements of stroke volume that are as accurate as those obtained by thermodilution in patients with suspected PAH. The presence of lung disease caused a marginal impairment in the accuracy of the IGR method.

Chapter 4

Comparison of right ventricular function, assessed by cardiac magnetic resonance imaging, in patients with idiopathic pulmonary arterial hypertension versus connective tissue disease associated pulmonary arterial hypertension: A cross-sectional study.

4 Comparison of right ventricular function, assessed by cardiac magnetic resonance imaging, in patients with idiopathic pulmonary arterial hypertension versus connective tissue disease associated pulmonary arterial hypertension: A cross-sectional study.

4.1 Introduction

Pulmonary arterial hypertension (PAH) is a progressive disease with a poor prognosis, although there have been recent improvements in survival with the introduction of disease targeted therapy. Idiopathic PAH (IPAH) is the most common cause of pulmonary arterial hypertension. An important clinical subgroup is PAH associated with connective tissue disease (CTDPAH), which is the second most prevalent type of PAH in the registries (8, 9). Systemic sclerosis (SSc) represents the main CTD associated with PAH (SSc-PAH). SSc-PAH is particularly aggressive and accounts for 30% of deaths among SSc patients (218). There is a relative paucity of literature regarding the outcome of CTDPAH in conditions other that SSc. The prognosis for patients with SSc-PAH remains poor and worse compared to other PAH subgroups. The 1 year mortality in IPAH is approximately 15% (219) versus 30% in PAH associated with scleroderma (220). A more recent prospective study has reported an improvement in survival in SSc-PAH patients at 1 year in the modern treatment era, although the outlook at 3 years remained very poor (221).

CTDPAH has a less favourable response to modern therapy and worse survival for reasons that remain unclear. Factors such as age and other comorbidities (e.g. cardiac and lung parenchymal involvement) do not fully account for this difference in outcomes (222). Baseline resting haemodynamic measurements offer valuable information in terms of severity and prognosis of PAH. Increased right atrial pressure (RAP), decreased cardiac index (CI), and increased mean pulmonary artery pressure (mPAP) are predictors of a poor prognosis in IPAH (4). Although these data have been validated in IPAH, they remain of unclear

usefulness in SSc-PAH. Recent studies have highlighted the lack of correlation between baseline haemodynamic data and clinical evolution in patients with SSc-PAH. These patients appear to have less severe alterations in haemodynamics compared with IPAH (8, 222, 223). In a retrospective analysis comparing baseline haemodynamic data in patients with IPAH and SSc-PAH, patients with SSc-PAH had a significantly lower mPAP and pulmonary vascular resistance (PVR), and equally depressed CI compared to patients with IPAH; However, follow up indicated they were 4 times more likely to die compared with patients with IPAH despite comparable therapy (222). These paradoxical findings suggest that the RV may have a reduced ability to adapt to increased PVR in SSc-PAH. RV adaptation and ventricular remodeling in PAH is a complex process that depends on multiple factors including the severity of pulmonary vascular disease, neurohormonal activation, myocardial perfusion, and myocardial metabolism (38, 42, 93, 224-231). Other factors that could influence RV adaptation include the rate and time of onset of PAH, its underlying aetiology, and genetic factors

Studies comparing haemodynamic measurements and survival of patients with IPAH and SSc-PAH suggest that increased myocardial dysfunction from failure to adapt to increased pulmonary vascular load might contribute to the poorer prognosis in SSc-PAH. Overbeek *et al* investigated the differences in RV pump function (using the pump function graph which relates mean RV pressure to SV index) between IPAH and SSc-PAH patient groups (232). They concluded that RV contractility was lower in SSc-PAH than in IPAH. More recently, Tedford and colleagues, using pulmonary resistance compliance relations and invasive PV loop analysis, concluded that intrinsic systolic RV dysfunction accounted for the poorer prognosis in the SSc-PAH patient cohort compared with IPAH (233). Patients with SSc-PAH have relatively depressed RV function, despite similarly augmented pulmonary afterload compared with IPAH.

The purpose of this study was to examine the haemodynamic and CMR findings, in the well-characterised populations of IPAH and CTDPAH, and to evaluate whether differences exist in cardiac structure and function that might affect survival. The reason for poorer survival in CTDPAH patient group remains poorly understood. We hypothesise that there will be a difference in right heart

adaptation, as determined by CMR, for a given mPAP that could account for the poorer prognosis in the CTDPAH group.

4.2 Methods

4.2.1 Study population

This was a cross-sectional study of fifty patients attending for assessment at the Scottish Pulmonary Vascular Unit (SPVU). The inclusion criteria were patients with a diagnosis of idiopathic pulmonary arterial hypertension (IPAH) or connective tissue disease related pulmonary arterial hypertension (CTDPAH). The study subjects were either incident patients attending the SPVU for initial diagnostic assessment or prevalent patients in whom disease targeted therapy was being modified. The diagnosis of PAH was based on RHC in accordance with contemporary guidelines (7). This study was approved by the West Glasgow Research Ethics Committee and written informed consent was obtained from all study participants.

4.2.2 Study design

All patients underwent CMR imaging followed by RHC within a 48 hour period. Conventional outcome measures including WHO functional class and 6 minute walk distance were also recorded.

4.2.3 Cardiac magnetic resonance (CMR) image acquisition and analysis

CMR imaging was performed on a 1.5 Tesla MRI scanner (Sonata Magnetom, Siemans, Germany). CMR was performed using a protocol described in detail in the materials and methods chapter of this thesis. All CMR images were analysed by a single operator (L.M.) using the Argus analysis software (Siemans, Erlangen, Germany). Individual scans were coded by number and analysed in batches by L.M. who was blinded to the haemodynamic and six minute walk distance results of any given subject at the time of analysis. Table 4.1 documents the measurements obtained from the CMR assessment.

Table 4-1: Measurements obtained in this study from cardiac magnetic resonance imaging.

Measurements obtained from CMR Imaging
Right ventricular end diastolic volume (RVEDV)
Right ventricular end systolic volume (RVESV)
Left ventricular end diastolic volume (LVEDV)
Left ventricular end systolic volume (LVESV)
Right ventricular mass (RVM)
Left ventricular mass (LVM)
Pulmonary artery flow analysis – stroke volume (PASV)
Aorta flow analysis – stroke volume (AoSV)

4.2.4 Right heart catheterisation

RHC was performed according to international recommendations (160). A 7F gauge, balloon tipped, flow directed, triple channel thermodilution Swan-Ganz catheter (Baxter Healthcare, Irvine, California, USA) was advanced through an 8F introducer sheath inserted into the right internal jugular vein or the right femoral vein. All measurements were recorded with the patient in a supine position, at rest, breathing room air or supplemental oxygen if required. Please refer to materials and methods section of this thesis for further information on RHC methodology.

4.2.5 Six-minute walk test

The 6MWT was performed on a 20-metre corridor, but otherwise according to the American Thoracic Society guidelines (234).

4.2.6 Statistical analysis

Statistical analysis was performed using SPSS version 15.0 (SPSS Inc., Chicago, Illinois, USA) and Graphpad Prism Version 6 (Graphpad Software, California, USA). Data are given as mean ± standard deviation (SD) unless otherwise stated. Correlation coefficients were calculated using the Pearson method.

4.3 Results

4.3.1 Patient characteristics

Fifty patients with PAH (30 IPAH and 20 CTDPAH) were recruited for this study. All patients underwent CMR imaging and RHC. 4 patients were unable to complete the full CMR protocol. 3 patients (WHO functional class IV) were unable to perform a 6 minute walk test. Table 4.2 presents the demographic data, WHO functional class, 6 minute walk distance and haemodynamic data for both groups of patients. There was no significant difference in age or BSA between the IPAH and CTDPAH patient groups. There was a higher proportion of female patients in the CTDPAH group. The functional status of both patient groups was similar. The majority of patients were in WHO functional class III. There was no significant difference in the 6 minute walk distance achieved between the 2 groups (252.7 ± 117.7 versus 262.4 ± 133.7, p=0.79). Haemodynamic measurements confirmed that all patients in this study had significant pulmonary hypertension. 50 patients had an elevated mPAP and PVR during RHC. The diagnosis of IPAH or CTDPAH was ascertained at the SPVU multidisciplinary meeting. There was no significant difference in mPAP (46.67 ± 10.72 versus 43.10 ± 15.13, p=0.33), cardiac index (2.14 ± 0.48 versus 2.27 ± 0.55, p=0.39) or PVRI (6.50 ± 3.46 versus 4.19, p=0.84) between these distinct patient groups.

Table 4-2: Baseline characteristics for patients enrolled in this study.

Characteristic	IPAH (n=30)	CTDPAH (n=20)	p value
Number of patients	30	20	
Age (years)	53.93 ± 17.69	57.88 ± 14.19	0.4079
Female:Male	21:9	18:2	
BSA	1.753 ± 0.2629	1.660 ± 0.2324	0.2044
mPAP (mmHg)	46.67 ± 10.72	43.10 ± 15.13	0.3337
CI (L/min/m2)	2.12 ± 0.42	2.26 ± 0.55	0.2949
PVRI (WU/m2)	6.62 ± 3.44	6.74 ± 4.59	0.9183
6 MWD (m)	252.7 ± 117.7	262.4 ± 133.7	0.7948

Baseline characteristics for the 50 patients enrolled in this study are documented. Data are expressed as mean ± standard deviation. BSA: body surface area; mPAP: mean pulmonary artery pressure: CI: cardiac index; PVRI: pulmonary vascular resistance index; 6MWD; six minute walk distance.

4.3.2 CMR measurements

Table 4.3 documents CMR measurements obtained from all patients in the study. 4 patients were unable to complete the full CMR protocol. 50 patients completed the mass and volumetric assessment. 49 patients completed pulmonary artery flow analysis and only 46 patients managed to complete aortic flow analysis. There was a significant difference in ventricular mass index (VMI). The CTDPAH group had a significantly lower VMI than the IPAH group (0.85 ± 0.23 versus 1.12 ± 0.44, p=0.01). Left ventricular ejection fraction (LVEF) was significantly higher in the CTDPAH group (62.08 ± 11.57 versus 50.91 ± 17.15, p=0.02). There were no further significant differences in CMR measurements between the 2 groups.

Table 4-3: Baseline cardiac magnetic resonance measurements for enrolled patients.

CMR Measurement	IPAH n = 30	CTDPAH n = 20	p value
RVEDVI	85.59 ± 26.16	77.58 ± 20.32	0.2536
RVESVI	57.95 ± 26.27	47.75 ± 24.58	0.1743
RVMI	55.77 ± 26.47	47.45 ± 16.70	0.2186
LVEDVI	46.68 ± 12.56	48.56 ± 15.72	0.6412
LVESVI	18.53 ± 6.876	17.19 ± 9.388	0.5627
LVMI	49.63 ± 10.09	55.76 ± 12.91	0.0661
VMI	1.124 ± 0.4418	0.849 ± 0.2278	0.0137 *
RVSVI (PA)	31.38 ± 11.78	29.64 ± 11.67	0.6084
LVSVI (Aorta)	25.11 ± 11.03	30.02 ± 7.366	0.1184
RVEF	38.52 ± 15.04	43.08 ± 23.66	0.4077
LVEF	50.91 ± 17.15	62.08 ± 11.57	0.0243 *

Ventricular dimensions and function measured by CMR imaging in 50 patients with pulmonary hypertension (30 IPAH and 20 CTDPAH). Data are expressed as mean ± standard deviation. IPAH; idiopathic pulmonary arterial hypertension. CTDPAH; pulmonary arterial hypertension associated with connective tissue disease. CMR; cardiac magnetic resonance. PA; pulmonary artery.

Figure 4-1: Bar graphs depicting ventricular dimensions and function measured by CMR in IPAH and CTDPAH patient groups

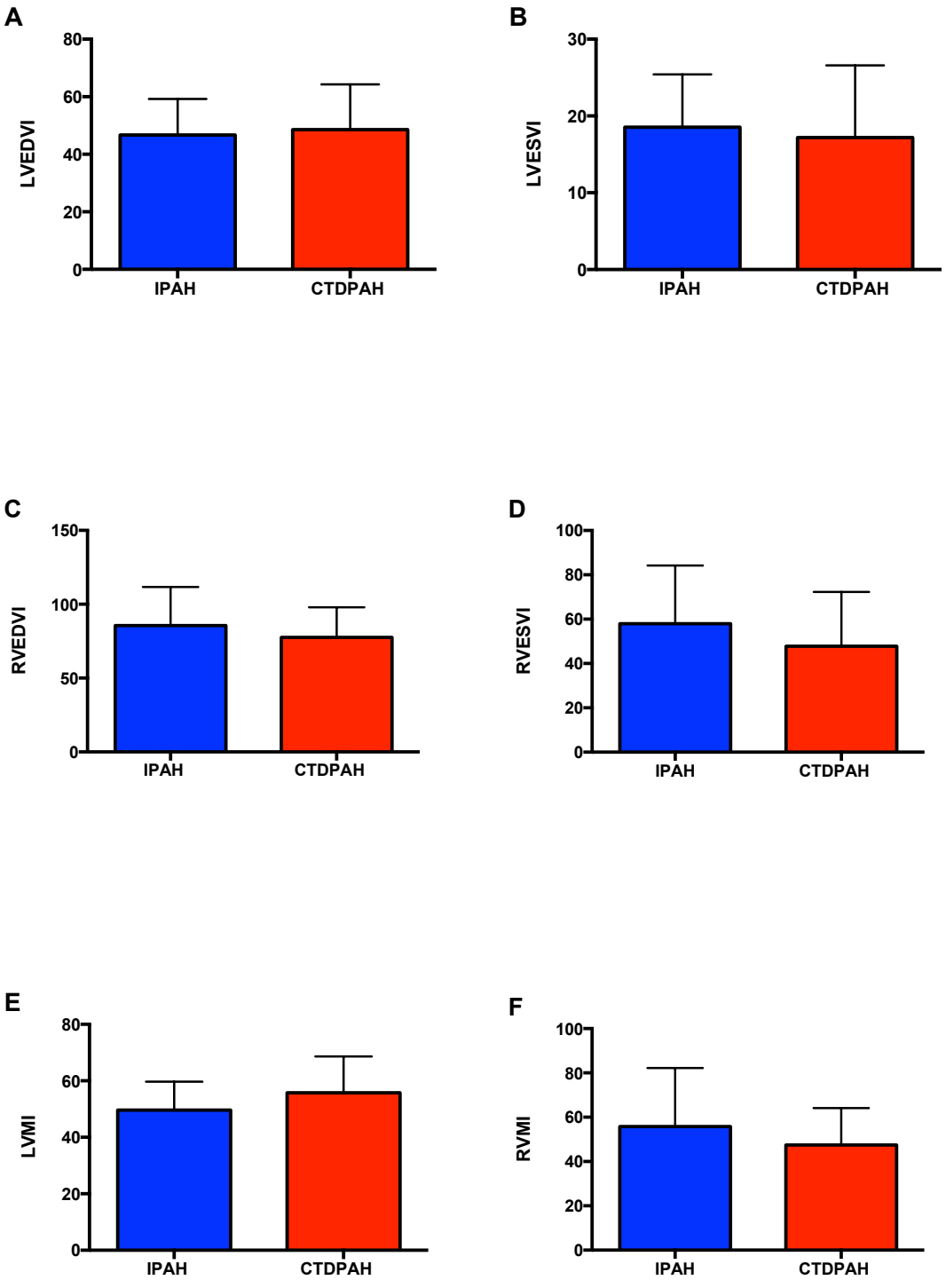

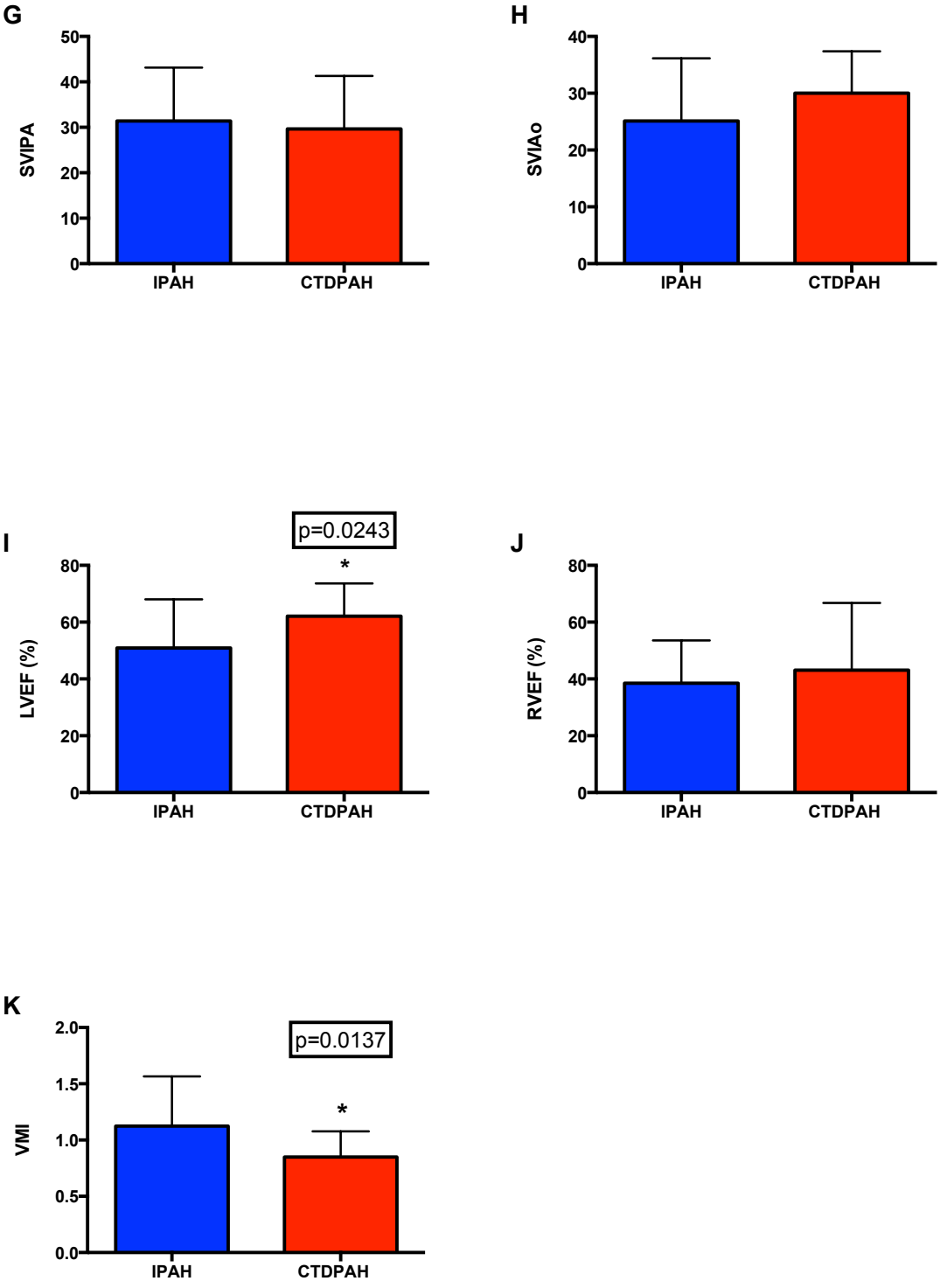
G
SVIPA
50
40
30
20
10
0
IPAH
CTDPAH
H
SVIAo
40
30
20
10
0
IPAH
CTDPAH
I
p=0.0243
*
LVEF (%)
80
60
40
20
0
IPAH
CTDPAH
J
RVEF (%)
80
60
40
20
0
IPAH
CTDPAH
K
p=0.0137
*
VMI
2.0
1.5
1.0
0.5
0.0
IPAH
CTDPAH

Legend for Figure 4.1

IPAH: idiopathic pulmonary arterial hypertension. CTDPAH: pulmonary arterial hypertension associated with connective tissue disease.

A: Bar graph demonstrating LVEDVI (left ventricular end diastolic volume index) measurements in IPAH and CTDPAH groups.

B: Bar graph demonstrating LVESVI (left ventricular end systolic volume index) measurements in IPAH and CTDPAH groups.

C: Bar graph demonstrating RVEDVI (right ventricular end diastolic volume index) measurements in IPAH and CTDPAH groups.

D: Bar graph demonstrating RVESVI (right ventricular end systolic volume index) measurements in IPAH and CTDPAH groups.

E: Bar graph demonstrating LVMI (left ventricular end mass index) measurements in IPAH and CTDPAH groups.

F: Bar graph demonstrating RVMI (right ventricular mass index) measurements in IPAH and CTDPAH groups.

G: Bar graph demonstrating SVIPA (stroke volume index measured from pulmonary artery) measurements in IPAH and CTDPAH groups.

H: Bar graph demonstrating SVIAo (stroke volume index measured from aorta) measurements in IPAH and CTDPAH groups.

I: Bar graph demonstrating LVEF (left ventricular ejection fraction) measurements in IPAH and CTDPAH groups. There was a significant difference between these patient groups ($p = 0.0243$)

J: Bar graph demonstrating RVEF (right ventricular ejection fraction) measurements in IPAH and CTDPAH groups.

K: Bar graph demonstrating VMI (ventricular mass index) measurements in IPAH and CTDPAH groups. There was a significant difference between these patient groups ($p = 0.0137$).

4.3.3 Correlation between mPAP and CMR measurements

Please refer to table 4.4 and Figure 4.2. The mPAP correlates significantly with CMR measurements of the right heart (RVEDVI, RVESVI, RVMI, RVEF and VMI) in both the groups. These results are in agreement with previously published literature. The mPAP correlated most strongly with RVMI and VMI, in both the IPAH and CTDPAH patient groups. There was a significant correlation between mPAP and LVEDVI ($p=0.02^*$) and LVSVI ($p=0.02^*$) in the CTDPAH group. A further significant correlation was also identified between mPAP and LVEF ($p=0.0058^{**}$) in the IPAH group only.

Multiple linear regression analysis identified no significant change in right heart structure and function (right heart adaptation) for a given mPAP between the IPAH and CTDPAH patient groups.

Table 4-4: Correlations between mean pulmonary artery pressure measurements and cardiac magnetic resonance measurements.

CMR measurement versus mPAP	IPAH	CTDPAH
RVEDVI	r = 0.4205 p = 0.0207 * n = 30	r = 0.4712 p = 0.0360 * n = 20
RVESVI	r = 0.4737 p = 0.0082 ** n = 30	r = 0.5906 p = 0.0061 ** n = 20
RVMI	r = 0.5097 p = 0.0040 ** n = 30	r = 0.6796 p = 0.0010 *** n = 20
LVEDVI	r = -0.1408 p = 0.4581 n = 30	r = -0.5131 p = 0.0207 * n = 20
LVESVI	r = -0.01688 p = 0.9294 n = 30	r = -0.1646 p = 0.4880 n = 20
LVMI	r = 0.09296 p = 0.6251 n = 30	r = 0.2462 p = 0.2954 n = 20
VMI	r = 0.5456 p = 0.0018 ** n = 30	r = 0.6493 p = 0.0019 ** n = 20
RVSVI (PA)	r = -0.3042 p = 0.1022 n = 30	r = -0.6086 p = 0.0057 ** n = 19
LVSVI (Aorta)	r = -0.3288 p = 0.0815 n = 30	r = -0.5623 p = 0.0234 * n = 16
RVEF	r = -0.6421 p = 0.0001*** n = 30	r = -0.5750 p = 0.0100 * n = 19
LVEF	r = -0.4915 p = 0.0058 ** n = 30	r = -0.1647 p = 0.5421 n = 16

CMR; cardiac magnetic resonance. mPAP; mean pulmonary artery pressure. IPAH; idiopathic pulmonary arterial hypertension. CTDPAH; pulmonary arterial hypertension associated with connective tissue disease. r = correlation coefficient. n = number of patients. p = value of significance.

Figure 4-2: Correlation plots between mean pulmonary artery pressure measurements and cardiac magnetic resonance measurements in IPAH and CTDPAH patients.

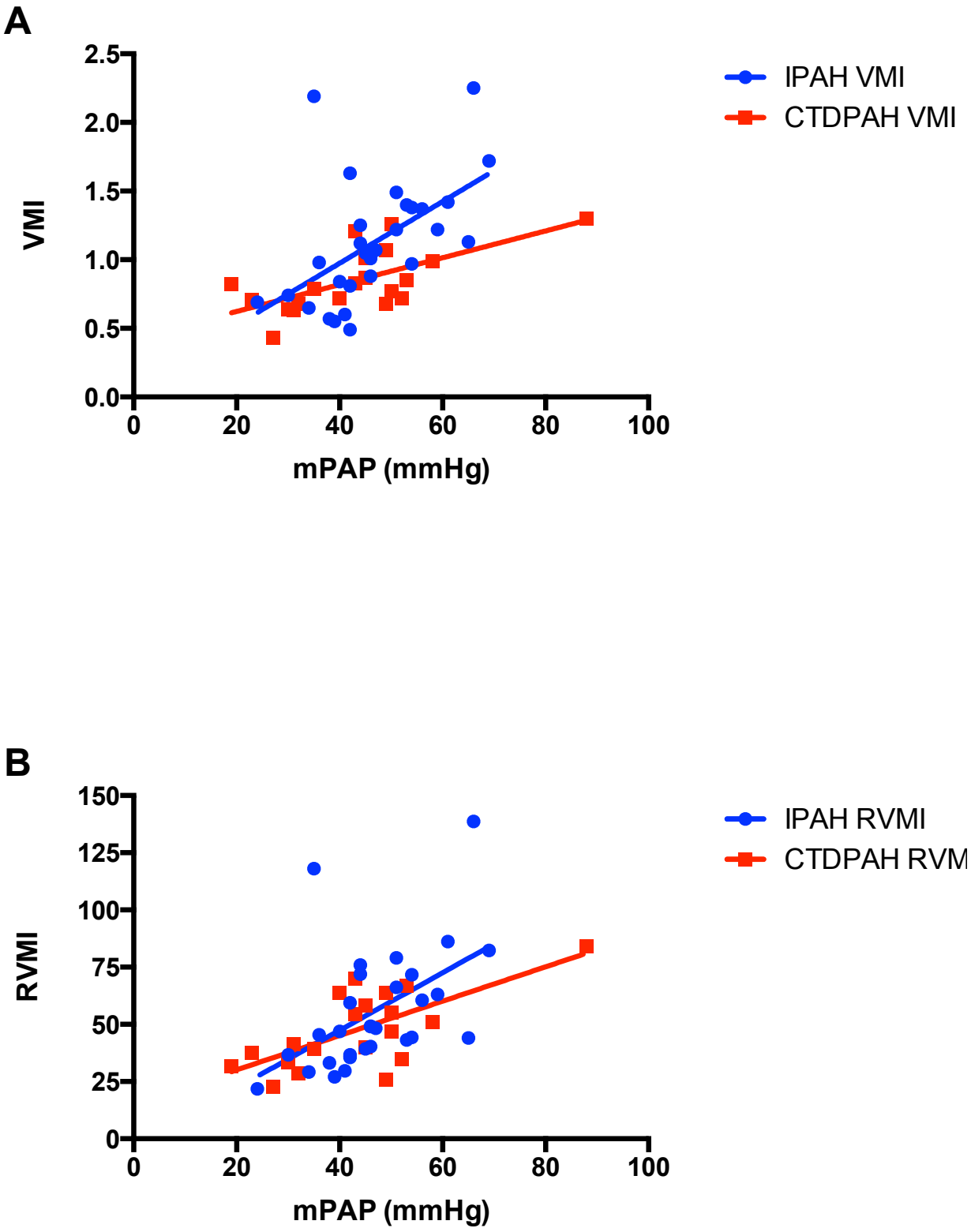

C

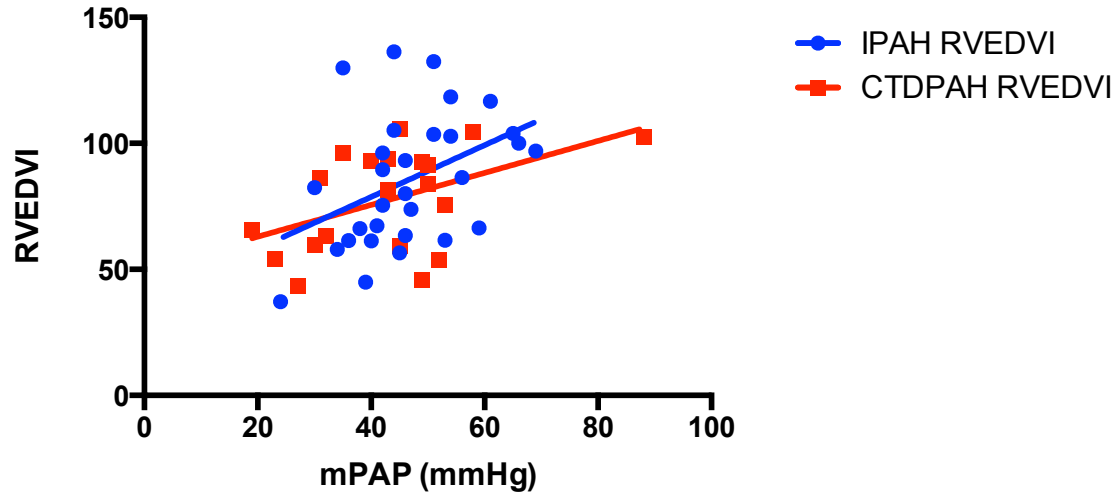
150
100
50
0
RVEDVI
0
20
40
60
80
100
mPAP (mmHg)
IPAH RVEDVI
CTDPAH RVEDVI

D

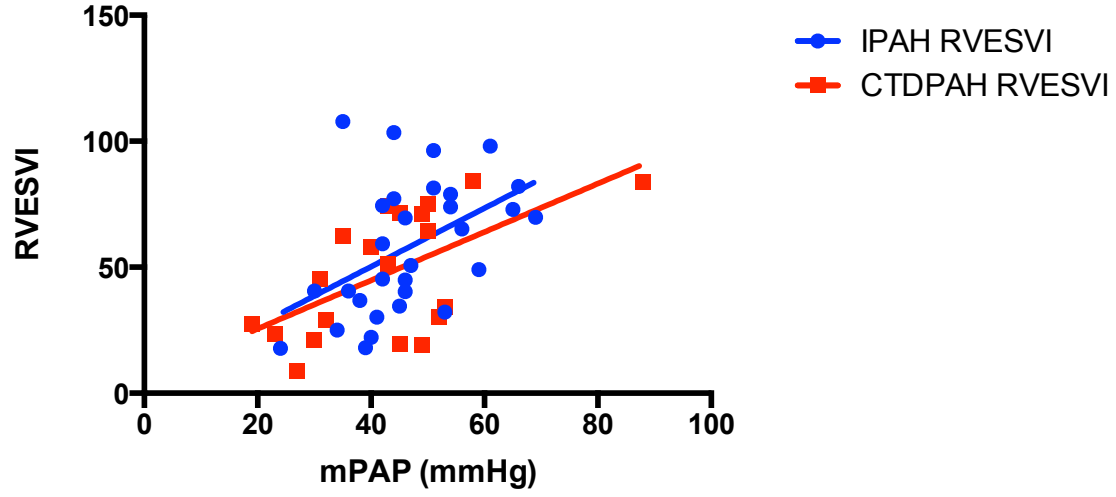
150
100
50
0
RVESVI
0
20
40
60
80
100
mPAP (mmHg)
IPAH RVESVI
CTDPAH RVESVI

E

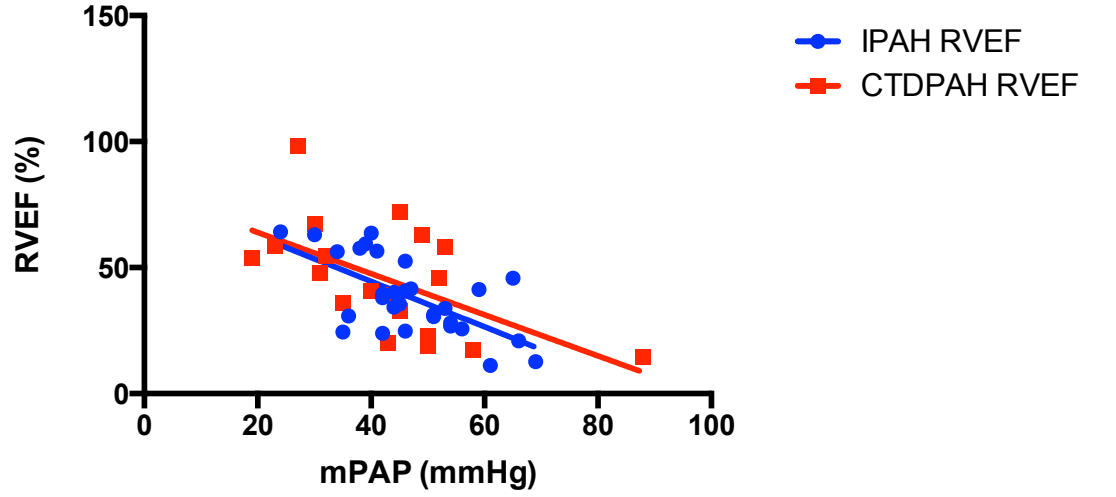
150
100
50
0
RVEF (%)
0
20
40
60
80
100
mPAP (mmHg)
IPAH RVEF
CTDPAH RVEF

Legend for Figure 4.2

A: The relationship between invasive mPAP and VMI in IPAH and CTDPAH patient groups. IPAH (p = 0.0018). CTDPAH (p = 0.0010).

B: The relationship between invasive mPAP and RVMI in IPAH and CTDPAH patient groups. IPAH (p = 0.004). CTDPAH (p = 0.001).

C: The relationship between invasive mPAP and RVEDVI in IPAH and CTDPAH patient groups. IPAH (p = 0.0207). CTDPAH (p = 0.036).

D: The relationship between invasive mPAP and RVESVI in IPAH and CTDPAH patient groups. IPAH (p = 0.0082). CTDPAH (p = 0.0661).

E: The relationship between invasive mPAP and RVEF in IPAH and CTDPAH patient groups. IPAH (p = 0.0001). CTDPAH (p = 0.01).

IPAH; idiopathic pulmonary arterial hypertension. CTDPAH; pulmonary arterial hypertension associated with connective tissue disease. mPAP; mean pulmonary arterial pressure. VMI; ventricular mass index. RVMI; right ventricular mass index. RVEDVI; right ventricular end diastolic volume index. RVESVI; right ventricular end systolic volume index. RVEF; right ventricular ejection fraction.

4.3.4 Survival analysis

Using the Kaplan-Meier method (Figure 4.3), significantly poorer survival is evident in patients with CTDPAH compared with IPAH. 19 patients died (8 IPAH, 11 CTDPAH) during the course of this study.

Figure 4-3: Kaplain-Meier survival curves for IPAH and CTDPAH patient groups.

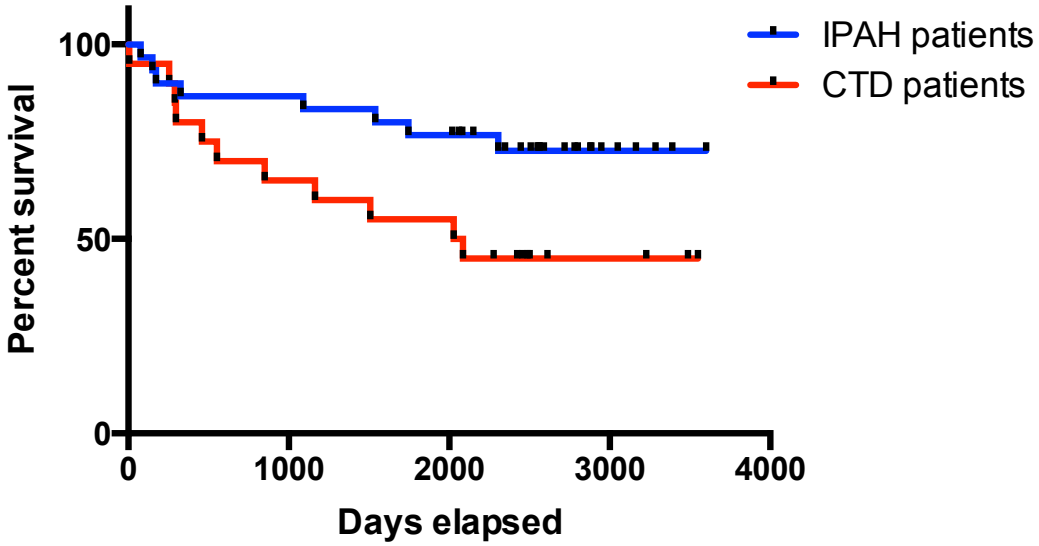

Kaplain-Meier survival curves according to diagnosis. p = 0.0461. Patients with a diagnosis of CTDPAH had a significantly poorer prognosis than IPAH patients. IPAH; idiopathic pulmonary arterial hypertension. CTDPAH; pulmonary arterial hypertension associated with connective tissue disease.

4.4 Discussion

Outcome prediction in patients with PAH has been extensively studied using large-cohort designs and smaller studies incorporating imaging parameters. The consistent finding among studies is that survival in PAH is closely related to RV adaptation to the increased pressure overload. The functional capacity of the RV is the major prognostic determinant in PAH, and death usually results from RV

failure (3-6). Haemodynamic studies have demonstrated the predictive value of RAP and CI. Echocardiographic studies have highlighted the predictive value of tricuspid annular plane systolic excursion (TAPSE) measurements, RV myocardial performance index, atrial size, and pericardial effusion. MRI studies have emphasized the predictive value of SVI, RVEF, and indexed RVESV and RVEDV.

Pulmonary arterial hypertension associated with connective tissue disease (CTDPAH) is associated with a high morbidity and mortality, and worse outcomes compared to the idiopathic form of the disease. Although responses to current PAH therapy have been reported to be effective in SSc-PAH (235, 236), some have reported less favourable responses as compared with IPAH (223, 237, 238). Survival analysis from our study confirmed a significantly poorer outlook in the CTDPAH cohort compared to the IPAH group. These data agree with published literature. The PAH Quality Enhancement Research Initiative (PAH-QuERI) enrolled 791 patients and the 3 year survival probability was significantly lower in patients with SSc-PAH than in patients with IPAH (60% vs 77%, $p<0.0001$). Further studies have confirmed patients with SSc-PAH have worse outcomes than other subgroups with PAH (11, 239) (240, 241).

The reasons for the striking difference in survival between IPAH and CTDPAH remain unclear. Compared with IPAH, patients with CTDPAH are mainly women (women/men ratio 4:1), are older (mean age at diagnosis 66 years) and may present with concomitant disorders (interstitial lung disease, left heart disease etc.). Fisher and colleagues (222) tested the hypothesis that an increased prevalence of left heart disease might explain the higher mortality in patients with SSc-PAH compared to patients with IPAH. Echocardiography revealed similar degrees of right ventricular dysfunction in the 2 groups, whereas a predominance of left heart dysfunction was observed in patients with PAH-SSc. It was concluded, however, that the presence of left heart disease, although more common in PAH-SSc, was not predictive of the higher mortality in these patients. Cardiac involvement in SSc has been reported since the 1960s on the basis of autopsy observations, which showed in 70-80% of cases a myocardial fibrosis pathway characterised by contraction band necrosis of both ventricles and replacement fibrosis, in the absence of concomitant coronary artery disease (242). The poorer prognosis in SSc-PAH has been confirmed, in the absence of

ILD, in the recent prospective study by Launay and colleagues (221). Overbeek *et al* explored patterns of vasculopathy in SSc-PAH patients and compared to IPAH patients (243). Lung tissue was obtained at autopsy, open lung biopsy or lung transplant. They concluded SSc-PAH is characterized by a small vessel intimal fibrosis, which is associated with a PVOD-like pattern in some cases and proposed that this may explain its different clinical behavior from IPAH (243).

The right ventricle (RV) is the main prognostic determinant in PAH. Recent studies have suggested intrinsic RV dysfunction may account for the differences in survival identified between these distinct patient groups. Overbeek *et al* investigated the differences in RV pump function (232) and concluded that RV contractility was lower in SSc-PAH than in IPAH. More recently, Tedford and colleagues, using pulmonary resistance compliance relations and invasive PV loop analysis (233) proposed patients with SSc-PAH have relatively depressed RV function, despite similarly augmented pulmonary afterload compared with IPAH.

A diagnosis of PAH was confirmed by right heart catheterisation in all our enrolled patients. We found no significant difference in the mPAP, PVRI or CI between the IPAH and CTDPAH patient groups in this study. These data are not in agreement with previously published literature. Fisher and colleagues demonstrated patients with SSc-PAH had a lower mPAP (46.6mmHg versus 54.4mmHg p=0.002) and PVRI (22.8 versus 17.5 p=0.026) than IPAH patients, despite similar levels of cardiac dysfunction (no significant difference between CI). Similar patterns were also found in a UK registry investigating the survival and characteristics of patients diagnosed with CTDPAH (11) and prospective US registry (PAH-QuERI) (244). The higher proportion of patients in WHO FC III/IV (IPAH 87%/CTDPAH 90%) in our study could explain this finding. Patients with a diagnosis of connective tissue disease (CTD) are often screened for development of pulmonary hypertension and, as such, identified at an early stage of disease. Our CTDPAH group had severe pulmonary hypertension confirmed at RHC and may reflect a late presenting group. In a recent prospective study, Launay and colleagues (221) identified that the SSc-PAH patients studied were mostly in NYHA FC III/IV and had severe PH at diagnosis. i.e. a late presentation in routine practice as opposed to studies who may have picked up patients during a screening process.

Recent studies have highlighted the lack of correlation between baseline haemodynamic data and clinical evolution in patients with SSc-PAH. Baseline haemodynamic abnormalities have been milder in the CTDPAH population i.e. significantly lower mPAP and PVR, and equally depressed CI compared to patients with IPAH; However, follow up indicated they were 4 times more likely to die compared with patients with IPAH despite comparable therapy (222). These seemingly paradoxical findings suggest that the RV may have a reduced ability to adapt to increased PVR in SSc-PAH, perhaps related in part to myocardial inflammation and scarring as supported by endomyocardial biopsies samples from patients with SSc (245).

CMR measurements obtained from both patient groups reflected the underlying diagnosis of pulmonary hypertension. Baseline CMR variables related to the right heart correlate with mPAP in both the IPAH and the CTDPAH patient groups. This is in agreement with previously published literature. There was a significant difference identified in the calculated ventricular mass index (VMI) for the IPAH and the CTDPAH groups. The VMI was significantly less in the CTDPAH group (0.849 ± 0.2278 versus 1.124 ± 0.4418). The VMI is calculated by dividing the right ventricular mass by the left ventricular mass [VMI = RVM/LVM]. Saba *et al* showed that a VMI > 0.6 had a sensitivity of 84% and specificity of 71% for detecting PAH of various aetiologies (75). VMI was more accurate than echocardiography in diagnosing PH and demonstrated excellent correlation (r=0.81) with the mPAP. (75). A larger study by Roeleveld *et al*, however, showed a much weaker correlation between the *VMI* and mPAP (r=0.56) although the *VMI* was found to be the best among five different CMR-based methods for the estimation of mPAP (76). The increased VMI in the IPAH patient group may reflect an improved cardiac adaptive process in the IPAH group to the increased pulmonary vascular afterload, despite no significant difference in indexed RVM being identified. It is well recognized that the left heart is involved in systemic sclerosis (246). LVEF was significantly higher in the CTDPAH group (62.08 ± 11.57 versus 50.91 ± 17.15, p=0.0243) compared to the IPAH group. These results are difficult to explain. Multiple linear regression analysis was applied to account for mPAP measurements. We were unable to identify any significant differences in

right heart adaptation (structure and function) for a given mPAP, which could account for the poorer prognosis in the CTDPAH group.

The prognosis of CTDPAH is confirmed to be significantly worse than IPAH. Previous studies have suggested intrinsic RV dysfunction may account for the differences in survival identified. We did not identify any significant differences in RV structure and function AT REST, for a given mPAP, between the 2 distinct patient groups. Perhaps exercise testing during CMR (e.g. MR-compatible ergometer, dobutamine administration) may be an avenue for further investigation. This may tease out subtle differences in RV/LV function between the groups. However, it should be noted that the majority of patients presented in WHO FC III and therefore exercise may be difficult to perform.

This study compared baseline CMR measurements between IPAH and CTDPAH patients. CTDPAH has a poorer prognosis than IPAH. RV function is the main prognostic determinant in PAH. We investigated whether there were detectable differences in baseline CMR, for a given mPAP, between IPAH and CTDPAH patient groups. Contrary to our hypothesis, we did not find any evidence of difference in right heart adaptation between the groups. It is likely that the survival difference observed is due to a combination of factors including RV function, impact of comorbidities, age, myocardial involvement, musculoskeletal involvement, presence of ILD and potential contributing element of PVOD.

Chapter 5

Changes in right ventricular function measured by CMR imaging in pulmonary hypertension patients receiving disease-targeted therapy: A longitudinal study.

5 Changes in right ventricular function measured by CMR imaging in pulmonary hypertension patients receiving disease-targeted therapy: A longitudinal study.

5.1 Introduction

Pulmonary hypertension (PH) is a progressive disorder affecting the pulmonary arteries. It is characterised by vascular proliferation and remodelling which results in a progressive increase in pulmonary vascular resistance (PVR) and subsequent right ventricular failure (RVF). The RV adapts to the increased afterload by increasing its wall thickness and contractility. In most patients, these compensatory mechanisms are insufficient and RV dysfunction occurs. Recent developments in imaging techniques, such as CMR and echocardiography, have improved our understanding of the structure and function of the RV. The initial insult involves the pulmonary vasculature yet survival of patients with pulmonary hypertension is closely related to right ventricular function (4, 247).

Over the last 20 years, several treatments targeting the pathological mechanisms of PH have been introduced. These agents have been approved largely based on improved haemodynamic variables on right heart catheterisation (RHC) or improved exercise capacity (increase in 6 minute walk distance [6MWD]) in randomised controlled trials (RCT). The current aim is for an early diagnosis of PH followed by treatment with first line monotherapy (26, 158). The importance of escalating therapy if a patient does not respond to initial treatment has been emphasized in recently published guidelines (7). Patients are closely followed up in the outpatient clinic every three to six months. Treatments for PH are always expensive, sometimes invasive and carry significant side effects. It is extremely important to be able to assess patients response to therapy with investigations of appropriate quality in order to convince patients, treating physicians, funding agencies, and regulatory bodies of the value of treatment. Physicians currently rely on the WHO functional class, exercise testing (6MWT and CPET), biomarkers (BNP levels), echocardiography

and RHC to assess disease progression and treatment efficacy in the clinic. These investigations have acknowledged limitations as discussed in the introduction.

The imperative role of the RV performance in the clinical status and long-term outcome of patients with PH is evident. This has raised the question that direct assessment of RV function may be a more appropriate way of determining response to therapy and monitoring disease progression in pulmonary hypertension. CMR provides a comprehensive overall picture of RV structure and function as it has unparalleled resolution, is reproducible and can provide three-dimensional images. CMR is well suited to longitudinal follow up as it is non-invasive and non-ionising. This imaging technique has gained a dominant role as the reference method for clinical trials assessing longitudinal changes in LV function after therapeutic interventions (57, 68). It provides a direct evaluation of right ventricular size, mass, morphology and function (151). The accuracy and reproducibility of CMR in assessing cardiac morphological and functional parameters leads to low interstudy variability, which translates into a significant reduction in sample size required to test the efficacy of therapeutic interventions (57, 248). Despite these clear advantages, the uptake of CMR in clinical practice has been limited. This may be partly attributable to cost but the lack of published data showing its use in PH patients, especially in those receiving treatment, may also be a contributing factor. This study aimed to evaluate the use of CMR in the longitudinal assessment of effects of treatment in patients with pulmonary hypertension.

This chapter presents the results obtained from my contribution to the EURO-MR study. EURO-MR was a prospective, longitudinal study conducted in four European centers: Scottish Pulmonary Vascular Unit, Glasgow, UK; Medical University Graz, Graz, Austria: Sapienza University of Rome, Rome, Italy and Department of Pulmonary Medicine, VU University Medical Center, Amsterdam, The Netherlands as part of the EU Framework 6 Pulmotension Initiative (249). Please refer to appendix 1 and 2 for the introductory letter and follow up newsletter. EURO-MR was designed to evaluate the performance of CMR imaging in the longitudinal assessment of pulmonary hypertension patients. I have presented the data for 34 patients who completed the baseline and 4 month assessment at the SPVU.

Table 5-1: EURO-MR: Outline and study timetable.

Timescale	CMR Protocol	Comparators
0 months / Baseline	CMR 1	• Haemodynamics • 6MWT • NTproBNP • WHO functional class • Genomics
4 months	CMR 2	• 6MWT • NTproBNP • WHO functional class
12 months	CMR 3	• 6MWT • NTproBNP • WHO functional class

This table outlines the EURO-MR study outline and timetable. 6MWT: six minute walk test. NT-proBNP: N-terminal pro–brain natriuretic peptide. WHO: World Health Organisation.

5.2 Materials and Methods

This was a prospective, longitudinal study of 34 patients attending for assessment at the Scottish Pulmonary Vascular Unit. This was the starting point of the multinational EURO-MR study, which was conducted in four European centers as part of the EU Framework 6 Pulmotension Initiative.

The study subjects were incident patients attending the SPVU for initial diagnostic assessment and subsequent follow up. The diagnosis of pulmonary hypertension was based on RHC in accordance with contemporary guidelines. The inclusion criteria were patients with a diagnosis of pulmonary hypertension: WHO group 1 (PAH including idiopathic PAH, heritable PAH, PAH associated with connective tissue disease and congenital heart disease), WHO Group 3 (PH due

to lung disease and/or hypoxia) and WHO Group 4 (Chronic thromboembolic pulmonary hypertension) if ineligible for pulmonary thromboendarterectomy. This study was approved by the West Glasgow Research Ethics Committee and written informed consent was obtained from all study participants.

5.2.1 Study design

Figure 5-1: Study protocol.

PH: pulmonary hypertension. WHO FC: World Health Organisation functional class. 6MWT: six minute walk test. CMR: cardiac magnetic resonance.

Baseline (0 month) assessment

This was performed during the subject's initial in-patient admission:

i. Full clinical history
ii. Full physical examination
iii. WHO functional class
iv. 6MWT
v. CMR imaging

4 month assessment

This visit comprised a morning or afternoon visit to the Western Infirmary.

i. Full clinical history
ii. Full physical examination
iii. WHO functional class
iv. 6MWT
v. CMR imaging

5.2.2 Cardiac magnetic resonance (CMR) image acquisition and analysis

CMR imaging was performed on a 1.5 Tesla MRI scanner (Sonata Magnetom, Siemens, Germany). CMR was performed using a protocol described in detail in the materials and methods chapter of this thesis. All CMR images were analysed by a single operator (L.M.) using the Argus analysis software (Siemans, Erlangen, Germany). Individual scans were coded by number and analysed in batches by L.M. who was blinded to the haemodynamic and six minute walk distance results of any given subject at the time of analysis.

Volumetric analysis: RV and LV volumes [RV end-diastolic volume (RVEDV), RV end-systolic volume (RVESV), LV end-diastolic volume (LVEDV) and LV end-systolic volume (LVESV)] were determined by manual planimetry as described previously (materials and methods section). RV and LV stroke volumes (RVSV and LVSV), ejection fractions (RVEF and LVEF) and mass (RVM and LVM) were determined as previously described. Ventricular mass index (VMI) was determined as RVM/LVM (75). RV and LV volumes and mass were then indexed to body surface area.

Flow analysis: Right ventricular SV was measured using MR phase-contrast flow quantification in an image plane positioned perpendicular to the main pulmonary artery, at least 1cm distal to the pulmonary valve. Left ventricular SV (aortic flow) was also measured, approximately 2 - 4cm above the aortic valve and distal to the coronary arterial ostia. A velocity encoded k-space segmented gradient-echo sequence was used to generate 45 matched pairs of anatomical

and velocity images. Retrospective ECG-gating was used to ensure coverage of the complete cardiac cycle. Patients were instructed to breath freely throughout this section of the protocol and the average time of acquisition was 2-3 minutes depending on the patient's heart rate. Please refer to the materials and methods section for further information.

Table 5-2: Measurements made from cardiac magnetic resonance imaging in this study.

Measurements from CMR imaging
• **RV/LV end diastolic volume index (RV/LVEDVI)**
• **RV/LV end systolic volume index (RV/LVESVI)**
• **RV/LV ejection fraction (RV/LVEF)**
• **RV/LV mass index (RV/LVMI)**
• **Ventricular mass index (VMI)**
• **Pulmonary artery flow analysis (PASVI)**
• **Aortic flow analysis (AoSVI)**

5.2.3 Right heart catheterisation

RHC was performed according to international recommendations (26) by SPVU physicians, in the catheterisation laboratory. A 7F gauge, balloon tipped, flow directed, triple channel thermodilution Swan-Ganz catheter (Baxter Healthcare, Irvine, California, USA) was advanced through an 8F introducer sheath inserted into the right internal jugular vein or the right femoral vein. All measurements were recorded with the patient in a supine position, at rest, breathing room air or supplemental oxygen if required. Please refer to materials and methods section of this thesis for further information on RHC methodology.

5.2.4 6-minute walk test

The 6MWT was performed by a respiratory physiologist or by a member of SPVU medical staff. The 6MWT was performed on a 20-metre corridor, but otherwise according to the American Thoracic Society guideline (139).

5.2.5 WHO functional class

Each patient was assigned to a WHO functional class, which is a four point scale to rate the impact of breathlessness and fatigue according to daily activity. Please refer to table 5.3 for WHO functional classification.

Table 5-3: World Health Organisation functional classification of pulmonary hypertension.

WHO FC	Description
Class I	Patients with PH but without resulting limitation of physical activity. Ordinary physical activity does not cause undue dyspnoea or fatigue, chest pain, or near syncope.
Class II	Patients with PH resulting in slight limitation of physical activity. They are comfortable at rest. Ordinary physical activity causes undue dyspnoea or fatigue, chest pain, or near syncope.
Class III	Patients with PH resulting in marked limitation of physical activity. They are comfortable at rest. Less than ordinary activity causes undue dyspnoea or fatigue, chest pain, or near syncope.
Class IV	Patients with PH with inability to carry out any physical activity without symptoms. These patients manifest signs of right heart failure. Dyspnoea and/or fatigue may even be present at rest. Discomfort is increased by any physical activity.

5.2.6 Statistical analysis

For demographic, haemodynamic and CMR measurements, mean values ± one standard deviation (± SD) were calculated. Comparison between baseline and 4 month follow up was performed using the paired t test. The correlation between the change in CMR measurements and 6MWD was determined by Pearson correlation. A significance level of 5% was used in all tests. Statistical analysis was performed using Graphpad Prism Version 6 (Graphpad Software, California, USA). Data are given as mean ± SD unless otherwise stated.

5.3 Results

5.3.1 Participants

In total, 34 patients underwent assessment at baseline and after 4 months of disease targeted therapy. Baseline characteristics for all patients are summarized in table 5.4. There were more female than male patients. Idiopathic pulmonary arterial hypertension (IPAH) was the most common aetiology. The majority of patients were in WHO functional class III. The patients had significant pulmonary hypertension confirmed by right heart catheterisation. Mean 6MWD at baseline was 319.7m ± 106.8m. Disease targeted therapy for pulmonary hypertension was commenced at baseline in all patients. Only 5 patients who were scanned at baseline did not attend for their interval CMR scan at 4 months and therefore could not be included in this longitudinal project. This highlighted that the vast majority of patients in this study tolerated the investigation well.

Table 5-4: Baseline characteristics for patients enrolled in this study.

Characteristic	Cohort (n = 34)
Age, mean ± SD, years	53.02 ± 21.60
Female:Male	21:13
Body surface area, mean ± SD, m^2	1.81 ± 0.22
Aetiology of PH, n (%)	
WHO Group 1	
IPAH	13 (38.2)
CTDPAH	6 (17.6)
CHDPAH	2 (5.9)
Other (FPAH)	1 (2.9)
WHO Group 3	
PH due to hypoxic lung disease	5 (14.7)
WHO Group 4	
CTEPH	7 (20.6)
WHO Functional Class, n (%)	
I	0
II	5 (14.7)
III	26 (76.5)
IV	3 (8.8)
Baseline 6MWD, mean ± SD, m	319.7 ± 106.8

Data are expressed as mean ± standard deviation.

IPAH: idiopathic pulmonary arterial hypertension; CTDPAH: pulmonary arterial hypertension associated with connective tissue disease; CHDPAH; pulmonary arterial hypertension associated with congenital heart disease; FPAH: familial pulmonary arterial hypertension; PH associated with hypoxic lung disease: pulmonary hypertension associated with hypoxic lung disease; CTEPH: chronic thromboembolic pulmonary hypertension; WHO: World Health Organisation; mPAP: mean pulmonary artery pressure; PVR: pulmonary vascular resistance; 6MWD 6 minute walk distance.

5.3.2 Response to disease-targeted therapy

There was a significant increase in 6MWD after 4 months of disease targeted therapy (319.7 ± 106.8m at baseline, 361 ± 90m at 4 months, p = 0.0005). One patient was unable to complete the 6 minute walk test at the 4 month assessment. 6 patients walked a shorter distance during the 6MWT at their 4 month review. All other patients improved their walk distance. Repeat WHO assessment at 4 months confirmed one patient had improved from WHO functional class III to II and one patient had deteriorated from WHO II to III. 32 patients remained in the same functional class at both assessments.

Figure 5-2: Change in 6 minute walk distance from baseline (0 months) to 4 months.

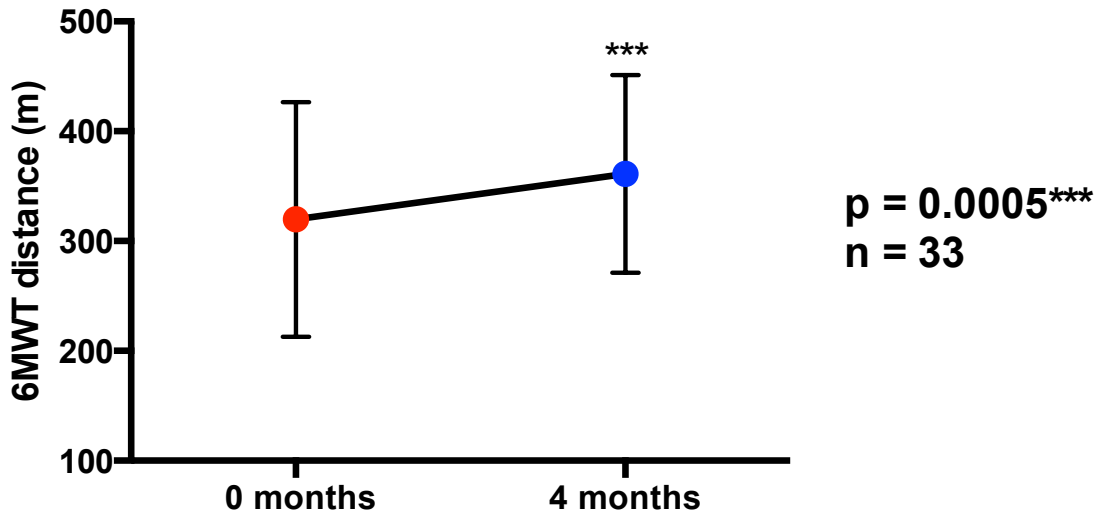

6MWT; six minute walk test. n; number of patients.

5.3.3 CMR assessments

CMR measurements at baseline and after 4 months of disease-targeted therapy are summarised in table 5.5. Following 4 months of disease targeted therapy, there were significant increases in RVEF (p < 0.0001), RVCI (p = 0.0219), RVSVI (p = 0.0102), LVEF (p = 0.0158), LVCI (p = 0.0071), LVSVI (p = 0.0025) and a significant decrease in the RVESVI (p = 0.0278).

Table 5-5: Baseline and four month cardiac magnetic resonance variables in the cohort group.

CMRI Variable	Baseline (n=34)	4 months (n=34)	P value
Right ventricle			
RVEDVI (ml/m^2)	83.92 ± 22.67	81.67 ± 24.70	p = 0.2916
RVESVI (ml/m^2)	52.50 ± 25.65	48.54 ± 23.60	p = 0.0278 *
SVI (ml/m^2) n=33	35.64 ± 13.54	39.91 ± 9.80	P = 0.0102 *
CI (L/min/m^2) n=33	2.58 ± 0.82	2.823 ± 0.70	P = 0.0219 *
EF (%) n=33	45.92 ± 20.93	52.57 ± 19.65	p = < 0.0001 ****
Mass (g/m^2)	51.59 ± 22.70	50.66 ± 21.72	p = 0.4350
Left ventricle			
LVEDVI (ml/m^2)	48.86 ± 11.53	52.71 ± 16.79	p = 0.0938
LVESVI (ml/m^2)	18.05 ± 6.22	17.93 ± 8.29	p = 0.9131
SVI (ml/m^2) n=33	27.88 ± 9.43	33.05 ± 9.81	p = 0.0025 **
CI (L/min/m^2) n=33	2.02 ± 0.59	2.324 ± 0.66	p = 0.0071 **
EF (%)n=33	57.40 ± 14.86	63.30 ± 9.19	P = 0.0158 *
Mass (g/m^2)	54.69 ± 9.93	54.08 ± 9.05	p = 0.5858
VMI	0.96 ± 0.39	0.95 ± 0.39	p = 0.7720

RVEDVI; right ventricular end diastolic volume index. RVESVI; right ventricular end systolic volume index. SVI; stroke volume index. CI; cardiac index. EF; ejection fraction. LVEDVI; left ventricular end diastolic volume index. LVESVI; left ventricular end systolic volume index. VMI; ventricular mass index.

All data are expressed as mean ± standard deviation.

Figure 5-3: Changes in cardiac magnetic resonance measurements from the left heart: Between baseline and 4 months of disease targeted therapy.

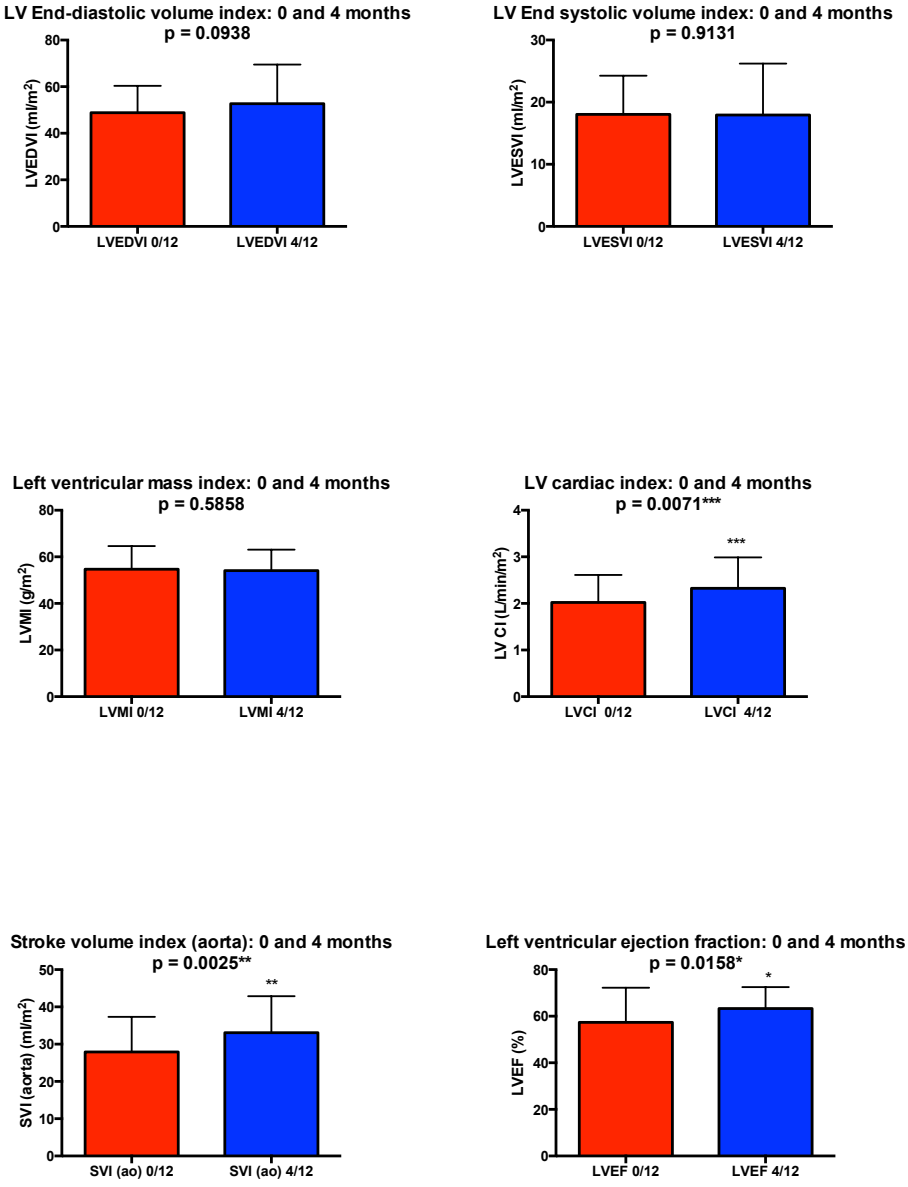

LVEDVI; left ventricular end diastolic volume index. LVESVI; left ventricular end systolic volume index. LVMI; left ventricular mass index. LVCI; left ventricular cardiac index. SVI; stroke volume index. LVEF; left ventricular ejection fraction.

Figure 5-4: Changes in cardiac magnetic resonance measurements from the right heart: Between baseline and 4 months of disease targeted therapy.

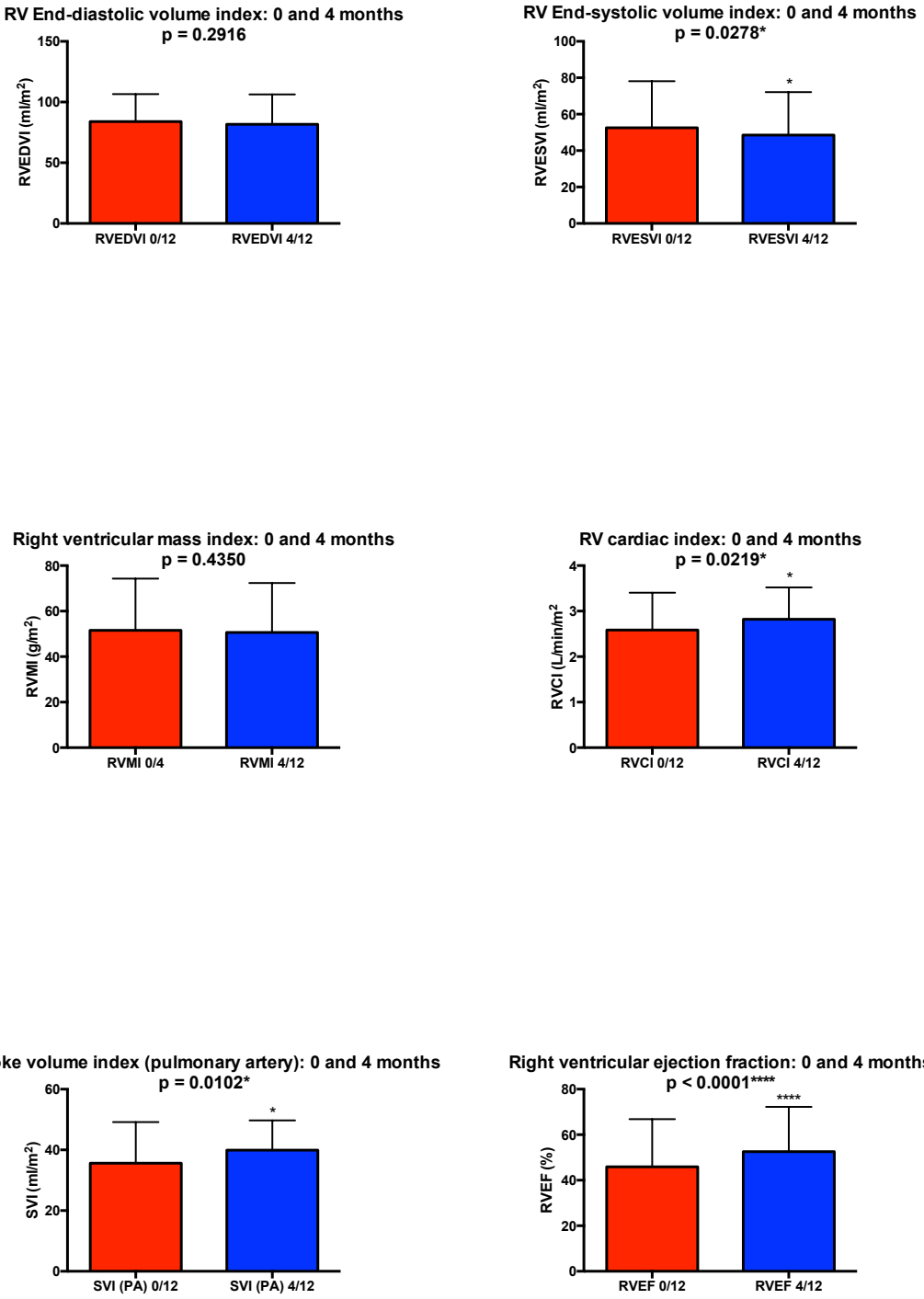

RVEDVI; right ventricular end diastolic volume index. RVESVI; right ventricular end systolic volume index. RVMI; right ventricular mass index. RVCI; right ventricular cardiac index. SVI; stroke volume index. RVEF; right ventricular ejection fraction.

Association of CMR measurements with 6MWD

6MWD increased from 319.7 ± 106.8m at baseline to 361 ± 90m at 4 months. CMRI variables that changed significantly during the 4 month treatment period were compared with the change in 6MWD during treatment. No significant correlations were identified between change in 6MWD and change in RVEF, RVSVI, RVCI, LVEF, LVSVI or LVCI. Please refer to Figure 5.5.

Figure 5-5: Pearson correlations between change in right ventricular function and change in six minute walk distance.

Pearson correlation between the change in RVEF vs change in 6MWD.

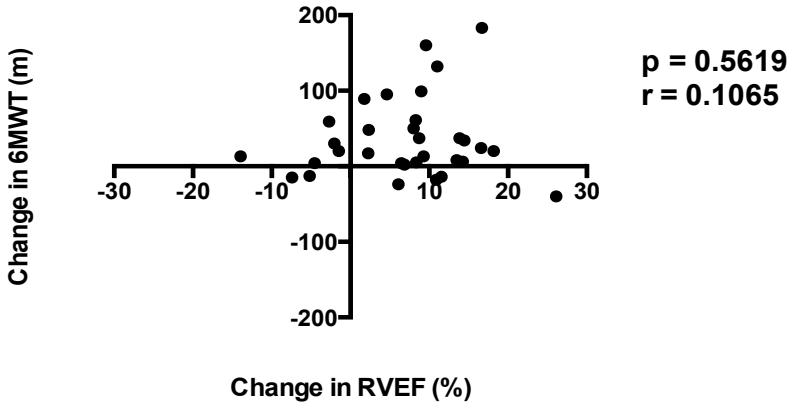

Pearson correlation between the change in SVI (PA) vs change in 6MWD.

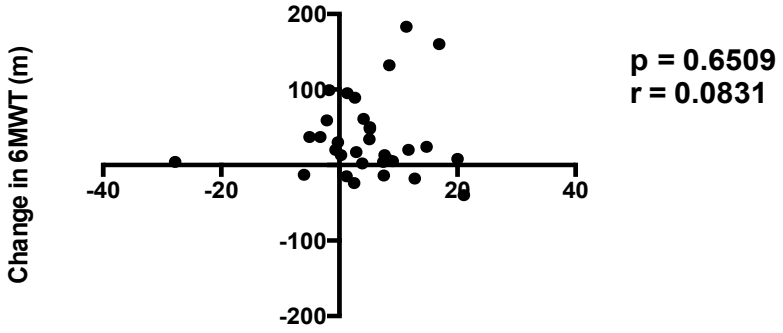

Pearson correlation between the change in RV CI vs change in 6MWD.

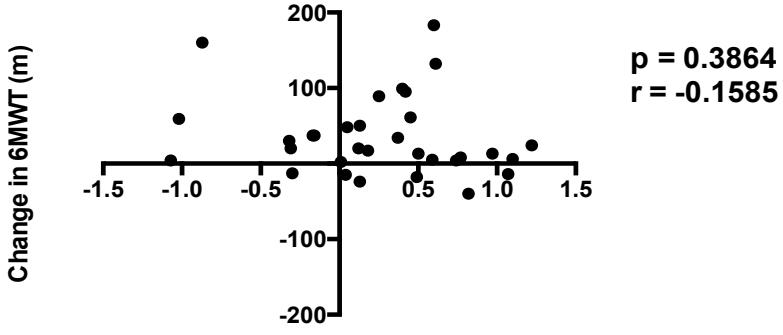

RVEF; right ventricular ejection fraction. 6MWD; six minute walk distance. 6MWT; six minute walk test. SVI; stroke volume index. PA; pulmonary artery. RVCI; right ventricular cardiac index.

Figure 5-6: Pearson correlations between change in left ventricular function and change in six minute walk distance.

Pearson correlation between the change in LVEF vs change in 6MWD.

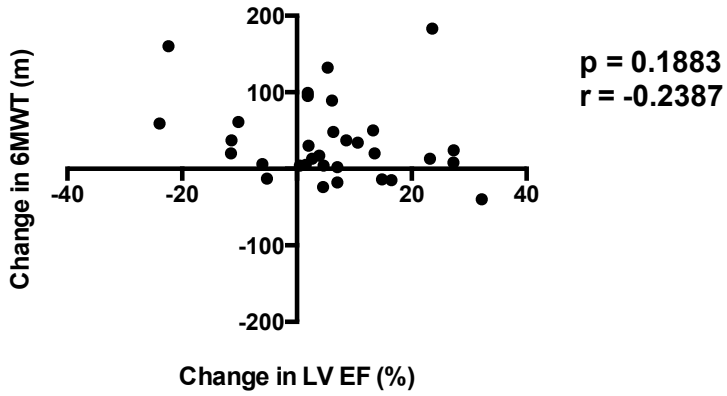

Pearson correlation between the change in SVI (aorta) vs change in 6MWD.

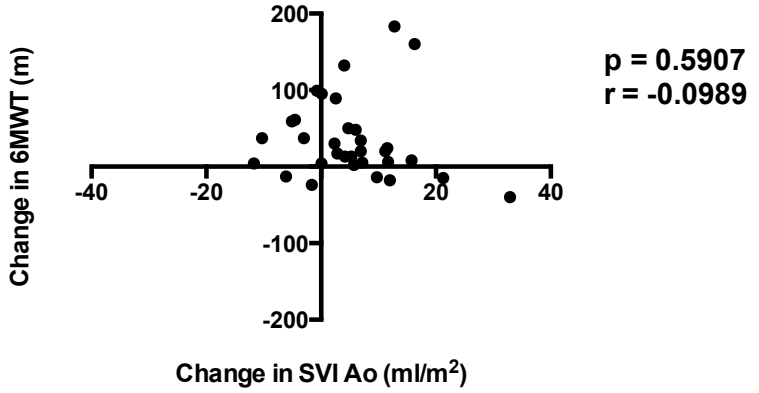

Pearson correlation between the change in LVCI vs change in 6MWD.

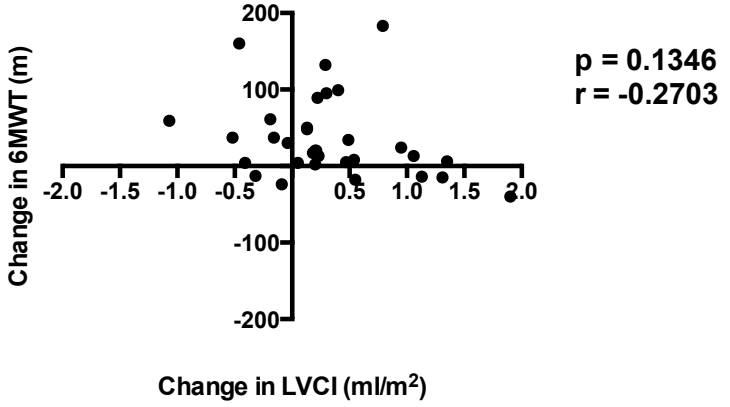

LVEF; left ventricular ejection fraction. 6MWD; six minute walk distance. 6MWT; six minute walk test. SVI; stroke volume index. Ao; aortic. LVCI: left ventricular cardiac index.

5.4 Discussion

The aim of this study was to evaluate the performance of CMR imaging in the longitudinal assessment of pulmonary hypertension patients. With the advent of multiple new disease-targeted therapies for PH it is increasingly important that we can assess the progress of patients in a non-invasive manner. This study was the starting point for the first multicenter study (EURO-MR) to prospectively assess the use of CMR imaging before and during disease-specific therapy (249).

In this longitudinal study, we investigated the effects of treatment on right and left ventricular function as assessed by CMR. A significant increase in 6MWD after 4 months of therapy was demonstrated in our cohort of patients. The CMR analysis confirmed there was a significant increase in stroke volume index, cardiac index and ejection fraction, when measured in either the left or right heart. There was also a significant reduction in right ventricular end-systolic volume index associated with treatment. These findings confirm that both left and right-sided measurements should be included in the analysis when assessing cardiac function in patients with pulmonary hypertension. In our study group, there was no change in left sided ventricular volumes with disease-targeted therapy. In addition, there was no significant change demonstrated in CMR-derived ventricular mass for either the left or right heart.

This current study complements data from several smaller trials studying changes in CMR derived variables during treatment of pulmonary hypertension. We did not, however, demonstrate any treatment related change in ventricular mass. In 2003, Michelakis and colleagues (189) performed a small non-randomised, pilot study of 5 patients with PH to investigate the effect of sildenafil 50mg tid. Sildenafil significantly reduced RVM and increased RVSV. In a prospective study (2004) of PH patients with prostacyclin (epoprostenol) therapy, the significant increase in RVSV (PA flow analysis) corresponded well with functional improvement (WHO functional class, 6MWT) (70). It was also demonstrated that epoprostenol therapy lowered PVR but did not affect RV dilatation or hypertrophy (70). The SERAPH study in 2006 (a comparison study between sildenafil and bosentan) demonstrated that RVM decreased significantly from baseline after 16 weeks of sildenafil therapy (n=13, p = 0.015) (191)

although this was not observed in the 12 patients receiving bosentan. There was no significant difference between treatments (p = 0.142). Similarly, Van Wolferen *et al* (2006) demonstrated by CMR that the addition of sildenafil reversed RV dilatation and hypertrophy in patients receiving endothelin receptor antagonist therapy (190). More recently, a single centre study assessed 16 patients with PAH by CMR at baseline and after 12 months treatment with bosentan (197). Cardiac index, PVR and 6MWT distance improved with treatment. There was a trend towards improvement in RV SV (p=0.08) although there was no change in RV ejection fraction or RVEDV. This study highlighted the need for further investigation of CMR variables associated with RV function and how they relate to variables such as 6MWD.

In PAH, vasoconstriction and vascular remodelling contribute to a progressive increase in PVR and PAP which have critical effects on the heart, and in particular, the right ventricle. The ability of the RV to adapt to the increased afterload resulting from the increased PVR is the main determinant of a patients functional capacity and survival. Changes to the RV due to pressure overload in PAH are complex, with an increased RV wall stress leading to RV dilatation and hypertrophy, which affects the structure and function of the RV as it adapts to increased PAP (250). Measurements of RV function have been shown to be important in determining patients prognosis and also, in some cases, response to treatment (4, 73, 147, 156, 199). The remodelling and RV myocardial hypertrophy, which occur in patients with PH, lead to a need for increased myocardial perfusion. However, increased wall tension leads to a reduction in oxygen supply, increased oxygen extraction and reduced perfusion secondary to compression of the coronary circulation and impairment of coronary flow (101, 251). This study confirmed that there was no significant change in RV or LV mass with disease-targeted therapy. It is unknown whether hypertrophy of the RV is protective or not. To date, two trials (36, 198) have used CMR-derived RVM as an end-point. This particular measurement remains unvalidated and may not be an ideal end point since it is unknown whether a hypertrophy of the RV is protective or not. There may be a maximal benefit obtained after which continued remodelling of the RV is deleterious to the patients condition.

Approval for disease-targeted therapy for pulmonary hypertension has been largely based on improved haemodynamic variables on RHC or improved exercise

capacity (increase in 6MWD) in RCTs. Consequently disease progression and treatment efficacy in the clinic are frequently assessed using 6MWT or RHC. These methods of assessment have acknowledged limitations as described in the introduction. With reference to this study, 6MWD provides limited information in patients with PAH associated with CTD, a patient group that made up 17.6% of the current study population. A baseline 6MWD is prognostic of survival (219) yet changes in 6MWD with treatment do not relate to outcomes in patients with PAH (252). In the SUPER trial, the significant improvement in 6MWD at week 12 did not translate into an increase in survival (253). Patients treated with the highest dose of sildenafil achieved the greatest improvements in 6MWD, but had the lowest long-term survival rates. A recent pooled analysis of data from 10 randomised controlled trials of PAH specific therapies showed that although the change in 6MWD from baseline to week 12 was a mediator of the relationship between treatment and the development of a clinical event, it accounted for under 25% of the total relationship (254). The findings of our analysis confirmed that the correlations between 6MWD and CMR variables were weak. This highlights the importance of monitoring right ventricular function directly to assess response to therapy.

The impact of a treatment on disease progression associated with PH can be measured by time to clinical worsening (TTCW). This endpoint is viewed as clinically relevant by clinicians and regulatory agencies and has been used in several clinical trials as a secondary, or more recently a primary end point. The composition of this end point varies from study to study. It has been confirmed that a uniform definition of TTCW should be used in future (phase III) RCTs in PAH. In the definition of TTCW, hard events should include all cause mortality, nonelective hospital stay due to PAH (with predefined criteria e.g. institution of iv prostatnoids, lung transplantation, or atrial septostomy) and disease progression defined as a reduction from baseline of 6MWD by 15% plus worsening functional class. Current therapies for PAH have been adopted on the basis of short term trials with exercise capacity as the primary end point. New studies in pulmonary hypertension medications are now using TTCW as a primary end point. The efficacy of macitentan (a dual endothelin receptor antagonist) was assessed using the primary end point of morbidity and mortality in a long term trial. The primary end point was the time from the initiation of treatment to the

first occurrence of a composite end point of death, atrial septostomy, lung transplantation, initiation of treatment with intravenous or subcutaneous prostanoids, or worsening of PAH (255). The AMBITION (A Study of First-Line Ambrisentan and Tadalafil Combination Therapy in Subjects with Pulmonary Arterial Hypertension) trial examined the effect of first-line combination therapy with ambrisentan and tadalafil versus first-line monotherapy with either ambrisentan or tadalafil in patients with PAH using a composite end-point which included an inadequate clinical response.

A wide range of CMR measurements have been identified in patients with PH and many have been shown to be strongly predictive of mortality and survival. These measurements offer the potential for monitoring and assessing response to treatment (256). Factors relating to the dynamic function of the right heart appear to be the most linked to outcome. Stroke volume (SV) is a key CMR prognostic measure in PAH patients. Maintenance of normal SV at rest and during exercise in pulmonary hypertension indicates right ventricular adaptation to the increase in afterload caused by an increasing PVR and PAP. A low SV is strongly linked to mortality in IPAH both at baseline and with treatment (73, 199), and in PAH related to systemic sclerosis (257). In PAH and CTEPH patients, 1 year of treatment with PAH-specific therapy resulted in significant improvements in stroke volume which was related to an increase in 6MWD (199). A recent CMR based study confirmed that a 10ml change in SV during follow up should be considered as clinically relevant. This value can be used to interpret changes in SV during clinical follow up in PH, although validation in a wider range of PAH aetiologies is required (199). RVEF is also as an important CMR-measured prognostic factor in PAH (73, 200). Prognosis of patients with PAH remains poor (219) despite the improvements in PVR or 6MWD seen during therapy. It has been suggested that RV function may be continuing to deteriorate despite the encouraging haemodynamic or functional signs e.g. Van de Veerdonk and colleagues demonstrated that 25% of patients with reduced PVR following 12 months of therapy had deteriorating RV function (assessed by RVEF) during this period, indicating that RV function does not necessarily adapt to treatment-induced changes in PVR. Deterioration in RVEF was associated with poor outcome, irrespective of improvements in PVR, emphasising the importance of monitoring RV function during the course of the disease (200). LV and RVEDV are

also independent predictors of prognosis in IPAH, and changes in following treatment are independent predictors of mortality (73, 258). A decline in both LV and RVEDV was seen in PAH patients who failed to survive in a recent study by Mauritz and colleagues (92). This study also compared changes in RV geometric shortening using RV longitudinal and transverse shortening and RV fractional area change, and found that longitudinal shortening, transverse shortening and RV fractional area change, measured at the beginning of the study and 1 year later, were significantly higher in subsequent 5-year survivors than in nonsurvivors. As transverse shortening incorporates both free-wall and septum movements, the authors suggest that this parameter could be used to monitor the decline in RV function in end-stage PAH (92).

The increasing importance of direct assessment of right ventricular function is highlighted by the incorporation of CMR measurements into the endpoints of upcoming trials. A prospective, multicenter trial (**REPAIR** – **R**ight v**E**ntricular remodeling in **P**ulmonary **A**rter**I**al hype**R**tension) is planned to evaluate the effects of macitentan on right ventricular and haemodynamic properties in patients with symptomatic PAH. Patients will be treated with macitentan for 1 year. CMR will be performed at baseline, week 26 and week 52. Change in RV stroke volume is a primary end point and change in arterial elastance (ventriculo-arterial coupling) is a secondary end point.

This study has limitations. The inclusion criteria allowed a heterogeneous population of PH patients to be enrolled and, unlike previous studies, it was not restricted to patients with pulmonary arterial hypertension (PAH). Although disease specific therapy is only recommended in management guidelines for PAH, in clinical practice these treatments are also used in WHO groups 3,4 and 5. Other CMR measurements that may be important prognostically and therapeutically were not included in the current analysis. These include pulmonary artery stiffness, pulmonary perfusion, right ventricular arterial coupling, transverse shortening etc. Clearly, these are important measurements and, as imaging techniques improve, will become part of the range of CMR derived measurements used to study patients with PH.

In conclusion, this study demonstrates that detailed CMR assessments at baseline and follow up in this patient cohort provide valuable information about response to disease-targeted therapy. There were treatment changes in CMR derived variables in both the left and right sided of the heart. These changes were not related to the changes in 6MWD and therefore, direct measurement of RV function is required in order for the potential benefits of PAH treatment to be fully appreciated. CMR imaging enables a unique combination of morphological and functional assessment of the right ventricle and pulmonary circulation. CMR has emerged as the gold standard for a detailed study of the RV and has become an established modality for the physiological assessment of PH patients in cross-sectional studies, longitudinal follow up studies and clinical trials of therapy. We anticipate that MR imaging will increasingly be utilised as the primary modality for combined anatomic and functional assessments that enable more complete and efficient evaluation of patients with PH.

Chapter 6

General Discussion and Summary

6 General discussion and summary

Pulmonary vascular medicine is a rapidly evolving clinical speciality in which huge progression in treatment options have been made over recent years. Pulmonary hypertension is characterised by increased pulmonary vascular resistance leading to chronic right ventricular pressure overload. The adaptation of the right ventricle is the major prognostic influence in pulmonary hypertension. Changes to the RV due to pressure overload in PAH are complex, with increased RV wall stress leading to RV dilatation and hypertrophy, which affect the structure and function of the RV as it adapts to increased PAP. Current methods of assessment of pulmonary hypertension patients are suboptimal. The aim of this thesis was to evaluate the role of CMR imaging in the assessment of right ventricular function in pulmonary hypertension patients and to provide clarity in its role as a non-invasive monitoring technique.

The results from this thesis have demonstrated that CMR imaging can be performed safely and can yield high-quality images in pulmonary hypertension patients. The vast majority of patients in our studies tolerated this investigation well. Despite frequent verbal reports of claustrophobia, this was rarely an insurmountable problem and patients managed with reassurance, distraction (music) and prism glasses. The CMR protocol used involved frequent breath holds, which could be arduous. The patients were mostly able to breath-hold adequately during the MR pulse sequences despite significant gas exchange abnormalities. All CMR scans performed in this study provided satisfactory images for analysis. 3 patients on a continuous epoprostenol infusion were scanned during my studies. These scans were performed with the assistance of a Clinical Nurse Specialist who managed the infusion pump located in the CMR control room. All patients enrolled in the longitudinal study returned (if physically fit enough) for their interval CMR scans highlighting that this investigation was tolerated well in our study.

A low baseline stroke volume index is predictive of a poor outcome in pulmonary hypertension. In addition, a further reduction in SV at 1 year follow up, predicted treatment failure and a poor long-term outcome. A non-invasive, accurate measure of SV would be beneficial to monitor disease progression in patients with PH. The widely accepted reference standard measurement of SV is

by thermodilution measured during right heart catheterisation. In chapter 3, we evaluated the accuracy of CMR imaging and inert gas rebreathing (using photoacoustic analysis) in the measurement of SV compared to the gold standard of thermodilution. We confirmed that CMR imaging and IGR provided non-invasive measurements of SV that were as accurate as those obtained by thermodilution. With the advent of multiple new disease targeted therapy, it is imperative that we can assess patients noninvasively. This study suggests that accurate assessment of a resting SV could be achieved by either of these non-invasive techniques.

The ability of the RV to adapt to the increased afterload resulting from rising PVR is the main determinant of a patient's functional capacity and survival. It is evident that CTDPAH patients have a much poorer prognosis than IPAH patients. We sought to evaluate whether there was any detectable difference in cardiac adaptation as assessed by CMR at baseline between these two patient groups, which could account for the poorer prognosis. We did not find any difference between these two distinct groups, which could be detected by resting CMR imaging, for a given mean pulmonary artery pressure.

The Task Force on Treatment Goals for PH confirms the need to analyse multiple goals for defining success of therapy including symptoms, exercise capacity and the right ventricular function (259). The importance of morbidity and mortality primary endpoints in future clinical trials (260) has been highlighted recently. The imperative role of RV performance in the clinical status and long-term outcome of patients with PH is evident. Direct assessment of RV function may be the most appropriate method of determining response to therapy and monitoring disease progression than the currently used assessment tools. The primary requirements for a monitoring tool for PH patients are that it should be reproducible and observer independent, non-invasive, cost-effective, standardised, prognostic and sensitive to treatment. Current guidelines recommend a number of techniques to assess disease severity, response to treatment and prognosis. Each technique has benefits and limitations as previously discussed. The longitudinal study (chapter 5) in this thesis aimed to clarify the role of CMR in monitoring PH patients. This study confirmed significant changes in CMR measurements with the introduction of disease-

targeted therapy. These changes were not related, however, to the change in 6MWD. The correlation between CMR measurements and 6MWD was weak in our patient group. Change in 6MWD has been used widely as a key endpoint in many PAH trials to date. The use of 6MWD, however, as a surrogate marker of outcome (in particular, mortality and morbidity) has been questioned in several recent studies.

CMR imaging is a non-invasive tool that provides high-resolution, three-dimensional images of the heart. The right ventricle is difficult to assess due to its geometry. CMR provides information about right heart structure, volumes and function that is not readily obtained via other methods, such as echocardiography and RHC. Given the important implications of RV structure and function in morbidity and mortality in PH, regular assessment is critical.

CMR imaging is associated with a range of limitations: higher cost, more limited availability relative to other methods, the need for more intensive and time consuming analysis, and the requirement for significant technical support and expertise. CMR is incompatible with pacemakers and certain infusion pumps, and the need for breath holding may be difficult for patients (256, 261). However, given the relevance of the right heart in PH, the advantages of this method may outweigh these disadvantages in the monitoring of patients with established PAH and in the assessment of treatment response in clinical trials.

Future research

Standardisation of CMR protocols and multicenter trials are needed to assess the optimal role of CMR imaging in patients with pulmonary hypertension. Longitudinal assessment of novel CMR measurements were not included in the current analysis e.g. pulmonary artery stiffness, right ventricular arterial coupling or transverse shortening. Further research should be directed towards identifying whether these are important prognostically or therapeutically. Further investigation into CMR assessment of PH patients during exercise should be explored e.g. MR compatible ergometer, dobutamine administration as exercise cardiac output is an important outcome measure in PH.

CMR imaging provides a unique combination of morphological and functional assessment of the right ventricle and pulmonary circulation. It has emerged as the gold standard for detailed study of the right ventricle. CMR imaging is a relatively new imaging technique in pulmonary hypertension. It is likely to provide a useful assessment and monitoring tool for physicians in clinical practice as techniques develop. An increasing number of measurements have been shown to be prognostic in PAH patients, and studies have shown that CMR imaging can be used to detect improvements in cardiac function in response to disease targeted therapy. As such, CMR imaging has great potential as a non-invasive monitoring tool.

7 Appendices

7.1 Appendix 1: Euro-MR introductory letter

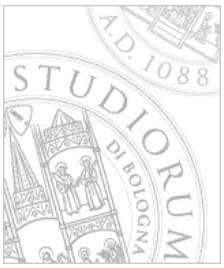

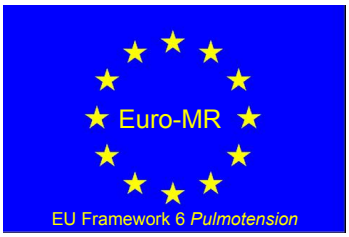

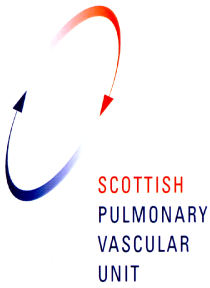

Longitudinal Assessment of Patients with Pulmonary Arterial Hypertension using Cardiac Magnetic Resonance Imaging: Relation to Genomics

Dear Colleague.

Welcome to the kick-off of "Euro-MR".

As you may know, the University of Bologna and ourselves were awarded EU Framework 6 funding to evaluate the use of cardiac MR in the assessment of changes in RV function in response to targeted therapy in patients with PAH. This will be a longitudinal study relating change in MR-derived variables to standard end points such as 6-MWD, NT pro-BNP, WHO class etc. In addition, we are interested in the influence of genomics upon the adaptation of the right ventricle and pulmonary circulation to treatment of PAH. Specifically we plan to assess the mutations of BMPR2 gene and polymorphisms of 5-HTT, endothelial NOS and ACE genes.

This is a golden opportunity to generate a Pan-European project in MR for PAH and we have received enthusiastic responses from most units we have contacted. We have undertaken to read all the scans using the attached protocol but each centre can also use the results for their own purposes.

We propose that patients are studied both within and without the context of clinical trials. Centres can decide whether or not they wish to be involved in the genetic side of the study.

Whilst some of you have already agreed to take part we are still awaiting news from others. Please take this opportunity to reply using the email address below to state whether you wish to participate. We have obtained funding to reduce the costs of CMR scans at each centre.

We would be grateful if you could forward contact details of relevant staff in your departments. When this information is collated a pack will be forwarded to every participant giving detailed information for your physicist and radiologists. We would welcome comments. It is our intention to send out a newsletter every 2 months informing centres of progress and recruitment numbers from each centre.

Best wishes,

Professor Andrew Peacock

SPVU STAFF

Director
Prof A Peacock

Senior Scientist
Dr D Welsh

MR Research Fellows
Dr L McLure
Dr K Blyth

CURRENTLY COMMITED CENTRES

SPVU
Prof A Peacock

Austria
Dr H Olschewski

Holland
Dr A Vonk- Noordegraaf

Italy
Dr N Galie

Scottish Pulmonary Vascular Unit, Level 8 Western Infirmary, Dumbarton Road, Glasgow, Scotland, G11 6NT
Telephone +44 141 211 6327 Facsimile +44 141 211 6334 e-mail david.welsh@bio.gla.ac.uk Web Site www.spvu.co.uk

7.2 Appendix 2: Euro-MR Newsletter

EURO MR Newsletter

October 2007

EU Framework 6: Pulmotension

Welcome to the first EURO-MR newsletter!

Recent expert opinion has stressed the importance of finding additional means of assessment of pulmonary hypertension (PHT). This includes both diagnostic and monitoring tools which can be used as end-points in therapeutic trials. The question of which end points are most relevant in the assessment of PHT has been the topic of intense discussion (End Points Meetings – Gleneagles May 2003, Turnberry June 2007).

Patients with PHT die from right ventricular (RV) failure. Measuring RV function is challenging. Cardiac magnetic resonance imaging (CMR) imaging is the most attractive modality for studying the complex geometry of the right ventricle and pulmonary vasculature. It is widely recognised as an accurate and reproducible means of measuring RV volume, RV mass, and pulmonary arterial flow in patients with PHT. This multinational EU funded Framework 6 EURO-MR study hopes to confirm that CMR will be a successful end point in PHT assessment.

To recap … EURO-MR Study Outline

Timescale	CMR Protocol	Comparators
0 weeks/Baseline • Disease targeted therapy introduction	CMR 1	• Haemodynamics • 6MWT • NTproBNP • WHO Functional class • Genomics; ACE, 5-HTT, BMPR2, eNOS
16 weeks	CMR 2	• 6MWT • NTproBNP • WHO Functional class
48 weeks	CMR 4	• 6MWT • NTproBNP • WHO Functional class

Right and left ventricular dimensions and function assessed by CMR:

- End diastolic volume (EDV)
- Stroke volume (SV)
- Mass
- Pulmonary artery flow analysis
- End systolic volume (ESV)
- Ejection fraction (EF)
- RV Mass Index ($^{RVM}/_{LVM}$)
- Pulmonary artery distensibility

Funding for EURO-MR

We have requested additional funding in the hope of extending the number of participating European centres. Costing for CMR scans varies between departments. Actelion have kindly offered to assist with funding for this exciting CMR study. Interested centres should contact us for further information on additional funding.

Participating European Centres so far ...

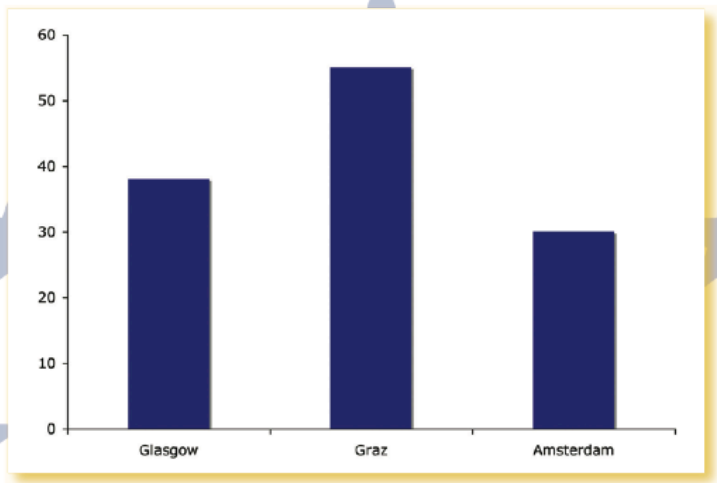

Further European Centres expressing interest in EURO-MR include Bologna, Papworth, Newcastle, Paris and Warsaw.

We would be delighted to hear from any interested groups and would welcome any comments. If you require any further details regarding EURO-MR please contact:

SCOTTISH PULMONARY VASCULAR UNIT

Dr. Lindsey McLure
Clinical Research Fellow
Scottish Pulmonary Vascular Unit
Western Infirmary
Glasgow G11 6NT
Tel: 0044 141 211 6327
Email: spvu@northglasgow.scot.nhs.uk

List of References

1. Rubin LJ. Primary pulmonary hypertension. N Engl J Med. 1997;336(2):111-7.
2. Runo JR, Loyd JE. Primary pulmonary hypertension. Lancet. 2003;361(9368):1533-44.
3. Fuster V, Steele PM, Edwards WD, Gersh BJ, McGoon MD, Frye RL. Primary pulmonary hypertension: natural history and the importance of thrombosis. Circulation. 1984;70(4):580-7.
4. D'Alonzo GE, Barst RJ, Ayres SM, Bergofsky EH, Brundage BH, Detre KM, et al. Survival in patients with primary pulmonary hypertension. Results from a national prospective registry. Ann Intern Med. 1991;115(5):343-9.
5. Kanemoto N. Natural history of pulmonary hemodynamics in primary pulmonary hypertension. Am Heart J. 1987;114(2):407-13.
6. Eysmann SB, Palevsky HI, Reichek N, Hackney K, Douglas PS. Two-dimensional and Doppler-echocardiographic and cardiac catheterization correlates of survival in primary pulmonary hypertension. Circulation. 1989;80(2):353-60.
7. Simonneau G, Gatzoulis MA, Adatia I, Celermajer D, Denton C, Ghofrani A, et al. Updated clinical classification of pulmonary hypertension. J Am Coll Cardiol. 2013;62(25 Suppl):D34-41.
8. Humbert M, Sitbon O, Chaouat A, Bertocchi M, Habib G, Gressin V, et al. Pulmonary arterial hypertension in France: results from a national registry. Am J Respir Crit Care Med. 2006;173(9):1023-30.
9. Peacock AJ, Murphy NF, McMurray JJ, Caballero L, Stewart S. An epidemiological study of pulmonary arterial hypertension in Scotland. Eur Respir J. 2007.
10. Sztrymf B, Coulet F, Girerd B, Yaici A, Jais X, Sitbon O, et al. Clinical outcomes of pulmonary arterial hypertension in carriers of BMPR2 mutation. American journal of respiratory and critical care medicine. 2008;177(12):1377-83.

11. Condliffe R, Kiely DG, Peacock AJ, Corris PA, Gibbs JS, Vrapi F, et al. Connective tissue disease-associated pulmonary arterial hypertension in the modern treatment era. Am J Respir Crit Care Med. 2009;179(2):151-7.

12. Mukerjee D, St George D, Coleiro B, Knight C, Denton CP, Davar J, et al. Prevalence and outcome in systemic sclerosis associated pulmonary arterial hypertension: application of a registry approach. Annals of the rheumatic diseases. 2003;62(11):1088-93.

13. Haas C. [Pulmonary hypertension associated with systemic lupus erythematosus]. Bull Acad Natl Med. 2004;188(6):985-97; discussion 97.

14. Hachulla E, Gressin V, Guillevin L, Carpentier P, Diot E, Sibilia J, et al. Early detection of pulmonary arterial hypertension in systemic sclerosis: a French nationwide prospective multicenter study. Arthritis and rheumatism. 2005;52(12):3792-800.

15. Dorfmuller P, Humbert M, Perros F, Sanchez O, Simonneau G, Muller KM, et al. Fibrous remodeling of the pulmonary venous system in pulmonary arterial hypertension associated with connective tissue diseases. Hum Pathol. 2007;38(6):893-902.

16. Chaouat A, Bugnet AS, Kadaoui N, Schott R, Enache I, Ducolone A, et al. Severe pulmonary hypertension and chronic obstructive pulmonary disease. American journal of respiratory and critical care medicine. 2005;172(2):189-94.

17. Thabut G, Dauriat G, Stern JB, Logeart D, Levy A, Marrash-Chahla R, et al. Pulmonary hemodynamics in advanced COPD candidates for lung volume reduction surgery or lung transplantation. Chest. 2005;127(5):1531-6.

18. Lettieri CJ, Nathan SD, Barnett SD, Ahmad S, Shorr AF. Prevalence and outcomes of pulmonary arterial hypertension in advanced idiopathic pulmonary fibrosis. Chest. 2006;129(3):746-52.

19. Cottin V, Nunes H, Brillet PY, Delaval P, Devouassoux G, Tillie-Leblond I, et al. Combined pulmonary fibrosis and emphysema: a distinct underrecognised entity. The European respiratory journal : official journal of the European Society for Clinical Respiratory Physiology. 2005;26(4):586-93.

20. Pengo V, Lensing AW, Prins MH, Marchiori A, Davidson BL, Tiozzo F, et al. Incidence of chronic thromboembolic pulmonary hypertension after pulmonary embolism. The New England journal of medicine. 2004;350(22):2257-64.

21. Hoeper MM, Lee SH, Voswinckel R, Palazzini M, Jais X, Marinelli A, et al. Complications of right heart catheterization procedures in patients with

pulmonary hypertension in experienced centers. J Am Coll Cardiol. 2006;48(12):2546-52.

22. Fedullo PF, Auger WR, Channick RN, Kerr KM, Rubin LJ. Chronic thromboembolic pulmonary hypertension. Clin Chest Med. 2001;22(3):561-81.

23. Galie N, Kim NH. Pulmonary microvascular disease in chronic thromboembolic pulmonary hypertension. Proceedings of the American Thoracic Society. 2006;3(7):571-6.

24. Lang IM. Chronic thromboembolic pulmonary hypertension--not so rare after all. The New England journal of medicine. 2004;350(22):2236-8.

25. Rich S, Dantzker DR, Ayres SM, Bergofsky EH, Brundage BH, Detre KM, et al. Primary pulmonary hypertension. A national prospective study. Ann Intern Med. 1987;107(2):216-23.

26. Galie N, Hoeper MM, Humbert M, Torbicki A, Vachiery JL, Barbera JA, et al. Guidelines for the diagnosis and treatment of pulmonary hypertension: the Task Force for the Diagnosis and Treatment of Pulmonary Hypertension of the European Society of Cardiology (ESC) and the European Respiratory Society (ERS), endorsed by the International Society of Heart and Lung Transplantation (ISHLT). European heart journal. 2009;30(20):2493-537.

27. Frishman WH, Landau A, Cretkovic A. Combination drug therapy with calcium-channel blockers in the treatment of systemic hypertension. J Clin Pharmacol. 1993;33(8):752-5.

28. Pitt B, Zannad F, Remme WJ, Cody R, Castaigne A, Perez A, et al. The effect of spironolactone on morbidity and mortality in patients with severe heart failure. Randomized Aldactone Evaluation Study Investigators. The New England journal of medicine. 1999;341(10):709-17.

29. Sitbon O, Humbert M, Jais X, Ioos V, Hamid AM, Provencher S, et al. Long-term response to calcium channel blockers in idiopathic pulmonary arterial hypertension. Circulation. 2005;111(23):3105-11.

30. Rich S, Kaufmann E, Levy PS. The effect of high doses of calcium-channel blockers on survival in primary pulmonary hypertension. The New England journal of medicine. 1992;327(2):76-81.

31. Jones DA, Benjamin CW, Linseman DA. Activation of thromboxane and prostacyclin receptors elicits opposing effects on vascular smooth muscle cell growth and mitogen-activated protein kinase signaling cascades. Mol Pharmacol. 1995;48(5):890-6.

32. Galie N, Hinderliter AL, Torbicki A, Fourme T, Simonneau G, Pulido T, et al. Effects of the oral endothelin-receptor antagonist bosentan on echocardiographic and doppler measures in patients with pulmonary arterial hypertension. J Am Coll Cardiol. 2003;41(8):1380-6.

33. Giaid A, Yanagisawa M, Langleben D, Michel RP, Levy R, Shennib H, et al. Expression of endothelin-1 in the lungs of patients with pulmonary hypertension. The New England journal of medicine. 1993;328(24):1732-9.

34. Stewart DJ, Levy RD, Cernacek P, Langleben D. Increased plasma endothelin-1 in pulmonary hypertension: marker or mediator of disease? Annals of internal medicine. 1991;114(6):464-9.

35. Galie N, Manes A, Branzi A. The endothelin system in pulmonary arterial hypertension. Cardiovascular research. 2004;61(2):227-37.

36. Wharton J, Strange JW, Moller GM, Growcott EJ, Ren X, Franklyn AP, et al. Antiproliferative effects of phosphodiesterase type 5 inhibition in human pulmonary artery cells. American journal of respiratory and critical care medicine. 2005;172(1):105-13.

37. Tantini B, Manes A, Fiumana E, Pignatti C, Guarnieri C, Zannoli R, et al. Antiproliferative effect of sildenafil on human pulmonary artery smooth muscle cells. Basic Res Cardiol. 2005;100(2):131-8.

38. Haddad F, Doyle R, Murphy DJ, Hunt SA. Right ventricular function in cardiovascular disease, part II: pathophysiology, clinical importance, and management of right ventricular failure. Circulation. 2008;117(13):1717-31.

39. Warnes CA. Adult congenital heart disease importance of the right ventricle. Journal of the American College of Cardiology. 2009;54(21):1903-10.

40. Rochais F, Mesbah K, Kelly RG. Signaling pathways controlling second heart field development. Circ Res. 2009;104(8):933-42.

41. Zaffran S, Kelly RG, Meilhac SM, Buckingham ME, Brown NA. Right ventricular myocardium derives from the anterior heart field. Circ Res. 2004;95(3):261-8.

42. Bogaard HJ, Abe K, Vonk Noordegraaf A, Voelkel NF. The right ventricle under pressure: cellular and molecular mechanisms of right-heart failure in pulmonary hypertension. Chest. 2009;135(3):794-804.

43. Urashima T, Zhao M, Wagner R, Fajardo G, Farahani S, Quertermous T, et al. Molecular and physiological characterization of RV remodeling in a murine

model of pulmonary stenosis. American journal of physiology Heart and circulatory physiology. 2008;295(3):H1351-H68.

44. Rudolph AM. Congenital cardiovascular malformations and the fetal circulation. Arch Dis Child Fetal Neonatal Ed. 2010;95(2):F132-6.

45. Kukulski T, Voigt JU, Wilkenshoff UM, Strotmann JM, Wranne B, Hatle L, et al. A comparison of regional myocardial velocity information derived by pulsed and color Doppler techniques: an in vitro and in vivo study. Echocardiography. 2000;17(7):639-51.

46. Redington AN. Physiopathology of right ventricular failure. Semin Thorac Cardiovasc Surg Pediatr Card Surg Annu. 2006:3-10.

47. Redington AN. Right ventricular function. Cardiol Clin. 2002;20(3):341-9, v.

48. Sheehan F, Redington A. The right ventricle: anatomy, physiology and clinical imaging. Heart. 2008;94(11):1510-5.

49. Boxt LM, Katz J, Kolb T, Czegledy FP, Barst RJ. Direct quantitation of right and left ventricular volumes with nuclear magnetic resonance imaging in patients with primary pulmonary hypertension. J Am Coll Cardiol. 1992;19(7):1508-15.

50. Doherty NE, 3rd, Fujita N, Caputo GR, Higgins CB. Measurement of right ventricular mass in normal and dilated cardiomyopathic ventricles using cine magnetic resonance imaging. Am J Cardiol. 1992;69(14):1223-8.

51. Katz J, Whang J, Boxt LM, Barst RJ. Estimation of right ventricular mass in normal subjects and in patients with primary pulmonary hypertension by nuclear magnetic resonance imaging. J Am Coll Cardiol. 1993;21(6):1475-81.

52. Pattynama PM, Willems LN, Smit AH, van der Wall EE, de Roos A. Early diagnosis of cor pulmonale with MR imaging of the right ventricle. Radiology. 1992;182(2):375-9.

53. Suzuki J, Caputo GR, Masui T, Chang JM, O'Sullivan M, Higgins CB. Assessment of right ventricular diastolic and systolic function in patients with dilated cardiomyopathy using cine magnetic resonance imaging. Am Heart J. 1991;122(4 Pt 1):1035-40.

54. Bottini PB, Carr AA, Prisant LM, Flickinger FW, Allison JD, Gottdiener JS. Magnetic resonance imaging compared to echocardiography to assess left ventricular mass in the hypertensive patient. Am J Hypertens. 1995;8(3):221-8.

55. Grothues F, Smith GC, Moon JC, Bellenger NG, Collins P, Klein HU, et al. Comparison of interstudy reproducibility of cardiovascular magnetic resonance with two-dimensional echocardiography in normal subjects and in patients with heart failure or left ventricular hypertrophy. Am J Cardiol. 2002;90(1):29-34.

56. Semelka RC, Tomei E, Wagner S, Mayo J, Kondo C, Suzuki J, et al. Normal left ventricular dimensions and function: interstudy reproducibility of measurements with cine MR imaging. Radiology. 1990;174(3 Pt 1):763-8.

57. Grothues F, Moon JC, Bellenger NG, Smith GS, Klein HU, Pennell DJ. Interstudy reproducibility of right ventricular volumes, function, and mass with cardiovascular magnetic resonance. Am Heart J. 2004;147(2):218-23.

58. Ley S, Kreitner KF, Fink C, Heussel CP, Borst MM, Kauczor HU. Assessment of pulmonary hypertension by CT and MR imaging. Eur Radiol. 2004;14(3):359-68.

59. Nayler GL, Firmin DN, Longmore DB. Blood flow imaging by cine magnetic resonance. J Comput Assist Tomogr. 1986;10(5):715-22.

60. Beerbaum P, Korperich H, Barth P, Esdorn H, Gieseke J, Meyer H. Noninvasive quantification of left-to-right shunt in pediatric patients: phase-contrast cine magnetic resonance imaging compared with invasive oximetry. Circulation. 2001;103(20):2476-82.

61. Robertson MB, Kohler U, Hoskins PR, Marshall I. Quantitative analysis of PC MRI velocity maps: pulsatile flow in cylindrical vessels. Magn Reson Imaging. 2001;19(5):685-95.

62. Holman ER, van Jonbergen HP, van Dijkman PR, van der Laarse A, de Roos A, van der Wall EE. Comparison of magnetic resonance imaging studies with enzymatic indexes of myocardial necrosis for quantification of myocardial infarct size. Am J Cardiol. 1993;71(12):1036-40.

63. Laissy JP, Messin B, Varenne O, Iung B, Karila-Cohen D, Schouman-Claeys E, et al. MRI of acute myocarditis: a comprehensive approach based on various imaging sequences. Chest. 2002;122(5):1638-48.

64. Lima JA, Judd RM, Bazille A, Schulman SP, Atalar E, Zerhouni EA. Regional heterogeneity of human myocardial infarcts demonstrated by contrast-enhanced MRI. Potential mechanisms. Circulation. 1995;92(5):1117-25.

65. Teraoka K, Hirano M, Ookubo H, Sasaki K, Katsuyama H, Amino M, et al. Delayed contrast enhancement of MRI in hypertrophic cardiomyopathy. Magn Reson Imaging. 2004;22(2):155-61.

66. McCann GP, Gan CT, Beek AM, Niessen HW, Vonk Noordegraaf A, van Rossum AC. Extent of MRI delayed enhancement of myocardial mass is related to right ventricular dysfunction in pulmonary artery hypertension. AJR Am J Roentgenol. 2007;188(2):349-55.

67. Uematsu H, Ohno Y, Hatabu H. Recent advances in magnetic resonance perfusion imaging of the lung. Top Magn Reson Imaging. 2003;14(3):245-51.

68. Bradlow WM, Hughes ML, Keenan NG, Bucciarelli-Ducci C, Assomull R, Gibbs JS, et al. Measuring the heart in pulmonary arterial hypertension (PAH): implications for trial study size. J Magn Reson Imaging. 2010;31(1):117-24.

69. Hoeper MM, Tongers J, Leppert A, Baus S, Maier R, Lotz J. Evaluation of right ventricular performance with a right ventricular ejection fraction thermodilution catheter and MRI in patients with pulmonary hypertension. Chest. 2001;120(2):502-7.

70. Roeleveld RJ, Vonk-Noordegraaf A, Marcus JT, Bronzwaer JG, Marques KM, Postmus PE, et al. Effects of epoprostenol on right ventricular hypertrophy and dilatation in pulmonary hypertension. Chest. 2004;125(2):572-9.

71. Vonk-Noordegraaf A, Marcus JT, Holverda S, Roseboom B, Postmus PE. Early changes of cardiac structure and function in COPD patients with mild hypoxemia. Chest. 2005;127(6):1898-903.

72. Vonk Noordegraaf A, Marcus JT, Roseboom B, Postmus PE, Faes TJ, de Vries PM. The effect of right ventricular hypertrophy on left ventricular ejection fraction in pulmonary emphysema. Chest. 1997;112(3):640-5.

73. van Wolferen SA, Marcus JT, Boonstra A, Marques KM, Bronzwaer JG, Spreeuwenberg MD, et al. Prognostic value of right ventricular mass, volume, and function in idiopathic pulmonary arterial hypertension. Eur Heart J. 2007;28(10):1250-7.

74. Gan CT, Lankhaar JW, Marcus JT, Westerhof N, Marques KM, Bronzwaer JG, et al. Impaired left ventricular filling due to right-to-left ventricular interaction in patients with pulmonary arterial hypertension. Am J Physiol Heart Circ Physiol. 2006;290(4):H1528-33.

75. Saba TS, Foster J, Cockburn M, Cowan M, Peacock AJ. Ventricular mass index using magnetic resonance imaging accurately estimates pulmonary artery pressure. Eur Respir J. 2002;20(6):1519-24.

76. Roeleveld RJ, Marcus JT, Boonstra A, Postmus PE, Marques KM, Bronzwaer JG, et al. A comparison of noninvasive MRI-based methods of estimating

pulmonary artery pressure in pulmonary hypertension. J Magn Reson Imaging. 2005;22(1):67-72.

77. King ME, Braun H, Goldblatt A, Liberthson R, Weyman AE. Interventricular septal configuration as a predictor of right ventricular systolic hypertension in children: a cross-sectional echocardiographic study. Circulation. 1983;68(1):68-75.

78. Roeleveld RJ, Marcus JT, Faes TJ, Gan TJ, Boonstra A, Postmus PE, et al. Interventricular septal configuration at mr imaging and pulmonary arterial pressure in pulmonary hypertension. Radiology. 2005;234(3):710-7.

79. Brechot N, Gambotti L, Lafitte S, Roudaut R. Usefulness of right ventricular isovolumic relaxation time in predicting systolic pulmonary artery pressure. European journal of echocardiography : the journal of the Working Group on Echocardiography of the European Society of Cardiology. 2008;9(4):547-54.

80. Gan CT, Holverda S, Marcus JT, Paulus WJ, Marques KM, Bronzwaer JG, et al. Right ventricular diastolic dysfunction and the acute effects of sildenafil in pulmonary hypertension patients. Chest. 2007;132(1):11-7.

81. Lindqvist P, Waldenstrom A, Wikstrom G, Kazzam E. Right ventricular myocardial isovolumic relaxation time and pulmonary pressure. Clinical physiology and functional imaging. 2006;26(1):1-8.

82. Dambrauskaite V, Delcroix M, Claus P, Herbots L, Palecek T, D'Hooge J, et al. The evaluation of pulmonary hypertension using right ventricular myocardial isovolumic relaxation time. J Am Soc Echocardiogr. 2005;18(11):1113-20.

83. Yeo TC, Dujardin KS, Tei C, Mahoney DW, McGoon MD, Seward JB. Value of a Doppler-derived index combining systolic and diastolic time intervals in predicting outcome in primary pulmonary hypertension. Am J Cardiol. 1998;81(9):1157-61.

84. Boissiere J, Gautier M, Machet MC, Hanton G, Bonnet P, Eder V. Doppler tissue imaging in assessment of pulmonary hypertension-induced right ventricle dysfunction. Am J Physiol Heart Circ Physiol. 2005;289(6):H2450-5.

85. Lakoumentas JA, Panou FK, Kotseroglou VK, Aggeli KI, Harbis PK. The Tei index of myocardial performance: applications in cardiology. Hellenic J Cardiol. 2005;46(1):52-8.

86. Lindqvist P, Caidahl K, Neuman-Andersen G, Ozolins C, Rantapaa-Dahlqvist S, Waldenstrom A, et al. Disturbed right ventricular diastolic function

in patients with systemic sclerosis: a Doppler tissue imaging study. Chest. 2005;128(2):755-63.

87. Yu CM, Sanderson JE, Chan S, Yeung L, Hung YT, Woo KS. Right ventricular diastolic dysfunction in heart failure. Circulation. 1996;93(8):1509-14.

88. Marcus JT, Gan CT, Zwanenburg JJ, Boonstra A, Allaart CP, Gotte MJ, et al. Interventricular mechanical asynchrony in pulmonary arterial hypertension: left-to-right delay in peak shortening is related to right ventricular overload and left ventricular underfilling. J Am Coll Cardiol. 2008;51(7):750-7.

89. Mauritz GJ, Marcus JT, Westerhof N, Postmus PE, Vonk-Noordegraaf A. Prolonged right ventricular post-systolic isovolumic period in pulmonary arterial hypertension is not a reflection of diastolic dysfunction. Heart. 2011;97(6):473-8.

90. Raymond RJ, Hinderliter AL, Willis PW, Ralph D, Caldwell EJ, Williams W, et al. Echocardiographic predictors of adverse outcomes in primary pulmonary hypertension. J Am Coll Cardiol. 2002;39(7):1214-9.

91. Kind T, Mauritz GJ, Marcus JT, van de Veerdonk M, Westerhof N, Vonk-Noordegraaf A. Right ventricular ejection fraction is better reflected by transverse rather than longitudinal wall motion in pulmonary hypertension. J Cardiovasc Magn Reson. 2010;12:35.

92. Mauritz GJ, Kind T, Marcus JT, Bogaard HJ, van de Veerdonk M, Postmus PE, et al. Progressive changes in right ventricular geometric shortening and long-term survival in pulmonary arterial hypertension. Chest. 2012;141(4):935-43.

93. Kuehne T, Yilmaz S, Steendijk P, Moore P, Groenink M, Saaed M, et al. Magnetic resonance imaging analysis of right ventricular pressure-volume loops: in vivo validation and clinical application in patients with pulmonary hypertension. Circulation. 2004;110(14):2010-6.

94. Sanz J, Garcia-Alvarez A, Fernandez-Friera L, Nair A, Mirelis JG, Sawit ST, et al. Right ventriculo-arterial coupling in pulmonary hypertension: a magnetic resonance study. Heart. 2012;98(3):238-43.

95. Kuehne T, Yilmaz S, Schulze-Neick I, Wellnhofer E, Ewert P, Nagel E, et al. Magnetic resonance imaging guided catheterisation for assessment of pulmonary vascular resistance: in vivo validation and clinical application in patients with pulmonary hypertension. Heart. 2005;91(8):1064-9.

96. Blyth KG, Groenning BA, Martin TN, Foster JE, Mark PB, Dargie HJ, et al. Contrast enhanced-cardiovascular magnetic resonance imaging in patients with pulmonary hypertension. Eur Heart J. 2005;26(19):1993-9.

97. Bradlow WM, Assomull R, Kilner PJ, Gibbs JS, Sheppard MN, Mohiaddin RH. Understanding late gadolinium enhancement in pulmonary hypertension. Circulation Cardiovascular imaging. 2010;3(4):501-3.

98. Kuribayashi T, Roberts WC. Myocardial disarray at junction of ventricular septum and left and right ventricular free walls in hypertrophic cardiomyopathy. Am J Cardiol. 1992;70(15):1333-40.

99. Holverda S, Gan CT, Marcus JT, Postmus PE, Boonstra A, Vonk-Noordegraaf A. Impaired stroke volume response to exercise in pulmonary arterial hypertension. J Am Coll Cardiol. 2006;47(8):1732-3.

100. Tulevski, II, Lee PL, Groenink M, van der Wall EE, Stoker J, Pieper PG, et al. Dobutamine-induced increase of right ventricular contractility without increased stroke volume in adolescent patients with transposition of the great arteries: evaluation with magnetic resonance imaging. Int J Card Imaging. 2000;16(6):471-8.

101. Vogel-Claussen J, Skrok J, Shehata ML, Singh S, Sibley CT, Boyce DM, et al. Right and left ventricular myocardial perfusion reserves correlate with right ventricular function and pulmonary hemodynamics in patients with pulmonary arterial hypertension. Radiology. 2011;258(1):119-27.

102. Mauritz GJ, Marcus JT, Boonstra A, Postmus PE, Westerhof N, Vonk-Noordegraaf A. Non-invasive stroke volume assessment in patients with pulmonary arterial hypertension: left-sided data mandatory. J Cardiovasc Magn Reson. 2008;10(1):51.

103. Bogren HG, Klipstein RH, Mohiaddin RH, Firmin DN, Underwood SR, Rees RS, et al. Pulmonary artery distensibility and blood flow patterns: a magnetic resonance study of normal subjects and of patients with pulmonary arterial hypertension. Am Heart J. 1989;118(5 Pt 1):990-9.

104. Kondo C, Caputo GR, Masui T, Foster E, O'Sullivan M, Stulbarg MS, et al. Pulmonary hypertension: pulmonary flow quantification and flow profile analysis with velocity-encoded cine MR imaging. Radiology. 1992;183(3):751-8.

105. Mousseaux E, Tasu JP, Jolivet O, Simonneau G, Bittoun J, Gaux JC. Pulmonary arterial resistance: noninvasive measurement with indexes of

pulmonary flow estimated at velocity-encoded MR imaging--preliminary experience. Radiology. 1999;212(3):896-902.

106. Kreitner KF, Ley S, Kauczor HU, Mayer E, Kramm T, Pitton MB, et al. Chronic thromboembolic pulmonary hypertension: pre- and postoperative assessment with breath-hold MR imaging techniques. Radiology. 2004;232(2):535-43.

107. Ley S, Puderbach M, Fink C, Eichinger M, Plathow C, Teiner S, et al. Assessment of hemodynamic changes in the systemic and pulmonary arterial circulation in patients with cystic fibrosis using phase-contrast MRI. Eur Radiol. 2005;15(8):1575-80.

108. Sanz J, Kuschnir P, Rius T, Salguero R, Sulica R, Einstein AJ, et al. Pulmonary arterial hypertension: noninvasive detection with phase-contrast MR imaging. Radiology. 2007;243(1):70-9.

109. Reiter G, Reiter U, Kovacs G, Kainz B, Schmidt K, Maier R, et al. Magnetic resonance-derived 3-dimensional blood flow patterns in the main pulmonary artery as a marker of pulmonary hypertension and a measure of elevated mean pulmonary arterial pressure. Circulation Cardiovascular imaging. 2008;1(1):23-30.

110. Mohiaddin RH, Yang GZ, Kilner PJ. Visualization of flow by vector analysis of multidirectional cine MR velocity mapping. J Comput Assist Tomogr. 1994;18(3):383-92.

111. Jardim C, Rochitte CE, Humbert M, Rubenfeld G, Jasinowodolinski D, Carvalho CR, et al. Pulmonary artery distensibility in pulmonary arterial hypertension: a MRI pilot study. Eur Respir J. 2006.

112. Gan CT, Lankhaar JW, Westerhof N, Marcus JT, Becker A, Twisk JW, et al. Noninvasively assessed pulmonary artery stiffness predicts mortality in pulmonary arterial hypertension. Chest. 2007;132(6):1906-12.

113. Sanz J, Kariisa M, Dellegrottaglie S, Prat-Gonzalez S, Garcia MJ, Fuster V, et al. Evaluation of pulmonary artery stiffness in pulmonary hypertension with cardiac magnetic resonance. JACC Cardiovascular imaging. 2009;2(3):286-95.

114. Laffon E, Laurent F, Bernard V, De Boucaud L, Ducassou D, Marthan R. Noninvasive assessment of pulmonary arterial hypertension by MR phase-mapping method. J Appl Physiol. 2001;90(6):2197-202.

115. Bradlow WM, Gatehouse PD, Hughes RL, O'Brien AB, Gibbs JS, Firmin DN, et al. Assessing normal pulse wave velocity in the proximal pulmonary arteries

using transit time: a feasibility, repeatability, and observer reproducibility study by cardiovascular magnetic resonance. J Magn Reson Imaging. 2007;25(5):974-81.

116. Ohno Y, Hatabu H, Murase K, Higashino T, Nogami M, Yoshikawa T, et al. Primary pulmonary hypertension: 3D dynamic perfusion MRI for quantitative analysis of regional pulmonary perfusion. AJR Am J Roentgenol. 2007;188(1):48-56.

117. Yock PG, Popp RL. Noninvasive estimation of right ventricular systolic pressure by Doppler ultrasound in patients with tricuspid regurgitation. Circulation. 1984;70(4):657-62.

118. Bouchard A, Higgins CB, Byrd BF, 3rd, Amparo EG, Osaki L, Axelrod R. Magnetic resonance imaging in pulmonary arterial hypertension. Am J Cardiol. 1985;56(15):938-42.

119. Saito H, Dambara T, Aiba M, Suzuki T, Kira S. Evaluation of cor pulmonale on a modified short-axis section of the heart by magnetic resonance imaging. Am Rev Respir Dis. 1992;146(6):1576-81.

120. Laffon E, Vallet C, Bernard V, Montaudon M, Ducassou D, Laurent F, et al. A computed method for noninvasive MRI assessment of pulmonary arterial hypertension. J Appl Physiol. 2004;96(2):463-8.

121. Lankhaar JW, Vonk Noordegraaf A, Marcus JT. A computed method for noninvasive MRI assessment of pulmonary arterial hypertension. J Appl Physiol. 2004;97(2):794; author reply -5.

122. Spindler M, Schmidt M, Geier O, Sandstede J, Hahn D, Ertl G, et al. Functional and metabolic recovery of the right ventricle during Bosentan therapy in idiopathic pulmonary arterial hypertension. J Cardiovasc Magn Reson. 2005;7(5):853-4.

123. Marcu CB, Beek AM, Van Rossum AC. Cardiovascular magnetic resonance imaging for the assessment of right heart involvement in cardiac and pulmonary disease. Heart Lung Circ. 2006;15(6):362-70.

124. Pennell DJ, Sechtem UP, Higgins CB, Manning WJ, Pohost GM, Rademakers FE, et al. Clinical indications for cardiovascular magnetic resonance (CMR): Consensus Panel report. Eur Heart J. 2004;25(21):1940-65.

125. Gabrielsen A, Videbaek R, Schou M, Damgaard M, Kastrup J, Norsk P. Non-invasive measurement of cardiac output in heart failure patients using a new foreign gas rebreathing technique. Clin Sci (Lond). 2002;102(2):247-52.

126. Ayotte B, Seymour J, McIlroy MB. A new method for measurement of cardiac output with nitrous oxide. J Appl Physiol. 1970;28(6):863-6.

127. Heneghan CP, Branthwaite MA. Non-invasive measurement of cardiac output during anaesthesia. An evaluation of the soluble gas uptake method. Br J Anaesth. 1981;53(4):351-5.

128. Hook C, Meyer M. Pulmonary blood flow, diffusing, capacity and tissue volume by rebreathing: theory. Respir Physiol. 1982;48(2):255-79.

129. Petrini MF, Peterson BT, Hyde RW. Lung tissue volume and blood flow by rebreathing theory. J Appl Physiol. 1978;44(5):795-802.

130. Agostoni P, Cattadori G, Apostolo A, Contini M, Palermo P, Marenzi G, et al. Noninvasive measurement of cardiac output during exercise by inert gas rebreathing technique: a new tool for heart failure evaluation. J Am Coll Cardiol. 2005;46(9):1779-81.

131. Peyton PJ, Thompson B. Agreement of an inert gas rebreathing device with thermodilution and the direct oxygen Fick method in measurement of pulmonary blood flow. J Clin Monit Comput. 2004;18(5-6):373-8.

132. Distler O, Behrens F, Pittrow D, Huscher D, Denton CP, Foeldvari I, et al. Defining appropriate outcome measures in pulmonary arterial hypertension related to systemic sclerosis: a Delphi consensus study with cluster analysis. Arthritis and rheumatism. 2008;59(6):867-75.

133. Voelkel MA, Wynne KM, Badesch DB, Groves BM, Voelkel NF. Hyperuricemia in severe pulmonary hypertension. Chest. 2000;117(1):19-24.

134. Nagaya N, Nishikimi T, Uematsu M, Satoh T, Kyotani S, Sakamaki F, et al. Plasma brain natriuretic peptide as a prognostic indicator in patients with primary pulmonary hypertension. Circulation. 2000;102(8):865-70.

135. Williams MH, Handler CE, Akram R, Smith CJ, Das C, Smee J, et al. Role of N-terminal brain natriuretic peptide (N-TproBNP) in scleroderma-associated pulmonary arterial hypertension. European heart journal. 2006;27(12):1485-94.

136. Fijalkowska A, Kurzyna M, Torbicki A, Szewczyk G, Florczyk M, Pruszczyk P, et al. Serum N-terminal brain natriuretic peptide as a prognostic parameter in patients with pulmonary hypertension. Chest. 2006;129(5):1313-21.

137. Andreassen AK, Wergeland R, Simonsen S, Geiran O, Guevara C, Ueland T. N-terminal pro-B-type natriuretic peptide as an indicator of disease severity in a heterogeneous group of patients with chronic precapillary pulmonary hypertension. The American journal of cardiology. 2006;98(4):525-9.

138. Torbicki A, Kurzyna M, Kuca P, Fijalkowska A, Sikora J, Florczyk M, et al. Detectable serum cardiac troponin T as a marker of poor prognosis among patients with chronic precapillary pulmonary hypertension. Circulation. 2003;108(7):844-8.

139. ATS statement: guidelines for the six-minute walk test. Am J Respir Crit Care Med. 2002;166(1):111-7.

140. Guyatt GH, Sullivan MJ, Thompson PJ, Fallen EL, Pugsley SO, Taylor DW, et al. The 6-minute walk: a new measure of exercise capacity in patients with chronic heart failure. Can Med Assoc J. 1985;132(8):919-23.

141. Miyamoto S, Nagaya N, Satoh T, Kyotani S, Sakamaki F, Fujita M, et al. Clinical correlates and prognostic significance of six-minute walk test in patients with primary pulmonary hypertension. Comparison with cardiopulmonary exercise testing. Am J Respir Crit Care Med. 2000;161(2 Pt 1):487-92.

142. Sun XG, Hansen JE, Oudiz RJ, Wasserman K. Exercise pathophysiology in patients with primary pulmonary hypertension. Circulation. 2001;104(4):429-35.

143. Raeside DA, Smith A, Brown A, Patel KR, Madhok R, Cleland J, et al. Pulmonary artery pressure measurement during exercise testing in patients with suspected pulmonary hypertension. The European respiratory journal : official journal of the European Society for Clinical Respiratory Physiology. 2000;16(2):282-7.

144. Oudiz RJ, Barst RJ, Hansen JE, Sun XG, Garofano R, Wu X, et al. Cardiopulmonary exercise testing and six-minute walk correlations in pulmonary arterial hypertension. The American journal of cardiology. 2006;97(1):123-6.

145. Wensel R, Opitz CF, Anker SD, Winkler J, Hoffken G, Kleber FX, et al. Assessment of survival in patients with primary pulmonary hypertension: importance of cardiopulmonary exercise testing. Circulation. 2002;106(3):319-24.

146. Tei C, Dujardin KS, Hodge DO, Bailey KR, McGoon MD, Tajik AJ, et al. Doppler echocardiographic index for assessment of global right ventricular function. J Am Soc Echocardiogr. 1996;9(6):838-47.

147. Forfia PR, Fisher MR, Mathai SC, Housten-Harris T, Hemnes AR, Borlaug BA, et al. Tricuspid annular displacement predicts survival in pulmonary hypertension. Am J Respir Crit Care Med. 2006;174(9):1034-41.

148. Tunariu N, Gibbs SJ, Win Z, Gin-Sing W, Graham A, Gishen P, et al. Ventilation-perfusion scintigraphy is more sensitive than multidetector CTPA in

detecting chronic thromboembolic pulmonary disease as a treatable cause of pulmonary hypertension. J Nucl Med. 2007;48(5):680-4.

149. Dartevelle P, Fadel E, Mussot S, Chapelier A, Herve P, de Perrot M, et al. Chronic thromboembolic pulmonary hypertension. The European respiratory journal : official journal of the European Society for Clinical Respiratory Physiology. 2004;23(4):637-48.

150. Reichelt A, Hoeper MM, Galanski M, Keberle M. Chronic thromboembolic pulmonary hypertension: evaluation with 64-detector row CT versus digital substraction angiography. European journal of radiology. 2009;71(1):49-54.

151. Lorenz CH, Walker ES, Morgan VL, Klein SS, Graham TP, Jr. Normal human right and left ventricular mass, systolic function, and gender differences by cine magnetic resonance imaging. J Cardiovasc Magn Reson. 1999;1(1):7-21.

152. Marcus JT, Vonk Noordegraaf A, Roeleveld RJ, Postmus PE, Heethaar RM, Van Rossum AC, et al. Impaired left ventricular filling due to right ventricular pressure overload in primary pulmonary hypertension: noninvasive monitoring using MRI. Chest. 2001;119(6):1761-5.

153. Paz R, Mohiaddin RH, Longmore DB. Magnetic resonance assessment of the pulmonary arterial trunk anatomy, flow, pulsatility and distensibility. Eur Heart J. 1993;14(11):1524-30.

154. Tardivon AA, Mousseaux E, Brenot F, Bittoun J, Jolivet O, Bourroul E, et al. Quantification of hemodynamics in primary pulmonary hypertension with magnetic resonance imaging. Am J Respir Crit Care Med. 1994;150(4):1075-80.

155. Jardim C, Rochitte CE, Humbert M, Rubenfeld G, Jasinowodolinski D, Carvalho CR, et al. Pulmonary artery distensibility in pulmonary arterial hypertension: an MRI pilot study. The European respiratory journal : official journal of the European Society for Clinical Respiratory Physiology. 2007;29(3):476-81.

156. van de Veerdonk MC, Kind T, Marcus JT, Mauritz GJ, Heymans MW, Bogaard HJ, et al. Progressive right ventricular dysfunction in patients with pulmonary arterial hypertension responding to therapy. J Am Coll Cardiol. 2011;58(24):2511-9.

157. Peacock A, Naeije R, Galie N, Reeves JT. End points in pulmonary arterial hypertension: the way forward. Eur Respir J. 2004;23(6):947-53.

158. Barst RJ, Gibbs JS, Ghofrani HA, Hoeper MM, McLaughlin VV, Rubin LJ, et al. Updated evidence-based treatment algorithm in pulmonary arterial

hypertension. Journal of the American College of Cardiology. 2009;54(1 Suppl):S78-84.

159. McLaughlin VV, Presberg KW, Doyle RL, Abman SH, McCrory DC, Fortin T, et al. Prognosis of pulmonary arterial hypertension: ACCP evidence-based clinical practice guidelines. Chest. 2004;126(1 Suppl):78S-92S.

160. Task Force for D, Treatment of Pulmonary Hypertension of European Society of C, European Respiratory S, International Society of H, Lung T, Galie N, et al. Guidelines for the diagnosis and treatment of pulmonary hypertension. Eur Respir J. 2009;34(6):1219-63.

161. McLaughlin VV, McGoon MD. Pulmonary arterial hypertension. Circulation. 2006;114(13):1417-31.

162. Peacock AJ, Naeije R, Galie N, Rubin L. End-points and clinical trial design in pulmonary arterial hypertension: have we made progress? The European respiratory journal : official journal of the European Society for Clinical Respiratory Physiology. 2009;34(1):231-42.

163. McKenna SP, Doughty N, Meads DM, Doward LC, Pepke-Zaba J. The Cambridge Pulmonary Hypertension Outcome Review (CAMPHOR): a measure of health-related quality of life and quality of life for patients with pulmonary hypertension. Qual Life Res. 2006;15(1):103-15.

164. Sitbon O, Humbert M, Nunes H, Parent F, Garcia G, Herve P, et al. Long-term intravenous epoprostenol infusion in primary pulmonary hypertension: prognostic factors and survival. J Am Coll Cardiol. 2002;40(4):780-8.

165. Paciocco G, Martinez FJ, Bossone E, Pielsticker E, Gillespie B, Rubenfire M. Oxygen desaturation on the six-minute walk test and mortality in untreated primary pulmonary hypertension. The European respiratory journal : official journal of the European Society for Clinical Respiratory Physiology. 2001;17(4):647-52.

166. Barst RJ, Langleben D, Frost A, Horn EM, Oudiz R, Shapiro S, et al. Sitaxsentan therapy for pulmonary arterial hypertension. American journal of respiratory and critical care medicine. 2004;169(4):441-7.

167. Barst RJ, McGoon M, McLaughlin V, Tapson V, Rich S, Rubin L, et al. Beraprost therapy for pulmonary arterial hypertension. Journal of the American College of Cardiology. 2003;41(12):2119-25.

168. Rich S. The current treatment of pulmonary arterial hypertension: time to redefine success. Chest. 2006;130(4):1198-202.

169. Mereles D, Ehlken N, Kreuscher S, Ghofrani S, Hoeper MM, Halank M, et al. Exercise and respiratory training improve exercise capacity and quality of life in patients with severe chronic pulmonary hypertension. Circulation. 2006;114(14):1482-9.

170. Sciurba F, Criner GJ, Lee SM, Mohsenifar Z, Shade D, Slivka W, et al. Six-minute walk distance in chronic obstructive pulmonary disease: reproducibility and effect of walking course layout and length. American journal of respiratory and critical care medicine. 2003;167(11):1522-7.

171. Nogueira PA, Leal AC, Pulz C, Nogueira ID, Filho JA. Clinical reliability of the 6 minute corridor walk test performed within a week of a myocardial infarction. Int Heart J. 2006;47(4):533-40.

172. Eaton T, Young P, Milne D, Wells AU. Six-minute walk, maximal exercise tests: reproducibility in fibrotic interstitial pneumonia. American journal of respiratory and critical care medicine. 2005;171(10):1150-7.

173. Macchia A, Marchioli R, Marfisi R, Scarano M, Levantesi G, Tavazzi L, et al. A meta-analysis of trials of pulmonary hypertension: a clinical condition looking for drugs and research methodology. American heart journal. 2007;153(6):1037-47.

174. Palange P, Ward SA, Carlsen KH, Casaburi R, Gallagher CG, Gosselink R, et al. Recommendations on the use of exercise testing in clinical practice. The European respiratory journal : official journal of the European Society for Clinical Respiratory Physiology. 2007;29(1):185-209.

175. Ross RM. ATS/ACCP statement on cardiopulmonary exercise testing. American journal of respiratory and critical care medicine. 2003;167(10):1451; author reply

176. West JB. Left ventricular filling pressures during exercise: a cardiological blind spot? Chest. 1998;113(6):1695-7.

177. Currie PJ, Seward JB, Chan KL, Fyfe DA, Hagler DJ, Mair DD, et al. Continuous wave Doppler determination of right ventricular pressure: a simultaneous Doppler-catheterization study in 127 patients. J Am Coll Cardiol. 1985;6(4):750-6.

178. Tei C, Ling LH, Hodge DO, Bailey KR, Oh JK, Rodeheffer RJ, et al. New index of combined systolic and diastolic myocardial performance: a simple and reproducible measure of cardiac function--a study in normals and dilated cardiomyopathy. Journal of cardiology. 1995;26(6):357-66.

179. Denton CP, Cailes JB, Phillips GD, Wells AU, Black CM, Bois RM. Comparison of Doppler echocardiography and right heart catheterization to assess pulmonary hypertension in systemic sclerosis. Br J Rheumatol. 1997;36(2):239-43.

180. Arcasoy SM, Christie JD, Ferrari VA, Sutton MS, Zisman DA, Blumenthal NP, et al. Echocardiographic assessment of pulmonary hypertension in patients with advanced lung disease. Am J Respir Crit Care Med. 2003;167(5):735-40.

181. Nagaya N, Nishikimi T, Okano Y, Uematsu M, Satoh T, Kyotani S, et al. Plasma brain natriuretic peptide levels increase in proportion to the extent of right ventricular dysfunction in pulmonary hypertension. J Am Coll Cardiol. 1998;31(1):202-8.

182. Gan CT, McCann GP, Marcus JT, van Wolferen SA, Twisk JW, Boonstra A, et al. NT-proBNP reflects right ventricular structure and function in pulmonary hypertension. Eur Respir J. 2006;28(6):1190-4.

183. Lankeit M, Dellas C, Panzenbock A, Skoro-Sajer N, Bonderman D, Olschewski M, et al. Heart-type fatty acid-binding protein for risk assessment of chronic thromboembolic pulmonary hypertension. The European respiratory journal : official journal of the European Society for Clinical Respiratory Physiology. 2008;31(5):1024-9.

184. Nickel N, Kempf T, Tapken H, Tongers J, Laenger F, Lehmann U, et al. Growth differentiation factor-15 in idiopathic pulmonary arterial hypertension. American journal of respiratory and critical care medicine. 2008;178(5):534-41.

185. Castelain V, Chemla D, Humbert M, Sitbon O, Simonneau G, Lecarpentier Y, et al. Pulmonary artery pressure-flow relations after prostacyclin in primary pulmonary hypertension. Am J Respir Crit Care Med. 2002;165(3):338-40.

186. Longmore DB, Klipstein RH, Underwood SR, Firmin DN, Hounsfield GN, Watanabe M, et al. Dimensional accuracy of magnetic resonance in studies of the heart. Lancet. 1985;1(8442):1360-2.

187. Moon JC, Lorenz CH, Francis JM, Smith GC, Pennell DJ. Breath-hold FLASH and FISP cardiovascular MR imaging: left ventricular volume differences and reproducibility. Radiology. 2002;223(3):789-97.

188. Moulton MJ, Creswell LL, Ungacta FF, Downing SW, Szabo BA, Pasque MK. Magnetic resonance imaging provides evidence for remodeling of the right ventricle after single-lung transplantation for pulmonary hypertension. Circulation. 1996;94(9 Suppl):II312-9.

189. Michelakis ED, Tymchak W, Noga M, Webster L, Wu XC, Lien D, et al. Long-term treatment with oral sildenafil is safe and improves functional capacity and hemodynamics in patients with pulmonary arterial hypertension. Circulation. 2003;108(17):2066-9.

190. van Wolferen SA, Boonstra A, Marcus JT, Marques KM, Bronzwaer JG, Postmus PE, et al. Right ventricular reverse remodelling after sildenafil in pulmonary arterial hypertension. Heart. 2006;92(12):1860-1.

191. Wilkins MR, Paul GA, Strange JW, Tunariu N, Gin-Sing W, Banya WA, et al. Sildenafil versus Endothelin Receptor Antagonist for Pulmonary Hypertension (SERAPH) study. Am J Respir Crit Care Med. 2005;171(11):1292-7.

192. Frist WH, Lorenz CH, Walker ES, Loyd JE, Stewart JR, Graham TP, Jr., et al. MRI complements standard assessment of right ventricular function after lung transplantation. Ann Thorac Surg. 1995;60(2):268-71.

193. Kasimir MT, Seebacher G, Jaksch P, Winkler G, Schmid K, Marta GM, et al. Reverse cardiac remodelling in patients with primary pulmonary hypertension after isolated lung transplantation. Eur J Cardiothorac Surg. 2004;26(4):776-81.

194. D'Armini AM, Zanotti G, Ghio S, Magrini G, Pozzi M, Scelsi L, et al. Reverse right ventricular remodeling after pulmonary endarterectomy. The Journal of thoracic and cardiovascular surgery. 2007;133(1):162-8.

195. Reesink HJ, Marcus JT, Tulevski, II, Jamieson S, Kloek JJ, Vonk Noordegraaf A, et al. Reverse right ventricular remodeling after pulmonary endarterectomy in patients with chronic thromboembolic pulmonary hypertension: utility of magnetic resonance imaging to demonstrate restoration of the right ventricle. The Journal of thoracic and cardiovascular surgery. 2007;133(1):58-64.

196. Mohiaddin RH, Paz R, Theodoropoulos S, Firmin DN, Longmore DB, Yacoub MH. Magnetic resonance characterization of pulmonary arterial blood flow after single lung transplantation. J Thorac Cardiovasc Surg. 1991;101(6):1016-23.

197. Chin KM, Kingman M, de Lemos JA, Warner JJ, Reimold S, Peshock R, et al. Changes in right ventricular structure and function assessed using cardiac magnetic resonance imaging in bosentan-treated patients with pulmonary arterial hypertension. Am J Cardiol. 2008;101(11):1669-72.

198. Wilkins MR, Ali O, Bradlow W, Wharton J, Taegtmeyer A, Rhodes CJ, et al. Simvastatin as a treatment for pulmonary hypertension trial. Am J Respir Crit Care Med. 2010;181(10):1106-13.

199. van Wolferen SA, van de Veerdonk MC, Mauritz GJ, Jacobs W, Marcus JT, Marques KM, et al. Clinically significant change in stroke volume in pulmonary hypertension. Chest. 2011;139(5):1003-9.

200. van de Veerdonk MC, Kind T, Marcus JT, Mauritz GJ, Heymans MW, Bogaard HJ, et al. Progressive right ventricular dysfunction in patients with pulmonary arterial hypertension responding to therapy. Journal of the American College of Cardiology. 2011;58(24):2511-9.

201. Sievers B, Kirchberg S, Bakan A, Franken U, Trappe HJ. Impact of papillary muscles in ventricular volume and ejection fraction assessment by cardiovascular magnetic resonance. J Cardiovasc Magn Reson. 2004;6(1):9-16.

202. Ganz W, Donoso R, Marcus HS, Forrester JS, Swan HJ. A new technique for measurement of cardiac output by thermodilution in man. Am J Cardiol. 1971;27(4):392-6.

203. McLaughlin VV, Shillington A, Rich S. Survival in primary pulmonary hypertension: the impact of epoprostenol therapy. Circulation. 2002;106(12):1477-82.

204. Hoeper MM, Maier R, Tongers J, Niedermeyer J, Hohlfeld JM, Hamm M, et al. Determination of cardiac output by the Fick method, thermodilution, and acetylene rebreathing in pulmonary hypertension. Am J Respir Crit Care Med. 1999;160(2):535-41.

205. Bland JM, Altman DG. Statistical methods for assessing agreement between two methods of clinical measurement. Lancet. 1986;1(8476):307-10.

206. Friedman M, Wilkins SA, Jr., Rothfeld AF, Bromberg PA. Effect of ventilation and perfusion imbalance on inert gas rebreathing variables. J Appl Physiol. 1984;56(2):364-9.

207. Fegler G. Measurement of cardiac output in anaesthetized animals by a thermodilution method. Q J Exp Physiol Cogn Med Sci. 1954;39(3):153-64.

208. Hillis LD, Firth BG, Winniford MD. Analysis of factors affecting the variability of Fick versus indicator dilution measurements of cardiac output. Am J Cardiol. 1985;56(12):764-8.

209. Cigarroa RG, Lange RA, Williams RH, Bedotto JB, Hillis LD. Underestimation of cardiac output by thermodilution in patients with tricuspid regurgitation. Am J Med. 1989;86(4):417-20.

210. Goldenheim PD, Kazemi H. Cardiopulmonary monitoring of critically ill patients (2). N Engl J Med. 1984;311(12):776-80.

211. Heerdt PM, Pond CG, Blessios GA, Rosenbloom M. Inaccuracy of cardiac output by thermodilution during acute tricuspid regurgitation. Ann Thorac Surg. 1992;53(4):706-8.

212. Kadota LT. Theory and application of thermodilution cardiac output measurement: a review. Heart Lung. 1985;14(6):605-16.

213. van Grondelle A, Ditchey RV, Groves BM, Wagner WW, Jr., Reeves JT. Thermodilution method overestimates low cardiac output in humans. Am J Physiol. 1983;245(4):H690-2.

214. Firmin DN, Nayler GL, Klipstein RH, Underwood SR, Rees RS, Longmore DB. In vivo validation of MR velocity imaging. J Comput Assist Tomogr. 1987;11(5):751-6.

215. Rebergen SA, van der Wall EE, Doornbos J, de Roos A. Magnetic resonance measurement of velocity and flow: technique, validation, and cardiovascular applications. Am Heart J. 1993;126(6):1439-56.

216. Lang CC, Karlin P, Haythe J, Tsao L, Mancini DM. Ease of noninvasive measurement of cardiac output coupled with peak VO2 determination at rest and during exercise in patients with heart failure. Am J Cardiol. 2007;99(3):404-5.

217. Kallay MC, Hyde RW, Smith RJ, Rothbard RL, Schreiner BF. Cardiac output by rebreathing in patients with cardiopulmonary diseases. J Appl Physiol. 1987;63(1):201-10.

218. Steen VD, Medsger TA. Changes in causes of death in systemic sclerosis, 1972-2002. Annals of the rheumatic diseases. 2007;66(7):940-4.

219. Humbert M, Sitbon O, Chaouat A, Bertocchi M, Habib G, Gressin V, et al. Survival in patients with idiopathic, familial, and anorexigen-associated pulmonary arterial hypertension in the modern management era. Circulation. 2010;122(2):156-63.

220. Tyndall AJ, Bannert B, Vonk M, Airo P, Cozzi F, Carreira PE, et al. Causes and risk factors for death in systemic sclerosis: a study from the EULAR Scleroderma Trials and Research (EUSTAR) database. Annals of the rheumatic diseases. 2010;69(10):1809-15.

221. Launay D, Sitbon O, Hachulla E, Mouthon L, Gressin V, Rottat L, et al. Survival in systemic sclerosis-associated pulmonary arterial hypertension in the modern management era. Annals of the rheumatic diseases. 2013;72(12):1940-6.

222. Fisher MR, Mathai SC, Champion HC, Girgis RE, Housten-Harris T, Hummers L, et al. Clinical differences between idiopathic and scleroderma-related pulmonary hypertension. Arthritis and rheumatism. 2006;54(9):3043-50.

223. Girgis RE, Mathai SC, Krishnan JA, Wigley FM, Hassoun PM. Long-term outcome of bosentan treatment in idiopathic pulmonary arterial hypertension and pulmonary arterial hypertension associated with the scleroderma spectrum of diseases. J Heart Lung Transplant. 2005;24(10):1626-31.

224. Voelkel NF, Quaife RA, Leinwand LA, Barst RJ, McGoon MD, Meldrum DR, et al. Right ventricular function and failure: report of a National Heart, Lung, and Blood Institute working group on cellular and molecular mechanisms of right heart failure. Circulation. 2006;114(17):1883-91.

225. Nagendran J, Michelakis ED. Mitochondrial NOS is upregulated in the hypoxic heart: implications for the function of the hypertrophied right ventricle. Am J Physiol Heart Circ Physiol. 2009;296(6):H1723-6.

226. Sutendra G, Bonnet S, Rochefort G, Haromy A, Folmes KD, Lopaschuk GD, et al. Fatty acid oxidation and malonyl-CoA decarboxylase in the vascular remodeling of pulmonary hypertension. Science translational medicine. 2010;2(44):44ra58.

227. Archer SL, Gomberg-Maitland M, Maitland ML, Rich S, Garcia JG, Weir EK. Mitochondrial metabolism, redox signaling, and fusion: a mitochondria-ROS-HIF-1alpha-Kv1.5 O2-sensing pathway at the intersection of pulmonary hypertension and cancer. Am J Physiol Heart Circ Physiol. 2008;294(2):H570-8.

228. Voelkel NF, Natarajan R, Drake JI, Bogaard HJ. Right ventricle in pulmonary hypertension. Comprehensive Physiology. 2011;1(1):525-40.

229. Dell'Italia LJ, Walsh RA. Application of a time varying elastance model to right ventricular performance in man. Cardiovascular research. 1988;22(12):864-74.

230. Michelakis ED, Wilkins MR, Rabinovitch M. Emerging concepts and translational priorities in pulmonary arterial hypertension. Circulation. 2008;118(14):1486-95.

231. Tanaka Y, Takase B, Yao T, Ishihara M. Right ventricular electrical remodeling and arrhythmogenic substrate in rat pulmonary hypertension. American journal of respiratory cell and molecular biology. 2013;49(3):426-36.

232. Overbeek MJ, Lankhaar JW, Westerhof N, Voskuyl AE, Boonstra A, Bronzwaer JG, et al. Right ventricular contractility in systemic sclerosis-

associated and idiopathic pulmonary arterial hypertension. Eur Respir J. 2008;31(6):1160-6.

233. Tedford RJ, Mudd JO, Girgis RE, Mathai SC, Zaiman AL, Housten-Harris T, et al. Right ventricular dysfunction in systemic sclerosis-associated pulmonary arterial hypertension. Circulation Heart failure. 2013;6(5):953-63.

234. Laboratories ATSCoPSfCPF. ATS statement: guidelines for the six-minute walk test. Am J Respir Crit Care Med. 2002;166(1):111-7.

235. Badesch DB, Hill NS, Burgess G, Rubin LJ, Barst RJ, Galie N, et al. Sildenafil for pulmonary arterial hypertension associated with connective tissue disease. The Journal of rheumatology. 2007;34(12):2417-22.

236. Badesch DB, Tapson VF, McGoon MD, Brundage BH, Rubin LJ, Wigley FM, et al. Continuous intravenous epoprostenol for pulmonary hypertension due to the scleroderma spectrum of disease. A randomized, controlled trial. Ann Intern Med. 2000;132(6):425-34.

237. Mathai SC, Girgis RE, Fisher MR, Champion HC, Housten-Harris T, Zaiman A, et al. Addition of sildenafil to bosentan monotherapy in pulmonary arterial hypertension. Eur Respir J. 2007;29(3):469-75.

238. Rubin LJ, Badesch DB, Barst RJ, Galie N, Black CM, Keogh A, et al. Bosentan therapy for pulmonary arterial hypertension. N Engl J Med. 2002;346(12):896-903.

239. Chung L, Liu J, Parsons L, Hassoun PM, McGoon M, Badesch DB, et al. Characterization of connective tissue disease-associated pulmonary arterial hypertension from REVEAL: identifying systemic sclerosis as a unique phenotype. Chest. 2010;138(6):1383-94.

240. Kawut SM, Taichman DB, Archer-Chicko CL, Palevsky HI, Kimmel SE. Hemodynamics and survival in patients with pulmonary arterial hypertension related to systemic sclerosis. Chest. 2003;123(2):344-50.

241. Koh ET, Lee P, Gladman DD, Abu-Shakra M. Pulmonary hypertension in systemic sclerosis: an analysis of 17 patients. Br J Rheumatol. 1996;35(10):989-93.

242. Follansbee WP, Miller TR, Curtiss EI, Orie JE, Bernstein RL, Kiernan JM, et al. A controlled clinicopathologic study of myocardial fibrosis in systemic sclerosis (scleroderma). The Journal of rheumatology. 1990;17(5):656-62.

243. Overbeek MJ, Vonk MC, Boonstra A, Voskuyl AE, Vonk-Noordegraaf A, Smit EF, et al. Pulmonary arterial hypertension in limited cutaneous systemic sclerosis: a distinctive vasculopathy. Eur Respir J. 2009;34(2):371-9.

244. Clements PJ, Tan M, McLaughlin VV, Oudiz RJ, Tapson VF, Channick RN, et al. The pulmonary arterial hypertension quality enhancement research initiative: comparison of patients with idiopathic PAH to patients with systemic sclerosis-associated PAH. Annals of the rheumatic diseases. 2012;71(2):249-52.

245. Fernandes F, Ramires FJ, Arteaga E, Ianni BM, Bonfa ES, Mady C. Cardiac remodeling in patients with systemic sclerosis with no signs or symptoms of heart failure: an endomyocardial biopsy study. J Card Fail. 2003;9(4):311-7.

246. Hachulla AL, Launay D, Gaxotte V, de Groote P, Lamblin N, Devos P, et al. Cardiac magnetic resonance imaging in systemic sclerosis: a cross-sectional observational study of 52 patients. Annals of the rheumatic diseases. 2009;68(12):1878-84.

247. Simonneau G, Galie N, Rubin LJ, Langleben D, Seeger W, Domenighetti G, et al. Clinical classification of pulmonary hypertension. J Am Coll Cardiol. 2004;43(12 Suppl S):5S-12S.

248. Bradlow WM, Hughes ML, Keenan NG, Bucciarelli-Ducci C, Assomull R, Gibbs JS, et al. Measuring the heart in pulmonary arterial hypertension (PAH): implications for trial study size. Journal of magnetic resonance imaging : JMRI. 2010;31(1):117-24.

249. Peacock AJ, Crawley S, McLure L, Blyth K, Vizza CD, Poscia R, et al. Changes in right ventricular function measured by cardiac magnetic resonance imaging in patients receiving pulmonary arterial hypertension-targeted therapy: the EURO-MR study. Circulation Cardiovascular imaging. 2014;7(1):107-14.

250. Ho SY, Nihoyannopoulos P. Anatomy, echocardiography, and normal right ventricular dimensions. Heart. 2006;92 Suppl 1:i2-13.

251. van Wolferen SA, Marcus JT, Westerhof N, Spreeuwenberg MD, Marques KM, Bronzwaer JG, et al. Right coronary artery flow impairment in patients with pulmonary hypertension. Eur Heart J. 2008;29(1):120-7.

252. Savarese G, Paolillo S, Costanzo P, D'Amore C, Cecere M, Losco T, et al. Do changes of 6-minute walk distance predict clinical events in patients with pulmonary arterial hypertension? A meta-analysis of 22 randomized trials. J Am Coll Cardiol. 2012;60(13):1192-201.

253. Galie N, Ghofrani HA, Torbicki A, Barst RJ, Rubin LJ, Badesch D, et al. Sildenafil citrate therapy for pulmonary arterial hypertension. N Engl J Med. 2005;353(20):2148-57.

254. Gabler NB, French B, Strom BL, Palevsky HI, Taichman DB, Kawut SM, et al. Validation of 6-minute walk distance as a surrogate end point in pulmonary arterial hypertension trials. Circulation. 2012;126(3):349-56.

255. Pulido T, Adzerikho I, Channick RN, Delcroix M, Galie N, Ghofrani HA, et al. Macitentan and morbidity and mortality in pulmonary arterial hypertension. N Engl J Med. 2013;369(9):809-18.

256. Vonk Noordegraaf A, Galie N. The role of the right ventricle in pulmonary arterial hypertension. European respiratory review : an official journal of the European Respiratory Society. 2011;20(122):243-53.

257. Campo A, Mathai SC, Le Pavec J, Zaiman AL, Hummers LK, Boyce D, et al. Hemodynamic predictors of survival in scleroderma-related pulmonary arterial hypertension. Am J Respir Crit Care Med. 2010;182(2):252-60.

258. Yamada Y, Okuda S, Kataoka M, Tanimoto A, Tamura Y, Abe T, et al. Prognostic value of cardiac magnetic resonance imaging for idiopathic pulmonary arterial hypertension before initiating intravenous prostacyclin therapy. Circulation journal : official journal of the Japanese Circulation Society. 2012;76(7):1737-43.

259. McLaughlin VV, Gaine SP, Howard LS, Leuchte HH, Mathier MA, Mehta S, et al. Treatment goals of pulmonary hypertension. J Am Coll Cardiol. 2013;62(25 Suppl):D73-81.

260. Gomberg-Maitland M, Bull TM, Saggar R, Barst RJ, Elgazayerly A, Fleming TR, et al. New trial designs and potential therapies for pulmonary artery hypertension. J Am Coll Cardiol. 2013;62(25 Suppl):D82-91.

261. Benza R, Biederman R, Murali S, Gupta H. Role of cardiac magnetic resonance imaging in the management of patients with pulmonary arterial hypertension. J Am Coll Cardiol. 2008;52(21):1683-92.